INFORMATION TO USERS

This manuscript has been reproduced from the microfilm master. UMI films the text directly from the original or copy submitted. Thus, some thesis and dissertation copies are in typewriter face, while others may be from any type of computer printer.

The quality of this reproduction is dependent upon the quality of the copy submitted. Broken or indistinct print, colored or poor quality illustrations and photographs, print bleedthrough, substandard margins, and improper alignment can adversely affect reproduction.

In the unlikely event that the author did not send UMI a complete manuscript and there are missing pages, these will be noted. Also, if unauthorized copyright material had to be removed, a note will indicate the deletion.

Oversize materials (e.g., maps, drawings, charts) are reproduced by sectioning the original, beginning at the upper left-hand corner and continuing from left to right in equal sections with small overlaps.

Photographs included in the original manuscript have been reproduced xerographically in this copy. Higher quality 6" x 9" black and white photographic prints are available for any photographs or illustrations appearing in this copy for an additional charge. Contact UMI directly to order.

Bell & Howell Information and Learning
300 North Zeeb Road, Ann Arbor, MI 48106-1346 USA
800-521-0600

GYPSUM SCALE FORMATION IN CONTINUOUS HYDROMETALLURGICAL NEUTRALIZATION REACTORS

by

Jeffrey F. Adams

A thesis submitted in conformity with the requirements
for the degree of Master of Applied Science
Graduate Department of Chemical Engineering and Applied Chemistry
University of Toronto

GYPSUM SCALE FORMATION IN CONTINUOUS HYDROMETALLURGICAL NEUTRALIZATION REACTORS

Master Of Applied Science 1999

Jeffrey F. Adams

Graduate Department of Chemical Engineering & Applied Chemistry
University of Toronto

Abstract

An experimental study was carried out to determine the rate and extent of scale formation of gypsum (calcium sulphate dihydrate) on stainless steel surfaces in two types of continuous hydrometallurgical sulphuric acid neutralization reactors: a calcium carbonate partial neutralization reactor, and a calcium oxide total neutralization reactor. The purpose of the study was to determine the effects of pH, temperature, residence time, presence of metal sulphates (Fe, Al, Ni, and Mg), addition of surfactants, and addition of gypsum seed on scale growth. The rate of scale formation was found to be reduced by lower temperatures, longer residence times, and the presence of nickel and magnesium. pH had no significant effect. The effect of these variables on the rate of scale formation was related to the degree of gypsum supersaturation. Scale reduction through the addition of sulphonated anionic surfactants was found to only be effective under certain conditions. However, gypsum seeding was found to be an effective method of scale reduction. Scale was reduced by 50% or more at a seed concentration of 10g/L.

Acknowledgements

I could not have completed this work without the following people:

First and foremost my parents, for their love, support and understanding for the last twenty six years, (especially the last three).

Dr. Vladimiros Papangelakis for his patience and guidance, as well as for believing in me and pushing me to always do "better".

Dr. Dmitri Rubisov for always leaving his door open, both literally and figuratively, and for never being too busy to answer questions or provide help.

Morteza Baghalha, Flora Nadafi, Pangiotis Perdikis, and Elena Rubisova for their help and assistance in the lab.

Fred Leslie for his friendly and prompt assistance.

INCO Ltd. for financial support of this project.

The CEGSA Group, for good times.

Table of Contents

List of Figures

1. Introduction

1.1 Industrial Scale Formation

Precipitation fouling or scale formation is a common problem encountered in many industrial process operations. It can best be described as the deposition of inorganic salts from aqueous solution onto surfaces. This includes everything from hard, crystalline, strongly adherent deposits, to soft, porous, loosely held sludge [1]. Scale formation is a problem because it fouls equipment surfaces, reducing process efficiency, and resulting in high maintenance costs. Industries and processes where scale formation is most common include oil and gas production, geothermal energy production, desalination operations, steam generation operations, heat transfer systems, water supply systems, and of course, hydrometallurgical operations.

Scale formation occurs in oil and gas production as a result of subsurface water coming into contact with well pipes, tubes and pumps [2]. As oil and/or gas are brought to the surface, ion-containing subsurface water is drawn along too. The drop in pressure and changes in temperature that occur during processing cause solubility to decrease, resulting in the deposition of $CaCO_3$, $CaSO_4$, and $BaSO_4$ scales [2], [3], [4].

In geothermal energy production, silica is the major component of scale. It deposits from hot brine solutions as they are pumped to the surface, resulting in clogged well lines, separators and discharge lines [1]. Minor contributors to this scale formation are iron and copper sulphides, $CaCO_3$, and $CaSO_4$.

Desalination operations also have scale formation problems, because sea water is rich in scale-forming ions such as Ca^{2+}, Mg^{2+}, SO_4^{2-}, and CO_3^{2-}. The salts of these ions, $CaCO_3$, $CaSO_4$, and $Mg(OH)_2$, precipitate on evaporator surfaces as a result of heating since these salts are inversely soluble with temperature [1]. In operations where reverse osmosis is used, scale is deposited on membrane surfaces, reducing their performance and efficiency [5]. These scales can also include strontium salts such as $SrCO_3$, and $SrSO_4$ [5], [6].

Boilers used in steam generation have always been plagued by scale formation. The type of salt that precipitates depends on the chemistry of the boiler feed water, but once again the most common scales are $CaCO_3$, $Mg(OH)_2$ and $CaSO_4$, with aluminum, iron and silica scales also occurring [2]. The result is poor heat conduction and therefore greater fuel consumption [7].

Similar scale formation is also encountered in heat transfer systems. Calcium and magnesium scales are especially a problem and can completely destroy the effectiveness of heat exchangers [7].

In water supply systems, $CaCO_3$ is the main component of scale [3]. This is especially a problem in southwestern Ontario where the water table is saturated with limestone. The result is clogged supply lines and reduced flow capacity.

In hydrometallurgical operations, many different types of scale formation occur. High temperatures and high ionic strengths make scale formation inevitable. One example is the formation of hematite and alunite scales on autoclave walls during high temperature leaching of nickeliferous laterites. A detailed study of this phenomenon was recently conducted at the University of Toronto [3].

Another example from the field of hydrometallurgy is the formation of $CaSO_4$ scales: mostly gypsum ($CaSO_4 \cdot 2H_2O$), but also hemihydrate ($CaSO_4 \cdot \frac{1}{2}H_2O$) and anhydrite ($CaSO_4$), depending on the temperature and reactor conditions. Because of the relative insolubility of the calcium sulphate hydrates, these scales are deposited almost anywhere calcium and sulphate are together in aqueous solution. The result is fouled reactor walls, impellers and pumps, as well as clogged pipes. What makes them such a problem is that they form even at low pH and can only be easily and effectively removed mechanically [8].

1.2 Gypsum Scale Formation in Continuous Hydrometallurgical Reactors

The largest occurrence of scale-forming calcium sulphate in hydrometallurgical processes is during the continuous partial neutralization or total neutralization of sulphuric acid leach solutions with calcium-containing bases, such as limestone ($CaCO_3$), and lime (CaO). The reactions are, respectively:

$$H_2SO_4 + CaCO_{3(s)} + H_2O \Rightarrow CaSO_4 \cdot 2H_2O_{(s)} + CO_{2(g)} \uparrow \qquad (1)$$

and

$$H_2SO_4 + CaO_{(s)} + H_2O \Rightarrow CaSO_4 \cdot 2H_2O_{(s)} \qquad (2)$$

In these two cases, gypsum ($CaSO_4 \cdot 2H_2O$) is the primary reaction product. The reason is that these reactors operate at atmospheric pressure, below 90°C. Under these conditions, gypsum is the precipitating phase, (see Section 2.2.1), [9], [10], [11].

Both (partial and total) neutralization steps are necessary in the processing of nickeliferous laterite ores. A simplified process flow diagram of this process is shown in Figure 1.

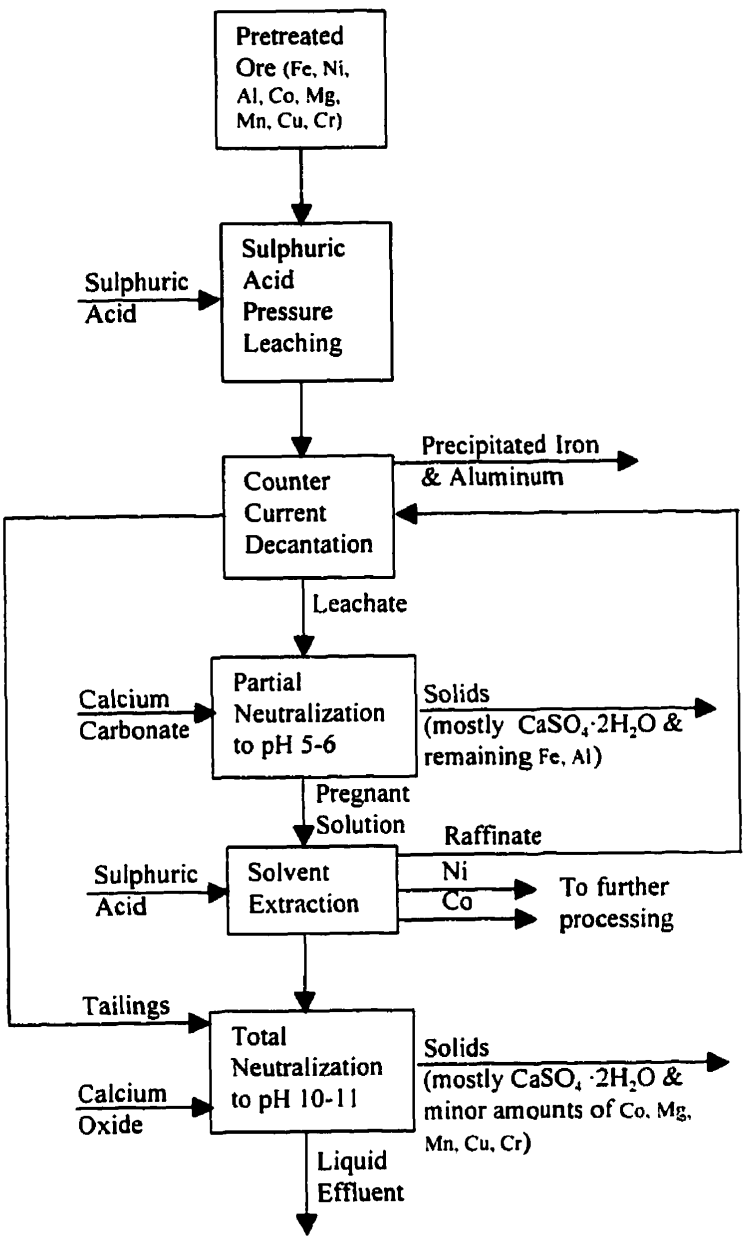

Figure 1: Simplified process flow diagram of nickeliferous laterite ore processing [12].

Briefly, neutralization (reaction 1) typically takes place immediately following high-temperature laterite leaching. The autoclave effluent is in the form of a slurry, containing precipitated iron and aluminum, as well as residual aqueous sulphuric acid, iron, aluminum, nickel, and minor amounts of cobalt, magnesium, manganese, chromium, copper, and other minor impurities. The temperature and pressure are reduced and the solids are separated by counter current decantation [3]. This leaves the leachate, which is partially neutralized to a pH of 5-6 with limestone (reaction 1) to precipitate the remaining iron, aluminum and sulphate, and to adjust the pH for downstream nickel/cobalt purification steps. Typical neutralization conditions are given in Table 1 (a). From here, the resulting slurry is again separated and a pregnant solution, (containing the target nickel and cobalt metals), continues to a solvent extraction operation for further processing. The solid gypsum, iron, and aluminum are disposed.

In the solvent extraction stage, stripping of the organic extractant occurs with sulphuric acid. The extracted, separated nickel and cobalt are sent for further processing while the remaining aqueous solution continues to a final neutralization/purification stage. The purpose of this total neutralization (reaction 2) is to neutralize the sulphuric acid and to render the solution safe for disposal, (by precipitating out all of the remaining metal ions). Typical reactor conditions for this process are given in Table 1 (b) below.

Table 1: Typical conditions for continuous (a) partial neutralization and (b) total neutralization of sulphate effluent during acid pressure leaching of laterites [13].

Calcium Base	Initial $[H_2SO_4]$	Temp.	Residence Time	pH	Major Entrained Metal Sulphates
(a) $CaCO_3$	30g/L	70°C	15-50min	4-6	1g/L Fe, 2g/L Al, 5g/L Ni
(b) CaO	10g/L	40°C	15-50min	10-11	0-10g/L Mg

The problem of gypsum scale formation arises in both neutralization stages. The reason is that not only does gypsum precipitate in the bulk solution, but it also precipitates and grows as scale on reactor surfaces and in pipes around the reactors.

1.3 Objectives

Although, as has been stated, gypsum scale formation is a common problem in continuous hydrometallurgical reactors, no work has ever been formally undertaken to study this phenomenon in depth under conditions relevant to hydrometallurgical processing. Thus, the purpose of this study was first to determine the rates of gypsum scale formation on stainless steel surfaces in simulated, bench-scale versions of the two different types of continuous neutralization reactors. (Stainless steel surfaces were used because it is the most common building material for reactors, pipes, impellers and other reactor components.) The next purpose of the study was to determine the effects of pH, temperature, residence time, presence of metal sulphates (Fe, Al, Ni, and Mg), addition of surfactants and addition of gypsum seed on scale growth. The ultimate goal of this was to identify trends in gypsum scale formation that might possibly lead to solutions to the problem.

2. Literature Review

Despite the lack of literature on the subject of gypsum scale formation in continuous hydrometallurgical reactors, there is a great deal of relevant background material in crystallization theory. The reason is that in order to understand how and why gypsum scale forms, it is necessary to review fundamental crystal theory. This includes crystal precipitation, nucleation, and growth theory.

2.1 Precipitation

Precipitation is defined "as reactive crystallization, i.e. the production of a solid compound out of a solution via a chemical reaction" [14]. Of course, it goes without saying that the solution must be supersaturated with respect to the precipitating compound before precipitation will occur.

Thus, precipitation will occur when:

$$\left(\frac{Q_{SP}}{K_{SP}}\right) > 1 . \qquad (3)$$

where Q_{sp} = concentration product of the solute in the solution

K_{sp} = solubility product constant of the solute at equilibrium

This ratio is defined as the saturation ratio, S. In dilute solutions, one can simplify this by taking Q_{sp} and K_{sp} to be equal to activities, and activities to be equal to concentrations:

$$S = \frac{Q_{SP}}{K_{SP}} \cong \frac{a}{a_o} \cong \frac{C}{C_{eq}} \qquad (4)$$

where a = activity of the solute in the initial solution

a_o = final activity of the solute in equilibrium with the solid species

C = concentration of the solute in the initial solution

C_{eq} = equilibrium concentration

The saturation ratio S, can also be used to define the supersaturation ratio:

$$S - 1 = \frac{C - C_{eq}}{C_{eq}} \qquad (5)$$

2.2 Nucleation

Once the conditions exist for precipitation to occur (i.e. S>1), the first stage of crystal formation can begin. This stage is called nucleation, and it has three main categories: (1) primary homogeneous, (2) primary heterogeneous, and (3) secondary heterogeneous [14].

Primary homogeneous nucleation occurs in bulk solution, in the absence of a solid interface [14]. This is through solute molecules combining to form embryos. These embryos either reach a critical size above which they are stable, or dissolve back into solution. Homogeneous nucleation occurs at relatively high values of S, (see Fig. 2), because the interfacial energy between the crystal and the solution is relatively high, and therefore a large driving force is necessary for it to occur [15].

Primary heterogeneous nucleation occurs in the presence of a foreign surface. Nuclei form on a solid surface such as dirt, reactor or pipe walls (beginning the process of scale formation), colloidal particles, etc. In this case, the interfacial energy between the

crystal and the solid is less than the interfacial energy between the crystal and solution. Thus, primary heterogeneous nucleation occurs at lower values of S than primary homogeneous nucleation, (see Fig. 2) [14],[15].

Secondary heterogeneous nucleation is nucleation that occurs on seed particles of the same composition and phase as the precipitating ones. When these seed particles are purposely added to the solution to induce precipitation, it is called apparent secondary nucleation. When the seed consists of fragments of crystals that are already present in the solution, (e.g. due to fluid motion), it is called true secondary nucleation. And when the seed is formed from crystals breaking due to collisions with other crystals, reactor walls, or impellers, it is called contact secondary nucleation [3]. Secondary heterogeneous nucleation occurs only in the presence of other like crystals. The interfacial energy between particles of the same composition and phase is generally fairly low, so that secondary heterogeneous nucleation occurs even at low values of S (see Fig. 2) [1],[3].

Therefore, nucleation can occur through several different reaction mechanisms, depending on the degree of saturation and reactor conditions. Of these, primary homogeneous nucleation occurs only at higher levels of S, primary heterogeneous nucleation occurs at lower values of S, and secondary heterogeneous nucleation can occur at even the lowest values of S provided there is seed present. This is best summarized by Figure 2, which shows a general plot of normalized nucleation rate versus saturation ratio S [3]. As can be seen, as long as there are seed crystals present, secondary heterogeneous nucleation has a high nucleation rate over the entire range of S.

Therefore, with respect to scale formation one would expect that primary heterogeneous nucleation would occur on new surfaces (e.g. reactors, pipes, impellers, etc.), followed by secondary heterogeneous nucleation which would lead to scale growth.

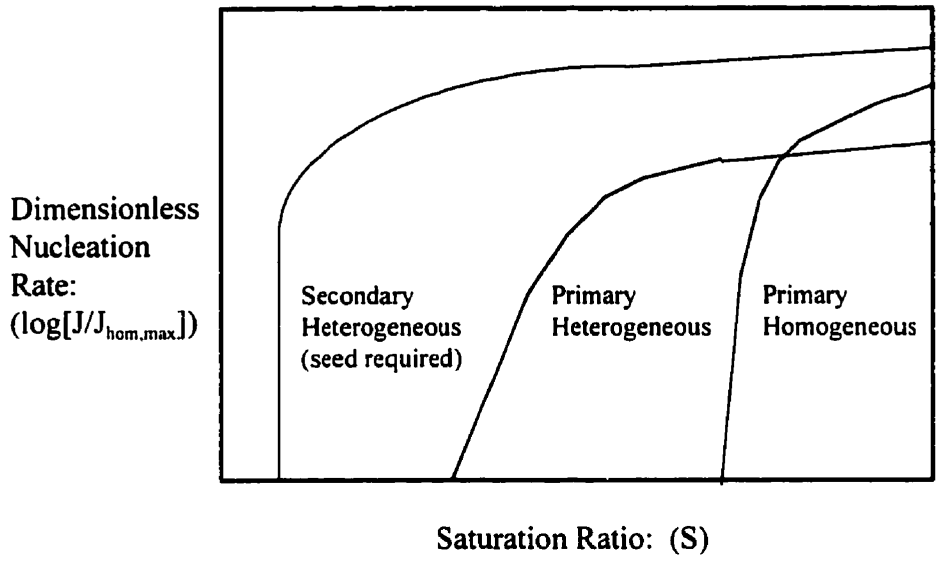

Figure 2: Nucleation rate vs saturation ratio Graph [3]

Before going any further, it is necessary to examine the case where a substance can precipitate as more than one phase. Calcium sulphate can precipitate as gypsum ($CaSO_4 \cdot 2H_2O$), hemihydrate ($CaSO_4 \cdot \frac{1}{2}H_2O$), or anhydrite ($CaSO_4$). Theoretically, the most thermodynamically stable phase is expected to precipitate. Furthermore, the most stable phase will have the lowest solubility as compared to the other, metastable phases. However, under conditions where primary homogeneous nucleation prevails, Stranski's Rule, (also known as Ostwald's Step Rule), states that "the precipitate with the highest solubility (i.e. the least stable solid phase) will form first in a consecutive precipitation reaction" [15].

This fundamental rule of precipitation has a profound effect on calcium sulphate scale formation, especially between 42 and 97°C. Although gypsum is the most common scale-forming phase of calcium sulphate, under some conditions it could be the hemihydrate or the anhydrite phases that are precipitating to form scale. The reason for this is the interweaving solubility curves of the three calcium sulphate phases.

Figure 3 shows a graph of solubility versus temperature for the three phases between 0 and 100°C. As can be seen, below 42°C gypsum is the least soluble phase, while above 42°C, anhydrite is the least soluble phase. One would therefore expect that gypsum would be the scale-forming phase below 42°C, while above 42°C, anhydrite would be the scale-forming phase. This is not the case however [11], [16].

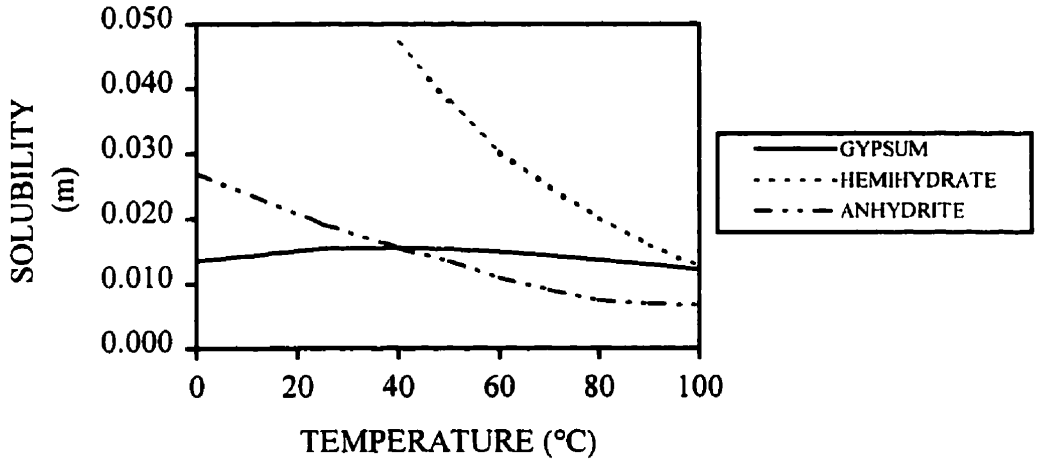

Figure 3: Solubility vs temperature for the three calcium sulphate phases [17]

According to Figure 3, above 42°C hemihydrate should be the first phase to form. Then it should convert to gypsum, which should then dehydrate to the anhydrite phase. However, only gypsum is found to precipitate [11], and once it is formed, it does not

dehydrate to form anhydrite. In fact, even when left for years, gypsum is still found to be the only phase present [11]. The reason is that the mechanism of gypsum dehydration involves two stages: a partial dehydration to hemihydrate, followed by the dehydration to anhydrite [10]. The former stage is not thermodynamically favoured below 97°C in pure water, and 90.5°C in concentrated salt solutions. (This was proven both thermodynamically and experimentally by Ostroff [10].) Thus although it is technically a metastable phase, gypsum is not converted to anhydrite between 42 and 90°C, and can therefore be considered stable.

Of course, it goes without saying that if the mechanism is secondary heterogeneous nucleation, and there is anhydrite seed present, anhydrite will be the precipitating, stable phase between 42 and 90°C. However, in this study anhydrite will not be purposely added as seed, and this scenario need not be considered.

Therefore, from this point on gypsum will be assumed to be the precipitating, scale-forming phase under all conditions, in both reactors.

2.3 Growth

Once nuclei are present, the second stage of crystal formation can begin. This stage is crystal growth. Crystal growth is obviously crucial to scale formation.

According to theory, growth occurs through the incorporation of solvated solute molecules, (or growth units), into step or kink sites on the crystal surface [14]. This occurs through the eight-step process that is illustrated in Figure 4:

(i) Transport of the growth unit from the bulk solution to the crystal surface.

(ii) Adsorption on the crystal surface.

(iii) Lateral diffusion over the surface.

(iv) Attachment to a step.

(v) Diffusion along a step.

(vi) Integration into the crystal at a kink site.

(vii) Diffusion of solvent molecules away from the crystal surface.

(viii) Liberation of heat of crystallization and its transport away from the crystal.

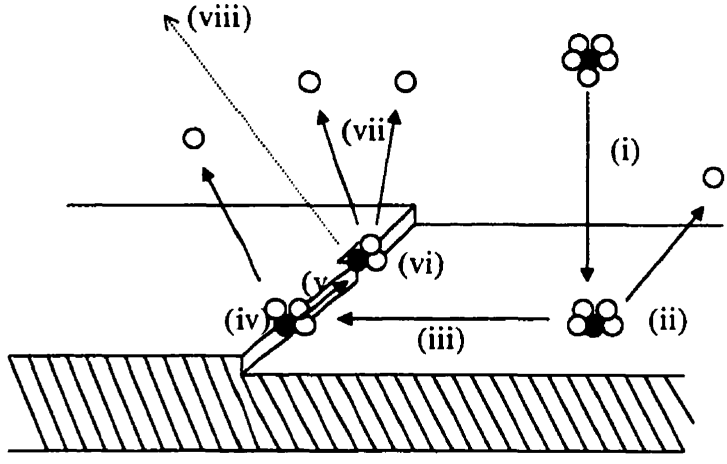

Figure 4: Stages of crystal growth [14]

Although crystal growth always occurs through the above eight-step process, the rate at which growth occurs depends on which of these eight steps is the rate-determining one. Thus, there are several different growth mechanisms that can be used to explain crystal growth rates, [3],[14],[15]:

(1) Mononuclear Growth (Figure 5a): One surface nucleus forms at a time on the surface of the crystal and then rapidly spreads across the surface to form a new growth layer. In this case, step (ii) in Figure 4 is the rate-determining step.

(2) Polynuclear Growth (Figure 5b): Many surface nuclei form on the crystal surface and grow together, until an entire growth layer is formed. In this case, once again step (ii) in Figure 4 is the rate-determining step.

(3) Screw Dislocation Growth (Figure 5c): New crystal molecules are absorbed onto the growth layer at the top step of a screw dislocation [3]. Thus, the dislocation grows up and up, (in a spiral), as new layers are added. In this case, step (iii) in Figure 4 is the rate-determining step.

(4) Diffusion-Controlled Growth: In this case, the rate-determining step in the growth of the crystal is diffusion of growth units to the crystal surface, (step (i) in Figure 4).

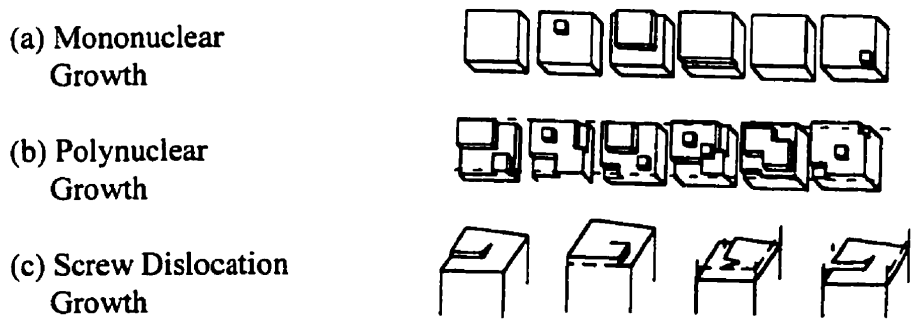

Figure 5: Crystal growth mechanisms (from Neilsen, (1964) [16])

From Dirksen and Ring (1991) [14], it is known that these four growth rate mechanisms can all be described by generalized growth rate expressions of the form:

$$\frac{dG}{dt} = C \cdot g(R) \cdot f(S) \qquad (6)$$

where $C \cdot g(R)$: is essentially a growth rate constant. It incorporates crystal volume and area factors $g(R)$, and other constants, (such as diffusion coefficients).

$f(S)$: is a saturation ratio function. Its form is given by:

$$f(S) = (S-1)^{n_1} \cdot (S)^{n_2} \cdot \exp\left(\frac{-n_3}{\ln S}\right) \qquad (7)$$

The coefficients n_1, n_2, n_3, and C, (from equation 6), depend on temperature and the mechanism of crystal growth [18]. (This will be discussed further in section 2.4). The mechanism of crystal growth in turn depends on the saturation ratio. For instance, screw dislocation growth occurs mostly under low supersaturation conditions. Mononuclear and polynuclear growth occur under higher supersaturation conditions, while bulk diffusion-controlled growth usually occurs under the highest supersaturation conditions.

For gypsum crystal growth systems, different researchers under different conditions have reported three of these four growth mechanisms. Christoffersen, Christoffersen, Weijnen and Van Rosmalen (1982) [17] reported screw dislocation growth in gypsum crystal growth systems in the saturation ratio range of 1.03 to 1.15. Pakter (1974) [16] found both mononuclear and polynuclear growth, depending on the time during batch crystallization. These experiments were in the saturation ratio range of 1.5 to 16. And finally, Tadros & Mayes (1979) [19], Klepetsanis & Koutsoukos (1989) [20], and Hamdona, Nessim & Hamza (1993) [21], all reported polynuclear growth for

gypsum crystals in different systems at varying saturation ratios. Thus it can be concluded there is no one mechanism for gypsum crystal growth; saturation ratio plays a large part in determining which mechanism is responsible for growth in any particular system.

2.4 Factors Affecting Crystal Growth

In addition to saturation ration, there are several other factors that can affect crystal growth and thus, scale formation. These can influence crystal shape, size, composition, properties, and growth kinetics. Some factors include temperature, matrix anion effects, impurity effects, presence of seed crystals, and presence of surfactants. These are summarized below.

2.4.1 Temperature

Temperature effects are highly significant. Besides merely influencing solubility and thus saturation ratio, high temperatures promote crystal formation and growth in a number of ways. The first way is by increasing the rate of diffusion of the growth unit (both step i and step iii in Fig. 4). Another way is by increasing the rate of integration of the growth unit into the crystal at the kink site (step vi in Fig. 4). The third way is by promoting dehydration (step vii in Fig. 4), which increases the rate of adsorption of the growth unit. All of these temperature effects are taken into account when determining the

coefficients (n_1, n_2, n_3, and C) for equation (6) and (7). In general, an increase in temperature usually (but not necessarily always) means an increase in crystal growth rate.

2.4.2 Matrix Anions

The solution matrix anion is another significant factor in crystal growth. It influences the shape and size of the precursor complex-cluster, which in turn affects the shape and size of the growing crystal. This would alter $g(R)$ in equation (6). The matrix anion can also be incorporated into the growing crystal as an impurity. This can cause deformities in the crystal structure, once again affecting g(R). The final way that the matrix anion can influence crystal growth is by interfering with the dehydration process (step vii in Fig. 4). This can impede incorporation of the growth units into the crystal lattice and slow down the rate of crystal growth [13]. This would be seen as a reduction in C in equation (6).

2.4.3 Impurities

Impurity effects are another significant factor in crystal growth. For example, adsorption of trace quantities of anions or cations can alter crystal morphology habit from needle-like to plate-like, (or vice versa), which would affect g(R) in equation (6). Adsorption may sometimes significantly inhibit growth by interfering with the supply of growth units to certain faces of the crystals. The impurities can also block kink sites

without being adsorbed themselves, and effectively retard crystal growth. And since they are not adsorbed, even trace amounts may have a strong effect.

A good example of crystals that are affected by impurities is gypsum crystals. In one study, divalent metals like magnesium, cadmium, lead and ferrous ions were all found to inhibit gypsum crystal growth [21]. It was postulated that the ions were adsorbed by the crystals in place of calcium. In another study, borax, citric, succinic, and tartaric acid salts were found to inhibit gypsum crystal growth by adsorbing onto the crystal surface and blocking adsorption of calcium and sulphate ions [22]. The effect of these impurities on the growth rate equation (6) would be a reduction in C and/or g(R). Thus, impurity effects are significant factors affecting gypsum crystal growth.

2.4.4 Surfactants

Surfactants can also block growth steps, thereby reducing or eliminating crystal growth. Or they can form surface complexes with the anions or cations of the crystal, making them unavailable for growth. Like other impurities, they can also alter the morphology of the growing crystal. This is as a result of preferential adsorption on one face of the crystal and either enhancing or inhibiting its growth. The effect of surfactants is usually seen as an alteration in C and/or g(R), in the growth rate equation (6).

Gypsum crystals are affected by many different types of surfactant [19], [22], [23], [24], [25], [26], [27], [28], [29]. Some of these include polyacrylate, polyaspartate, and polycarboxylate polymers, as well as different phosphonates and sulphonates. These are all anionic surfactants and they have been shown to be effective in inhibiting gypsum

crystal growth over a wide range of pH. It is *hypothesized* that they work by physically blocking the incorporation of calcium and sulphate, or by forming surface complexes with calcium, preventing its adsorption. In most cases their effect can be seen in the crystal morphology which is altered from needle-like to block-like, due to adsorption on the top [111] crystal face [19]. When this occurs, only the [110] and [010] crystal faces grow outward, resulting in short, stubby crystals. Figure 6 shows the different faces of a gypsum crystal.

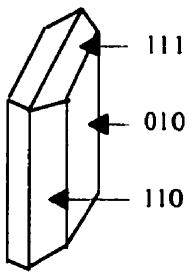

Figure 6: Crystal faces of gypsum [19]

The only problem with surfactants is that it is extremely hard to predict in which gypsum applications they will be effective. The reason is that gypsum defies conventional surfactant theory. Anionic surfactants are negatively charged, and should therefore only be adsorbed by and inhibit the growth of positively charged crystals. However, gypsum crystal growth is inhibited by anionic surfactants at neutral pH, even though gypsum crystals are negatively charged between pH's of 2.3 and 10.7. A plot of zeta potential versus pH for gypsum in saturated solution is shown in Figure 7.

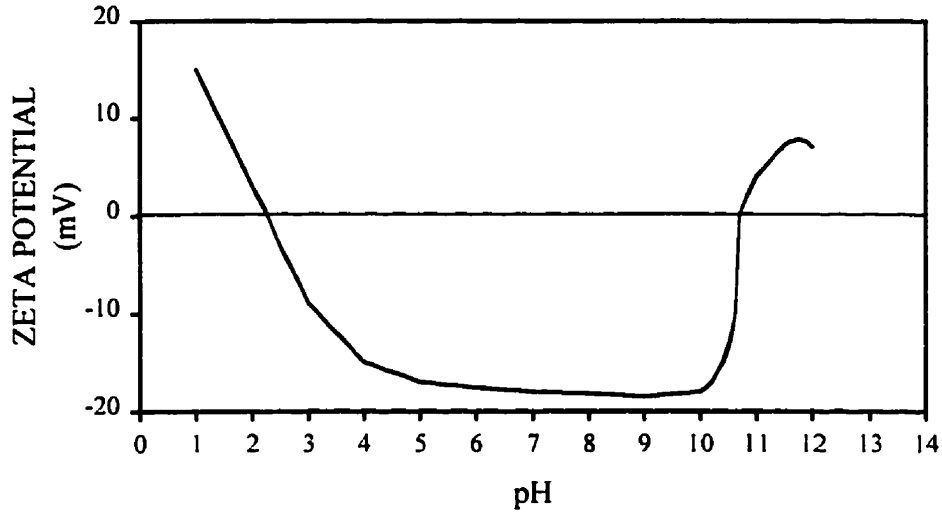

Figure 7: Zeta potential vs pH for gypsum in saturated calcium sulphate solution [30]

Therefore, the problem with surfactants as crystal growth inhibitors is that not enough is known about how they work. Thus, they are extremely application-specific. Finding one that works for any gypsum system is difficult and usually involves a fair amount of luck.

2.4.5 Seed Crystals

The presence of seed crystals is the last significant factor that can affect crystal growth. Recall from section 2.2 that seed crystals provide a surface for secondary nucleation and secondary nucleation rates are higher than homogeneous or heterogeneous nucleation rates at equivalent saturation ratios. In other words, crystal growth on seed particles is faster and requires less of a driving force than growth on foreign surfaces. The presence of additional, added seed also provides a larger surface area on top of which

growth can occur. This means that the more seed particles there are, the lower the individual growth rates for each crystal. The effect of seeding is seen in the growth rate constant C in equation (6).

There are several good examples of these principles in literature. Liu & Nancollas found that the gypsum crystal growth rate constant was proportional to the amount of seed added [31]. Omelon & Demopoulos (1997) used repeated seed recycling and low supersaturation to produce larger gypsum crystals with more favourable settling properties [32]. Another study used seeding to reduce calcium sulphate scale formation in a distillation plant [33]. In this case, the seed provided a surface for calcium sulphate to precipitate on in the bulk solution (through secondary nucleation), rather than the heat exchanger walls (through heterogeneous nucleation).

Therefore, there are many factors that affect crystal growth (i.e. scale growth). Temperature, matrix anions, impurities, surfactants and seed crystals can each exert significant influence on the crystal shape, size, composition, properties and growth kinetics. An understanding of these factors can help to predict when and how fast scale crystals will grow, as well as the properties that they will have.

3. Experimental

3.1 Scope of Experiments

Experiments were performed to assess the effect of process variables on gypsum scale formation in two cases: calcium carbonate partial neutralization, and calcium oxide total neutralization. These variables included pH, temperature, and residence time, which were investigated in both the absence and presence of foreign metal sulphates. After this, means of scale reduction were investigated through the addition of surfactants and gypsum seeding. SEM examination of the scale was also performed.

All of the scale growth experiments were performed in a continuous 425 mL glass reactor, using simulated waste acid solutions. Raw data for all of the scale growth experiments will be presented in Appendix A.

3.2 Equipment

Figure 8 shows the arrangement of the continuous reactor apparatus. The limestone/lime slurry feed tank and sulphuric acid tank were both HDPE carboys, 25L and 20L in volume respectively. The base slurry was kept continuously in suspension by the action of a Cole Parmer laboratory mixer (model 4554-10) in conjunction with a Cole Parmer Stir-Pack controller and a 45cm HDPE stirrer shaft. The peristaltic pumps were both Cole Parmer L/S variable speed digital pumps (model E-07523) capable of pumping 0.6-1680mL/min (± 0.1mL/min) depending on the tubing size. Tubing between the tanks

and the reactor was black Norprene LS 16. A Corning Hot Plate/Stirrer (model PC-351) provided temperature control (±2°C) and magnetic agitation (700-1000rpm).

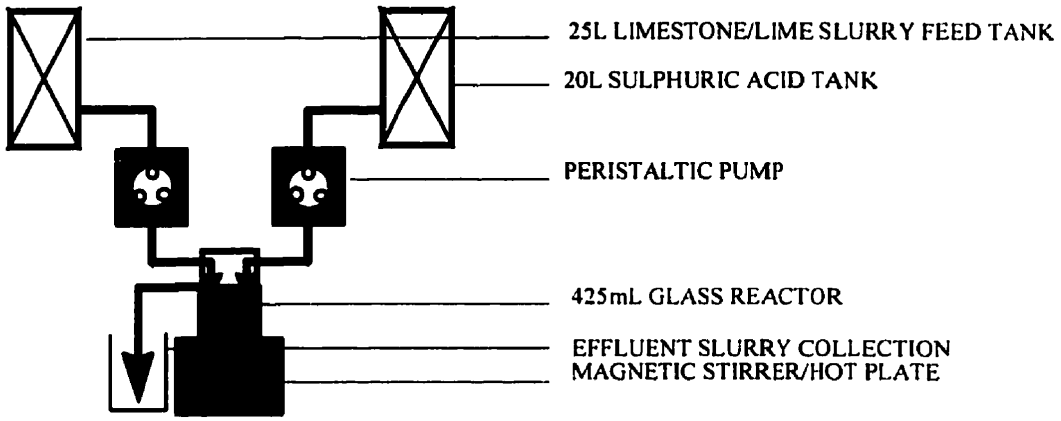

Figure 8: Continuous reactor apparatus

The continuous reactor employed was a novel experimental design and is shown in Figure 9. It was made of glass and was cylindrical in shape with approximate dimensions 8.5cm I.D., 13.5cm height. The inlets to the reactor were placed at a 120° angle from one another, 9cm from the bottom of the reactor. The outlet was placed 120° from both inlets, 7cm from the bottom of the reactor. Both of the inlets and the outlet were constructed of 0.75cm I.D. glass tubes, 2cm in length, molded onto the cylinder. The volume of liquid that would fill the reactor cylinder to the mouth of the outlet was approximately 425mL. A 1cm I.D. rubber hose was attached to the mouth of the outlet. The other end of this hose emptied into a waste container.

Scale was grown on 3/16" 316SS sample rods, (17cm in length), that were held suspended in the reactor solution by a custom-made aluminum sample holder. Details are shown in Figure 9.

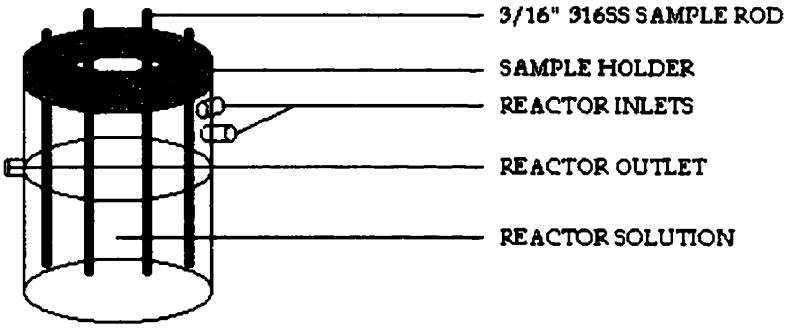

Figure 9: Glass reactor with sample rods

3.3 Materials

Nickel sulphate, ferric sulphate, aluminum sulphate, magnesium sulphate, calcium sulphate, and calcium carbonate were all technical grade chemicals from Fisher Scientific. Sulphuric acid was 97% pure and was diluted to the appropriate concentration with distilled water. Dow Chemical supplied surfactant's Dowfax 2A1 and 3B2, while Aerosol OS surfactant was supplied by Cytec Industries Incorporated.

3.4 Experimental Preparation

Because the scale growth experiments involved the use of a continuous reactor, considerable preparation was required for each run. First, six sample rods were cut in the machine shop and their rough edges were filed down. They were then cleaned with acetone, rinsed with distilled water and allowed to dry in air overnight. At this point, the rods were marked with the numbers 1-6 and weighed to the nearest tenth of a milligram

using an AND model ER-120A balance. Rods were handled with vinyl gloves at all times to avoid contamination.

Next, the acid tank was prepared. First, a clamp was placed at the end of the attached tubing to prevent leakage. The tank was then filled with distilled water and the appropriate amount of acid. For the experiments involving partial neutralization with calcium carbonate, this meant that the solution was made up to a concentration of 30g/L. For the experiments involving total neutralization with calcium oxide, this meant that the solution was made up to a concentration of 10g/L. If the experiments included metal sulphates in the acid solution, the appropriate amount of each sulphate was weighed and added. (Exact metal sulphate concentrations were given in Table 1.) The acid solution could be prepared well in advance.

The base (calcium carbonate or calcium oxide) slurry was prepared next. This was done approximately 30min before the start of the experimental run. The reason is that base slurries, especially calcium oxide slurries, tend to absorb carbon dioxide from the air when agitated. This forms carbonic acid, which partially neutralizes the base and leaves calcium carbonate deposits on the walls of the tank and on the slurry stirrer.

To prepare the slurry, first a clamp was placed at the end of the attached tubing to prevent leakage. Next, the tank was filled with distilled water and the appropriate amount of base, which was weighed out ahead of time. The amount of calcium carbonate was 45g/L in the partial neutralization experiments. This amount was chosen to ensure that calcium carbonate dissolution would not affect the overall reaction kinetics, and to ensure that there would be enough calcium carbonate to completely precipitate iron and aluminum in the metal sulphate experiments. It represented approximately 1.5 times the

stoichiometric amount of calcium carbonate that would completely consume the 30g/L of sulphuric acid. For a sample calculation showing the determination of the stoichiometric amount, see Appendix B.1.

For total neutralization experiments, the amount of calcium oxide was either 8.55g/L or 6.5g/L, depending on whether there was magnesium in the acid feed or not. The reason that these latter two were different from each other was that calcium oxide was partially consumed by magnesium to form magnesium oxide, so that the experiments with magnesium sulphate in the acid feed required more calcium oxide in the base feed. Both of these concentrations were determined by calculating the stoichiometric ratio that would theoretically consume the 10g/L of sulphuric acid, and then running several experiments (without scale sample rods) using increasing amounts of calcium oxide until a steady state pH of 9-11 was achieved.

When the base slurry was completely prepared, the stirrer was turned on to approximately 50% of full power to ensure a homogeneous suspension.

3.5 Experimental Procedure

The first set of scale growth experiments that were performed were in the continuous partial neutralization reactor. In these experiments, 30g/L of sulphuric acid was continuously partially neutralized with calcium carbonate (limestone).

The second set of scale growth experiments were in the continuous total neutralization reactor. In these experiments, 10g/L of sulphuric acid was being continuously neutralized with calcium oxide (lime).

Once preparation was complete, (in either reactor), the reactor was filled with distilled water and the magnetic stirrer was turned on. The stirrer was turned to a speed of approximately 850rpm. This speed was chosen because it was just fast enough to keep the solid products in suspension. It was also slow enough to prevent any splash and leakage.

Next, the peristaltic base and acid pumps were turned on and adjusted to a flow rate of 7mL/min ± 0.1mL/min each, to produce the desired residence time of 30min ± 0.5min. At this point, the hot plate was turned on. The hot plate was adjusted to a calibrated setting to produce the desired steady state temperature. In the calcium carbonate partial neutralization reactor, the desired temperature was 70°C. In the calcium oxide alkalization reactor, the desired temperature was 40°C.

The system was then allowed to reach steady state. Depending on the residence time, this could take anywhere from thirty minutes (for a residence time of 15min) to an hour and a half (for a residence time of 50min). As soon as the system had reached steady state, (constant temperature and pH), the sample rods were placed in the sample holder and the sample holder was placed in the reactor.

To measure scale growth, one sample rod was removed from the reactor every hour or two, (depending on the growth rate), and a dummy rod was put in its place to preserve the same hydrodynamics. The scaled sample rod was rinsed with distilled water to remove loosely attached scale and reactor particles. This was repeated for the other rods, until the run was over, (which was usually six to twelve hours, depending on the growth rate). The rods were allowed to dry in air overnight and then weighed. The

amount of scale formed was determined by subtracting the mass of the rods before the run, from the mass of the rods after the run. These numbers were divided by the surface areas of the scale-covered portions of the rods to determine "specific growth" in g/cm^2.

To calculate scale growth rates, the mass of deposited gypsum per unit area was plotted versus time. A "specific growth rate" was thus defined. A typical specific growth versus time graph is shown in Figure 10. An induction period was always seen, after which the plots were linear. The slope of the line was the specific scale growth rate, and was determined using linear regression. For a sample calculation of specific growth rate, see Appendix B.2.

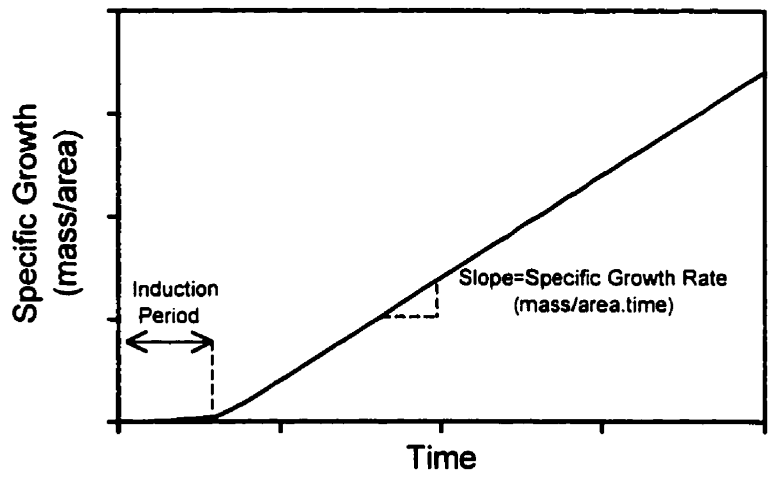

Figure 10: Specific growth vs time graph.

3.5.1 Effect of pH

pH was varied by changing the concentration of the base in the base slurry. In the calcium carbonate partial neutralization experiments, calcium carbonate slurry concentrations of 30g/L and 60g/L were used, (which were different from the original experiment which used a slurry concentration of 45g/L). These concentrations represented approximately 0.98 and 1.96 times the stoichiometric amount of calcium carbonate that would completely consume the 30g/L of sulphuric acid. The temperature and residence time were held steady at 70°C and 30min respectively.

In the calcium oxide total neutralization experiments without magnesium sulphate, calcium oxide slurry concentrations of 5.8g/L and 7.125g/L were used, (which were different from the original experiment, which used a slurry concentration of 6.5g/L). In the experiments with magnesium sulphate, slurry concentrations of 6.5g/L and 26g/L were used. The reason that these latter two were different was that calcium oxide was partially consumed by magnesium to form magnesium oxide. All four of these slurry concentrations were determined by running several experiments (without scale sample rods) using increasing amounts of calcium oxide until a range of steady state pH's was determined. The extremes of this range were chosen for investigation. Finally, the temperature and residence time were held steady at 40°C and 30min respectively.

pH was measured to one decimal place using an Accumet® 925 pH/ion Meter. Samples were collected from the outlet of the reactor every hour for testing, and an average was calculated at the end of the experiment.

3.5.2 Effect of Temperature

Temperature was varied by changing the setting on the hot plate. At first, this involved trial and error, but then the hot plate setting was calibrated for a given set of conditions. In the calcium carbonate partial neutralization experiments, temperatures of 50°C and 90°C were used, (which were different from the original experiment which used a temperature of 70°C). The calcium carbonate slurry concentration was 45g/L to produce approximately the same pH of 5.8-6.3. The residence time was held steady at 30min in all four experiments.

In the calcium oxide total neutralization experiments temperatures of 24°C and 60°C were used, (which were different from the original experiment which used a temperature of 40°C). The calcium oxide slurry concentration was 6.5g/L, to produce approximately the same pH of 10.3-11.0 in the two experiments without magnesium sulphate. With magnesium sulphate, the concentration was 8.55g/L to produce a pH in the range of 9.3-10.0. The residence time was held steady at 30min in all four experiments.

Steady state temperature in the reactor was measured every hour using a standard mercury thermometer with an accuracy of ± 0.2°C.

3.5.3 Effect of Residence Time

Residence times were varied from the standard 30min ± 0.5min by changing the flow rates of the acid and base feeds. To produce a residence time of 15min ± 0.5min, the

flow rates of the acid and base were 14mL/min each. To produce a residence time of 50min ± 0.5min, the acid feed was 4.2mL/min and the base feed was 4.3mL/min. These last two were not identical but were as close as possible to produce a residence time of 50min. (i.e. The pumps only pump to the nearest 0.1mL/min.)

3.5.4 Effect of Metal Sulphates

All of the experiments in sections 3.5.1-3.5.3 were performed both in the absence and presence of metal sulphates. In the calcium carbonate partial neutralization reactor experiments, 5g/L of nickel (as nickel sulphate), 2g/L of aluminum (as aluminum sulphate), and 1g/L of iron (III) (as ferric sulphate) were dissolved in the 30g/L sulphuric acid feed tank. In the calcium oxide total neutralization reactor experiments, 10g/L of magnesium (as magnesium sulphate) was dissolved in the 10g/L sulphuric acid feed tank. These concentrations were suggested by Inco Technical Services Limited [13], as being representative of typical laterite leach effluent, (see section 1.2).

3.5.5 Scale Reduction

Two different methods of scale reduction were tried: addition of surfactants to the acid feed and addition of gypsum seed to the base feed. The surfactants were Dowfax 2A1 and 3B2 from Dow Chemical, and Aerosol OS from Cytec Industries Incorporated. All three surfactants were anionic, having sulphonate groups. They were chosen because

of their acid resistance. Their effect was tested at several concentrations, which included 1ppm, 10ppm, and 100ppm.

Gypsum seed was made from powdered calcium sulphate hemihydrate. It was dissolved in the base slurry tank the night before an experimental run. It would immediately reprecipitate as solid gypsum particles through the following reaction:

$$CaSO_4 \cdot 1/2\,H_2O_{(s)} \Rightarrow CaSO_{4\,(aq)} + 1/2\,H_2O_{(l)} + 3/2\,H_2O_{(l)} \Rightarrow CaSO_4 \cdot 2H_2O_{(s)} \quad (8)$$

This seed was kept suspended in solution with the slurry stirrer. Seed concentrations of 5g/L and 10g/L were tested under several different reactor conditions.

3.5.6 Chemical Analysis, Scale Characterization, and Particle Size Analysis

In order to determine the steady state calcium and metal sulphate concentrations, three samples were collected from the outlet of the reactor during the course of the run. These were filtered using Fisher P2 Filter paper, diluted, and analyzed using a Perkin Elmer Optima 3000 inductively coupled plasma – atomic emission spectroscope (ICP-AES). ICP was chosen over atomic absorption spectroscopy (AAS) because calcium is prone to ionization in the latter method, which introduces large errors into the results. An average of the three samples was used to calculate the steady state calcium concentration. To determine the saturation ratio, this was divided by the solubility of calcium in the system, which was calculated using the computer program MINTEQA2 [34]. MINTEQA2 is discussed further in Appendix C.2. For a sample calculation of saturation ratio, see Appendix B.3.

In order to characterize scale, some sample rods were selected for viewing under the scanning electron microscope (SEM). The procedure of Perdikis (1996) [3] was used. Briefly, the scaled ends of rods were inserted into a sample holder which was then filled with an epoxy – hardener mixture. This was allowed to cure for 24 hours at room temperature and then the sample was cut in half, leaving a cross section of the scaled rod. The cross section was polished with finer and finer grit grinding disks up to 800 grit, and then further polished using a 1μm aerosol diamond spray. It was sputter-coated with gold and viewed using a Hitachi S-570 scanning electron microscope. Leco Corporation provided the epoxy – hardener mixture, grinding disks and diamond spray. A gallery of these SEM pictures is presented in Appendix D.

Particle size distributions of the particles formed in the bulk solution were also measured. To accomplish this, a 30mL sample of reactor solution was collected at the outlet of the reactor. This was stirred with a glass rod and then approximately 10-15mL of each sample was poured into a Malvern Mastersizer S particle size analyzer, and the distribution was recorded. Before pouring the samples in however, the analyzer was filled with approximately 1L of a saturated calcium sulphate solution, in order to avoid gypsum particle dissolution. The results of these analyses were not used in this study but are presented in Appendix E for future study.

3.6 Sources of Error

3.6.1 Reproducibility

The reproducibility of the scale growth rate measurement technique was the first source of error. In order to determine its effect, five experiments were performed in the calcium carbonate partial neutralization reactor at a temperature of 70°C, a pH of 6.2, and a residence time of 30 min. The results are presented in Appendix C.1. The conclusion of this study is that the technique is highly reproducible. (i.e. All five specific scale growth rates were within the 95% confidence interval, were within 3% of the average, and the scatter was good.)

3.6.2 Filtering of Samples

When samples of supersaturated gypsum slurry were taken from the outlet of the reactor, they were filtered using Fisher P2 Filter paper. This is a slow filter paper, which was necessitated by the small size of the gypsum slurry particles. During filtration, gypsum may have further precipitated. Thus, the saturation ratio may have dropped somewhat. An attempt was made to extract samples directly from the reactor using a syringe with a syringe filter, but the suspension was too dense and the filters clogged up immediately.

3.6.3 Rinsing of Sample Rods

The amount and force of the rinse had an effect on the amount of loose scale that was removed. To ensure consistency, the rinse was always directed at the non-scaled half of the rod and was allowed to flow over the scaled half. Also, because gypsum is soluble in water, it was possible that some of the crystals were being dissolved by the rinse. To ensure that this was not a significant error, a test was performed in which dry scaled sample rods were weighed, rinsed, allowed to dry, and then weighed again. The results are presented in Appendix C.2. The conclusion of this study was that this error only affects the induction period, which was not specifically studied, and could therefore be ignored.

3.6.4 Specific Scale Measurement

The first error in the specific scale measurement was in the actual weighing of the samples. Gypsum scale crystals are in the form of needles. In the process of drying and weighing the sample rods, some of these needles were broken off. This resulted in a small error in scale mass, but was compensated for by the fact that every rod underwent the same procedure, and was therefore exposed to the same physical stress.

The other error in the specific scale measurement was in the calculation of surface area. Scale formed halfway down the rod, and the side that was facing the reactor flow had a slightly higher surface length due to fluid dynamics. Therefore, an average of the front and back sides was used to calculate the scale surface area.

3.6.5 Calculation of Gypsum Solubility & Saturation Ratios

As was mentioned in section 3.5.6, the computer program MINTEQA2 was used to calculate the solubility values that were used in calculating saturation ratios. The reason for this was that there were no relevant literature studies related to gypsum solubility in mixed metal sulphate solutions, (see Appendix C.3). A potential error arises from the use of MINTEQA2 because MINTEQA2 has its own database of thermodynamic constants (such as K_{SP}) that it uses to calculate equilibrium aqueous species concentrations. It also allows for input of new or different constants.

In the case of gypsum, the choice of K_{SP} has a significant effect on solubility calculations. This can in turn affect saturation ratios, sometimes by more than 50%! In order to ensure that the K_{SP} values used in this study would produce accurate solubility results, K_{SP} values from different literature studies were used in MINTEQA2 to calculate total calcium solubility in a saturated gypsum solution. The results were compared with experimentally determined solubilities from several researchers. This comparison can be found in Appendix C.3. Based on this comparison, the K_{SP} values of Langmuir & Melchior (1985) [35] were chosen because they predicted the experimental solubility results to within 2%.

4. Results & Discussion

4.1 Calcium Carbonate Partial Neutralization Reactor

Scale growth was observed to occur in this reactor under all conditions after an induction period that was generally two to six hours long, depending on the scale growth rate. Usually, the higher the rate, the shorter the induction period. During the induction period, heterogeneous nucleation of gypsum seed was probably occurring on the 316SS rods. This resulted in a thin layer of gypsum covering the surface of the rods. Once this surface layer was formed, secondary nucleation and scale growth would begin to occur on top of it. Scale growth was in the form of gypsum needles that grew straight outward (or on a slight angle), from the surface layer. A single gypsum needle is shown growing outward from a typical surface layer in Figure 11 below.

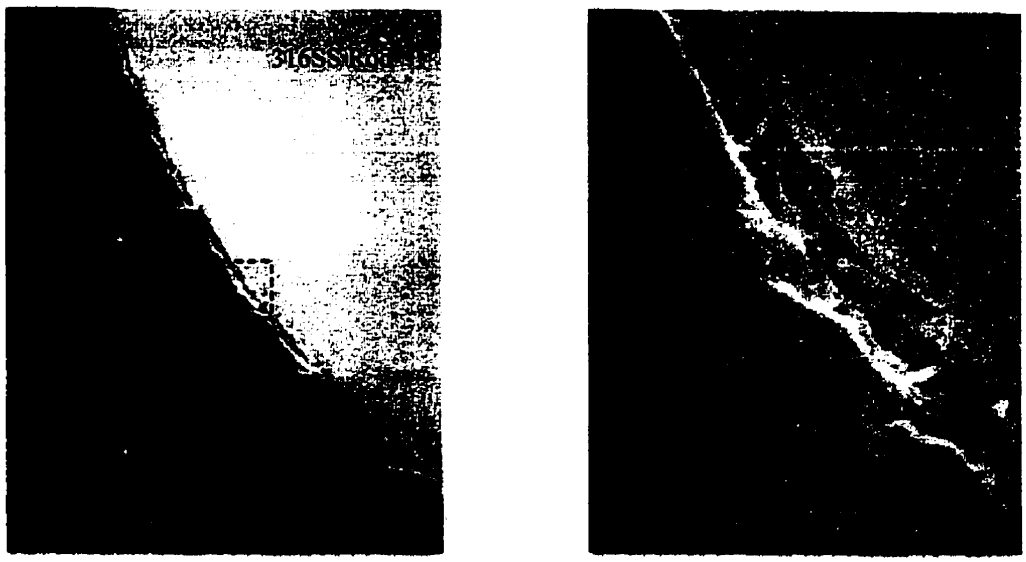

Figure 11: SEM cross-section of a scale growth rod at the end of the induction period. The picture on the right is an enlargement of the area enclosed by the dashed line at left.

Reactor conditions: 70°C, residence time = 30min, pH = 6.2, no metal sulphates in the acid feed.

The enlargement of the surface layer in Figure 11 shows the surface layer to be porous. This further indicates that heterogeneous nucleation was occurring and that the resulting nuclei were growing together in a somewhat non-uniform manner.

After several hours of scale growth, a typical rod was covered in growing gypsum needles. One example is shown in Figure 12. In this picture, the unattached gypsum needles were broken off from the surface layer during SEM sample preparation. This was a common problem during sample preparation, because the needles were quite fragile and fairly loosely attached. It is only on the macroscopic scale, when they are combined with millions of other needles, that they become a problem as gypsum scale. This should be taken into account whenever pictures of scale growth are shown.

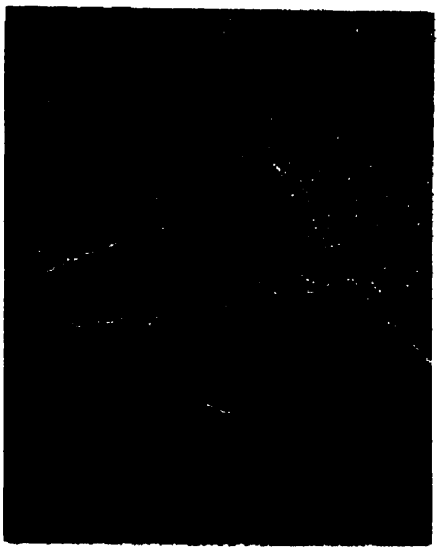

Figure 12: SEM cross-section of a scale growth rod 8h after the end of the induction period. Reactor conditions: 70°C, residence time = 30min, pH = 6.2, no metal sulphates in the acid feed.

At the end of the induction period linear growth (with time) of gypsum scale was observed. R^2 values calculated by linear regression on the growth portion of the curves, were always greater than 0.98.

One other point that should be mentioned was the effect of agitation speed on the growing gypsum scale needles. An agitation speed of 850rpm was chosen for all experiments to minimize splashing while ensuring 100% slurry suspension, (see section 3.5). However, it was noticed that gypsum scale needles initially grew on the rods parallel to the direction of flow in the reactor caused by the rotating magnetic stir bar. The side of the rods that was being directly hit by the flow generally had fewer and smaller needles than the back side during the early stages of an experimental run. An exaggerated diagram of this phenomenon is shown in Figure 13.

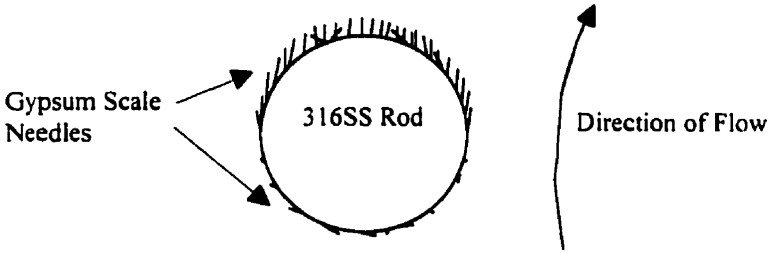

Figure 13: Effect of agitation on gypsum scale needle growth. (Diagram is not to scale.)

Also, it is known that agitation speed can affect crystal growth either through mechanical shear, or through increased mass transport [14]. In order to determine the effect of agitation in this reactor, experiments were performed at three different agitation speeds: 700rpm, 850rpm, and 1000rpm. The results are shown in Figure 14.

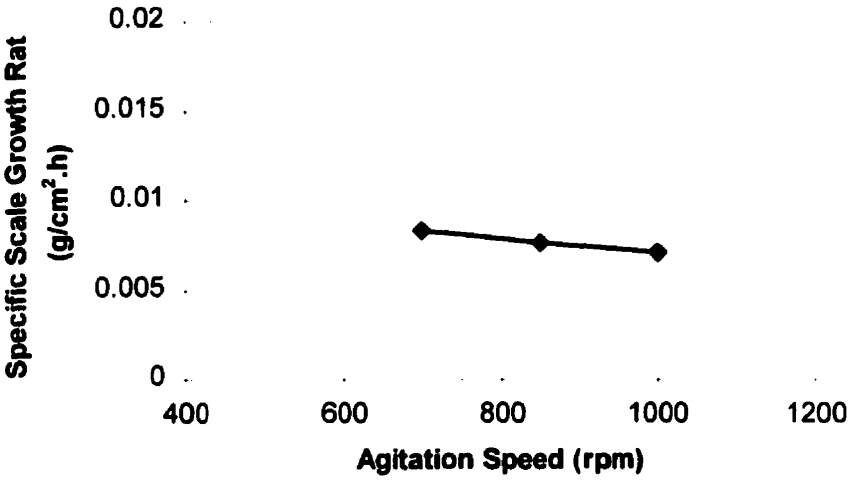

Figure 14: Effect of agitation on the specific scale growth rate in the calcium carbonate partial neutralization reactor.

Reactor conditions: Temperature=70°C, residence time=30min, pH=6.2, no metal sulphates in the acid feed.

As can be seen, increasing the agitation speed decreases the scale growth rate by 13% between 700 and 1000 rpm. If the effect of agitation is increased mass transport, one would expect to see an increase in scale growth rate when the agitation speed is increased. Therefore agitation speed seems to affect scale growth in a purely mechanical way. The increased shear probably breaks the larger fragile gypsum needles off.

The fact that gypsum needles grow away from the direction of flow, (as seen in Figure 13), also indicates that agitation speed does not have a mass transport effect. If a higher speed was increasing the transport of growth units to the scale crystals, one would expect to see the needles growing straight *into* the direction of flow.

Therefore, this is a type of mechanical effect that depends on reactor design. As long as it remains constant, the effect will be similar under all other reactor conditions. Thus, the constant agitation speed of 850 rpm that was used for all experiments ensured that hydrodynamics were the same for all experiments. Thus, agitation speed need not be considered a factor in this study.

4.1.1 Effect of pH

Figure 15 shows the specific gypsum scale growth rates at different pH values, in the calcium carbonate partial neutralization reactor, (represented by the solid lines). The graph also shows the corresponding saturation ratio versus pH data, (represented by the dashed lines). It also compares the system with no metal sulphates in the 30g/L sulphuric acid feed, to the system with metal sulphates (5g/L nickel, 2g/L aluminum, and 1g/L iron (III)) in the 30g/L sulphuric acid feed. For each of these experiments, the temperature was held constant at 70°C, and the residence time was 30min.

As can be seen, there was only a slight increase in the rate of specific gypsum scale formation over the range of pH that was studied. This was the case for the system where no metal sulphates were present in the acid feed, as well as the system where they were. The reason can be seen in the saturation ratios. They showed only a slight increase from low to higher pH. This was due to the fact that calcium solubility, (which is plotted for these systems in Figure 16), is fairly constant between pH=2.2 and pH=7. Thus, with temperature and saturation ratio essentially constant, the rate of gypsum scale formation

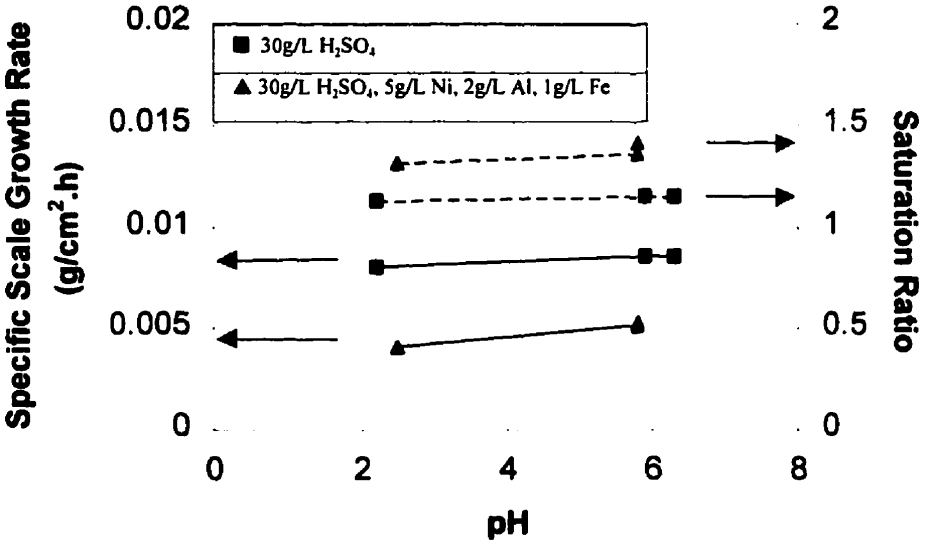

Figure 15: Specific gypsum scale growth rate and saturation ratio vs pH for the calcium carbonate partial neutralization reactor. The legend denotes the concentration of the inlet acid feed.

Reactor conditions: 70°C, residence time = 30min

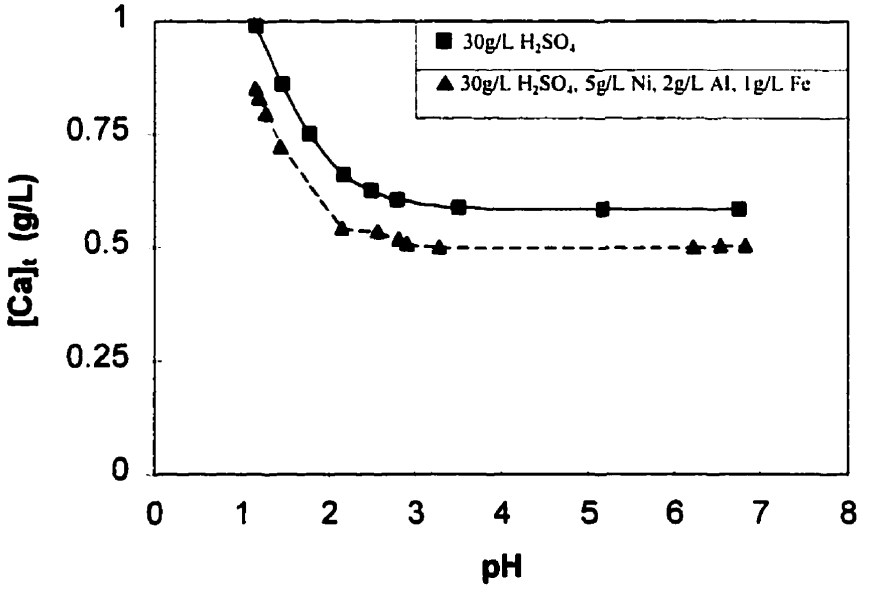

Figure 16: Total calcium solubility in a saturated gypsum solution vs pH at 70°C for the two systems studied. (Calculated using MINTEQA2 [34].) The legend denotes the concentration of the inlet acid feed.

did not vary with pH. Therefore, pH can be ignored as a factor in gypsum scale growth in the calcium carbonate neutralization reactor.

This is one of the reasons that gypsum scale is such an insidious form of fouling. It can not be avoided simply by altering the pH of a system.

The other interesting feature of the specific gypsum scale growth versus pH plots is the difference between the two systems studied. The system with no metal sulphates present in the acid feed had higher specific scale growth rates than the system with metal sulphates, despite having lower saturation ratios. This will be explained in section 4.1.4.

4.1.2 Effect of Temperature

Figure 17 shows the specific growth rate of gypsum scale at three different temperatures, in the calcium carbonate partial neutralization reactor. As can be seen, in both systems there was an increase in specific scale growth rate from 50 to 70°C, followed by a decrease in specific scale growth rate from 70 to 90°C. This strange trend can be explained by two offsetting factors. The first is the inverse solubility of calcium (in saturated gypsum solution), with temperature. As can be seen in Figure 18, above approximately 45°C gypsum solubility decreases with increasing temperature. This would primarily affect the saturation ratio and cause it to increase, which would in turn cause an increase in scale growth rate, (which is seen in the system with metal sulphates in the acid feed).

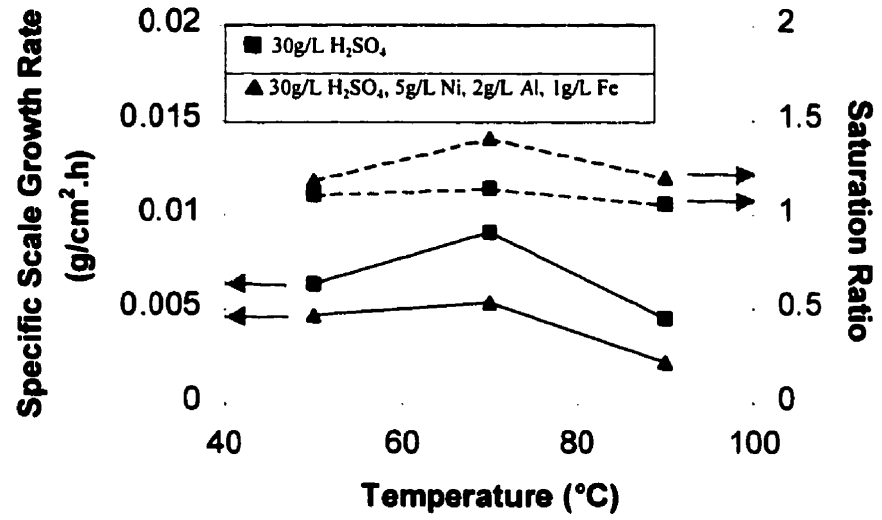

Figure 17: Specific gypsum scale growth rate and saturation ratio vs temperature for the calcium carbonate partial neutralization reactor.

Reactor conditions: pH≈5.8-6.3, residence time = 30min

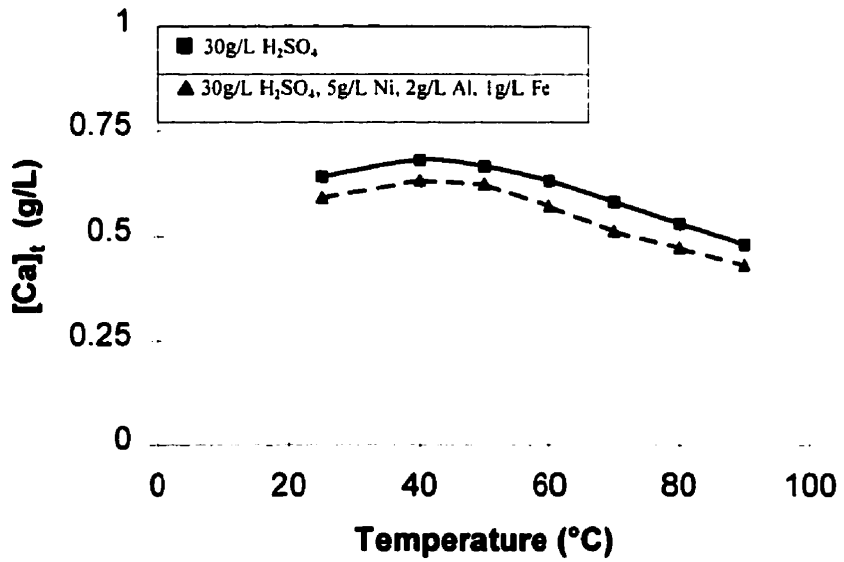

Figure 18: Total calcium solubility in a saturated gypsum solution vs temperature graph for the two systems studied. (Calculated using MINTEQ [34].)

Offsetting this solubility effect, is the kinetics of the neutralization reaction. It was shown by Barton and Vatanatham (1976) [36], that the kinetics of this reaction progressively increase with increasing temperature. This means that the subsequent gypsum precipitation in the bulk solution proceeds faster as temperature increases. Indeed, Smith and Sweet (1971) [37] found that gypsum precipitation in bulk solution was "too rapid" to study at 90°C.

It is also possible that more growth is occurring on free gypsum particles in the bulk solution (as opposed to the fixed scale particles) at 90°C. Recall from section 2.4.1 that increases in temperature result in increases in crystal growth rates through enhanced diffusion, dehydration, and integration of growth units. The greater contact with the reactor solution that the bulk solution particles are subject to, could further enhance these effects.

In order to better determine the exact effect of temperature on scale growth rates, more experiments would have to be done. The purpose would be to find out how the coefficients in equations 6 and 7 in section 2.3.1 are affected by temperature, and by how much.

Finally, the other feature of the specific gypsum scale growth versus temperature plots is the difference between the two systems studied. The system with no metal sulphates present in the acid feed has higher specific scale growth rates than the system with metal sulphates present in the acid feed, despite having lower saturation ratios. This will be explained in section 4.1.4.

4.1.3 Effect of Residence Time

Figure 19 shows the specific growth rate of gypsum scale at three different residence times, in the calcium carbonate partial neutralization reactor. A trend can be seen in the three data points for each system. At the shortest residence time, (15min), the scale growth rate was the highest. As the residence time was increased, the scale growth rate decreased. This corresponded with a similar decrease in saturation ratio as residence time was increased.

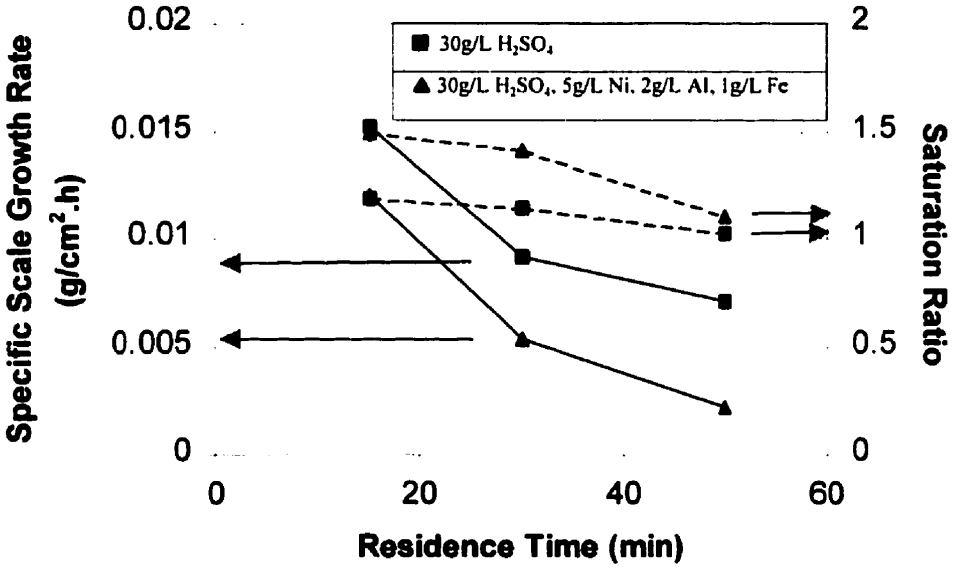

Figure 19: Specific gypsum scale growth rate and saturation ratio vs residence time for the calcium carbonate partial neutralization reactor.

Reactor Conditions: 70°C, pH≈5.7-6.3

The reason is that with a long residence time, the solution has longer to reach equilibrium. There is more time for bulk solution particles to nucleate and grow, and thus more surface area in the bulk solution on top of which new gypsum can precipitate. The result is that growth is spread out over a larger surface area, and therefore a lower specific scale growth rate.

It should be noted that it is not clear whether increasing the residence time beyond 50min would continue to produce a reduction in scale growth rate. However it is logical that a further increase in residence time would lower the saturation ratio to the point where the saturation ratio would be equal to 1 (or close enough to it), and no more gypsum would precipitate. It was not possible to test this hypothesis however because of the small size of the reactor and the nature of the slurry pump, (which could not pump the calcium carbonate slurry slower than 4ml/min.)

Another interesting feature of the specific scale growth rate versus residence time graph was the increase in saturation ratio along with the increase in growth rate. Between a residence time of 50min and 30min, a small increase in saturation ratio (<5%), resulted in a large increase in specific scale growth rate (>25%) for both reactors. However between a residence time of 30min and 15min, an even smaller increase in saturation ratio (<1%), resulted in an even larger increase in growth rate (>100%) for both reactors. This means that gypsum scale growth rate has a greater dependence on saturation ratio at a short residence time, than at the longer residence times.

This would seem to indicate that the exponent on the saturation ratio or the supersaturation ratio in equation (7) changes from one residence time to another. Such a difference in the exponent would seem to indicate a change in the scale growth

mechanism from one set of conditions to another. Actually determining the different scale growth mechanisms accurately would require more experimental data. However, looking at the morphology of the scale crystals at different residence times might offer a clue as to the mechanism(s).

Figure 20 shows SEM cross-sections of scale growth at residence times of 50min, 30min and 15min. At 50min the gypsum needles were smooth and well defined. At this stage, (2h after the end of the induction period), they were still rather small and squat, but were beginning to show signs of developing into well-formed gypsum crystals. They were also evenly spaced, and fragile on a microscopic scale. Therefore, because the saturation ratio was also low, this indicates that the growth mechanism was either screw dislocation, or possibly mononuclear growth [14].

At a residence time of 30min the scale crystals had a different shape: they were now long, thin and straight. The fact that they were slanted up toward the left-hand side was caused by the agitation of the bulk solution, and was therefore a hydrodynamic effect. This was discussed in section 5.1. The length of these needles indicates that the top [111] crystal face was growing faster than the sides. Thus, the faces with the lower nucleation rates (the sides) dictated the crystal shape. This type of morphology is indicative of mononuclear growth [14].

At a residence time of 15min the scale crystals again had a different shape: they were now longer, thinner (almost pointy), and dendritic. The scale was also thick and densely packed. This appears to be diffusion-controlled growth morphology [14], although this is by no means certain. The relatively low specific scale growth rate would make diffusion-controlled growth seem unlikely.

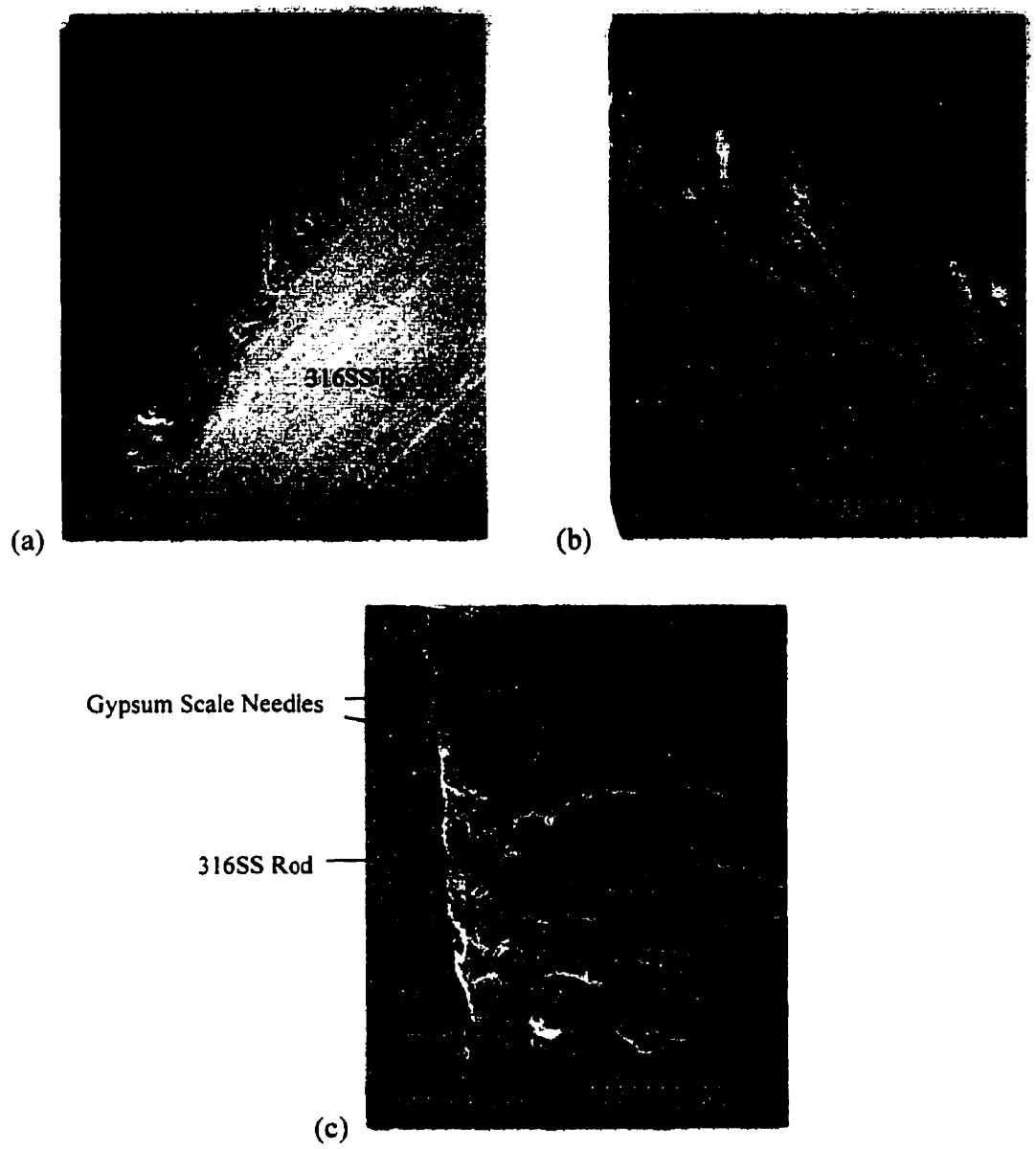

Figure 20: SEM cross-section of scale growth at residence times of: (a) 50min, (b) 30min, (c) 15min, after 8h in the reactor.

Reactor conditions: 70°C, pH = 6.0, 5.8, 5.7 (respectively), with metal sulphates in the acid feed.

Therefore, under three different sets of conditions, two or possibly three different scale morphologies were produced. This would not seem odd if not for the fact that the saturation ratios were so low. In fact, they were less than 1.5 in every case. According to

Dirksen and Ring (1991) [14], screw dislocation growth usually occurs below a saturation ratio of 1.5, mononuclear and polynuclear growth occur at higher saturation ratios, and diffusion-controlled growth occurs at the highest saturation ratios. In these experiments, the saturation ratios were all low, and the difference between them was very small. This could mean that the above crystal growth mechanisms occur at lower saturation ratios in the present system where the crystals are fixed to a surface as scale and are therefore not free floating in the bulk solution. Or this could even mean that the measured saturation ratios were lower than the actual saturation ratios, because of the slow filtration of the reactor solution in the sampling procedure. This was mentioned as a possible source of error in section 3.6.2.

The final consistent feature of the specific gypsum scale growth versus residence time is the difference between the two systems studied. The system with no metal sulphates present in the acid feed once again had higher specific scale growth rates than the system with metal sulphates present in the acid feed, despite having lower saturation ratios. This will be explained in the next section.

4.1.4 Effect of Metal Sulphates

One of the most curious aspects of the experimental results for the calcium carbonate neutralization reactor was the effect of the metal sulphates Fe (III), Al (III), and Ni (II) on scale growth. As has been mentioned in the previous three sections, scale growth rates were systematically lower when metal sulphates were present in the acid feed, than in their absence. This was occurring despite the fact that the saturation ratios

were significantly higher. The reason for the increase in the saturation ratios was that gypsum solubility was lower due to the common ion effect. The extra sulphate in the system naturally reduced the solubility of the calcium in the system. But this increase in saturation ratios should have increased scale growth rates too. Thus, one or more of the metal sulphates must have been inhibiting scale growth.

It is already known from literature that some metals inhibit crystal growth, possibly by preferentially adsorbing onto growth sites [13],[22],[38]. Gypsum crystallization has been shown to be inhibited by magnesium, cadmium, lead, and ferrous ions [38]. Iron, aluminum, and nickel, like calcium, are all positively charged and have a hydration number of six [39]. Also, none of them are larger than calcium in ionic form: the radius of Ca^{2+}=0.094nm, while Fe^{3+}=0.064nm, Al^{3+}=0.051nm and Ni^{2+}=0.069nm. Therefore it seemed likely that one or all of iron, aluminum, and nickel were adsorbing onto growth sites and inhibiting scale growth.

However, because this was a neutralization reactor, the steady state pH was above 5.5 in all but the 'Effect of pH' experiments. This meant that iron and aluminum, which precipitate as hydroxides at pH≈2.5 and 4 respectively, were not present in ionic form in the bulk solution at steady state. Of course, they could have been precipitating on the gypsum scale and thus inhibiting scale growth. But recall from section 4.1.1 that even at a steady state pH of 2.2, the inhibition in the metal sulphate system was approximately the same. Thus it seemed unlikely that either of iron or aluminum could have been inhibiting scale growth. This left nickel.

An experiment was performed with the same initial concentrations of iron and aluminum in the acid feed, but with no nickel. The results are shown in Figure 21.

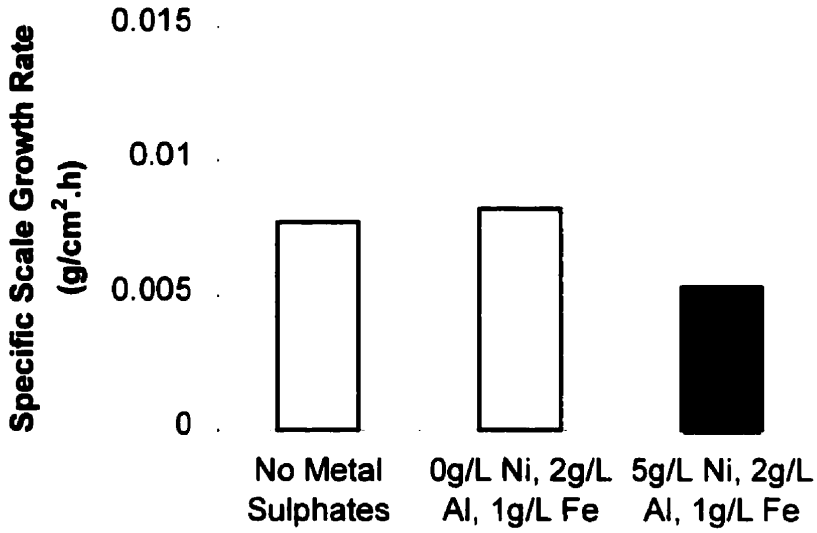

Figure 21: Effect of nickel sulphate on the specific gypsum scale growth rate for the calcium carbonate partial neutralization reactor.

Reactor Conditions: 70°C, pH≈5.7-6.2, residence time=30min

The system with no nickel in the acid feed had statistically the same scale growth rate as the system with no metal sulphates at all. Thus, nickel ions must inhibit scale growth (by 33%) under these conditions. Whether nickel simply blocks the growth sites, or actually is adsorbed and incorporated into the gypsum crystal lattice, is not known.

Of course, these results do not mean that adding more and more nickel sulphate to the acid feed would continue to reduce scale growth rates. Eventually, the common ion effect would increase the saturation ratios high enough that the effect of nickel would be cancelled, and scale growth rates would actually start to increase. More experiments would be needed to determine when this would occur however.

4.1.5 Scale Reduction

Since the addition of nickel is not a practical method of scale reduction, (because nickel is an environmental toxin as well as a valuable product), the use of additives was tried. The first types of additives were anionic surfactants, which have been shown to be effective in reducing gypsum scale, (see section 2.4.4). The other type of additive was gypsum seed. The latter worked better and more consistently than the former.

Three surfactants were tried in an attempt to reduce scale. These were Dowfax 2A1 and 3B2, made by Dow Chemical, and Aerosol OS, made by Cytec. The results of these experiments are shown in Figure 22, Figure 23, and Figure 24.

It is clear from these figures that surfactants only seemed to work when there were no metal sulphates present in the acid feed. They inhibit crystal growth by inhibiting growth of the top [111] crystal face, forming short, stumpy, plate-like scale crystals. (See Figure 26 at the end of this section for an SEM cross-section.) However in these systems, 50% reductions in scale growth rates were only achieved when concentrations of 100ppm were used. This is an unacceptably high concentration. In an industrial process, the continuous addition of surfactants at a concentration of 100ppm would be prohibitively expensive, as well as environmentally unfriendly. Especially for such a small decrease in scale growth rates.

In the systems where metal sulphates were present in the acid feed, there was either no benefit in adding surfactants, (as was the case for Dowfax 2A1 and 3B2), or there was even an increase in scale growth rate, (as was the case for the Aerosol OS surfactant). The first case is easily explained. It is hypothesized that surfactants work by

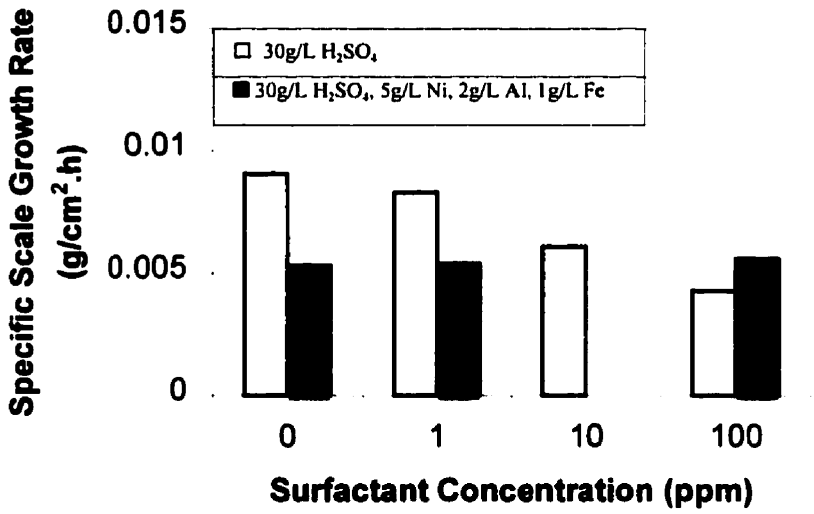

Figure 22: Effect of Dowfax 2A1 surfactant on the specific gypsum scale growth rate during calcium carbonate partial neutralization.

Reactor Conditions: 70°C, pH≈5.5-6.2, residence time=30min

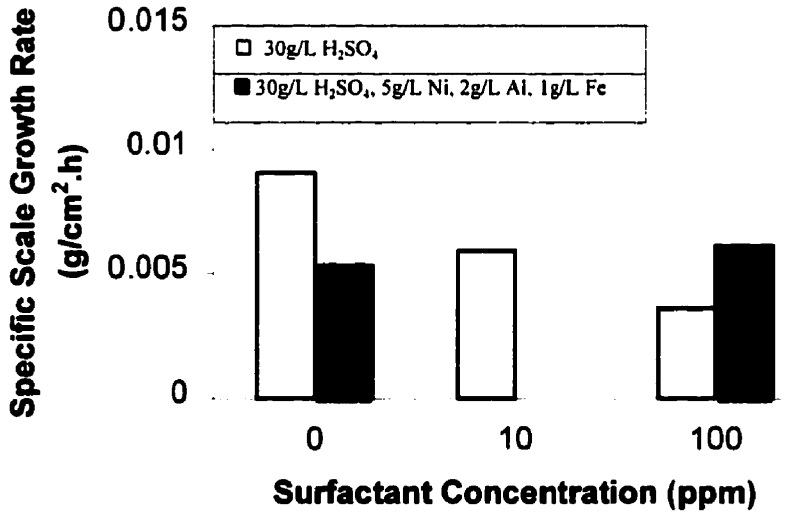

Figure 23: Effect of Dowfax 3B2 surfactant on the specific gypsum scale growth rate during calcium carbonate partial neutralization.

Reactor Conditions: 70°C, pH≈5.4-6.2, residence time=30min

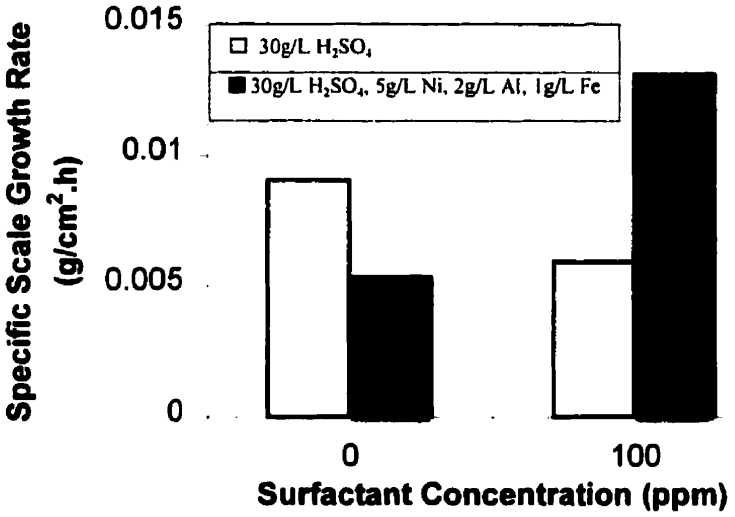

Figure 24: Effect of Aerosol OS surfactant on the specific gypsum scale growth rate during calcium carbonate partial neutralization.

Reactor Conditions: 70°C, pH≈5.4-6.2, residence time=30min

physically blocking surface growth sites. In this study, it was also hypothesized that nickel was blocking surface growth sites. Thus, if nickel was already blocking the surface growth sites, the surfactants may not have been able to provide any additional reduction. Or they could have been poisoned by nickel, or adsorbed by the precipitating iron and aluminum, so that they were made ineffective.

In the case of the OS Aerosol surfactant, the scale growth rate was actually higher in the presence of the surfactant. In fact, it was actually 50% higher than the system with no metal sulphates and no surfactants in the acid feed! There is no easy explanation for this. It would seem that the surfactant was actually facilitating gypsum scale growth, and yet it inhibited it in the system with no metal sulphates. Perhaps it reacted with nickel

and formed a scale growth-enhancing surfactant complex. More tests would have to be done, to determine what was actually happening.

Figure 25 shows the effect of adding gypsum seed to the base slurry. The clear bars represent the system with no metal sulphates in the acid feed, and the solid bars represent the system with metal sulphates present in the acid feed. Reductions in scale growth rates of 71% and 60% were achieved in the systems without metal sulphates in the acid feed, and with metal sulphates in the acid feed, respectively, when a seed concentration of 10g/L was used. It did this by providing a surface on which gypsum could precipitate, other than the scale growth rods.

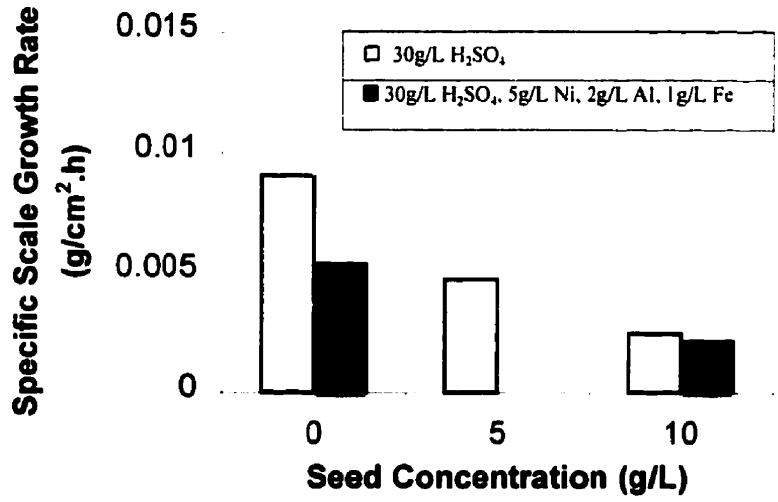

Figure 25: Effect of gypsum seed on the specific gypsum scale growth rate during calcium carbonate partial neutralization.

Reactor Conditions: 70°C, pH≈6.0-6.4, residence time=30min

It should also be remembered from section 3.5.5 that this was artificial gypsum seed made from powdered hemihydrate. It would be more economical and probably

more effective to recycle seed from the outlet of the reactor. In this case, there would be an unlimited supply of aged particles to use that would already be acclimatized to the reactor environment. Thus, they would be able to begin incorporating new gypsum immediately.

Figure 26(a) shows SEM cross-sections of gypsum scale grown in the presence of 100ppm Dowfax 2A1 surfactant. Figure 26(b) shows gypsum scale grown in the presence of 10g/L artificial gypsum seed. These were the two most successful examples of scale reduction. The surfactant has inhibited the growth of the top [111] crystal face, while the seed has simply provided an alternate surface for gypsum to precipitate. This reduced the amount of total scale and resulted in smaller, more scattered gypsum scale needles.

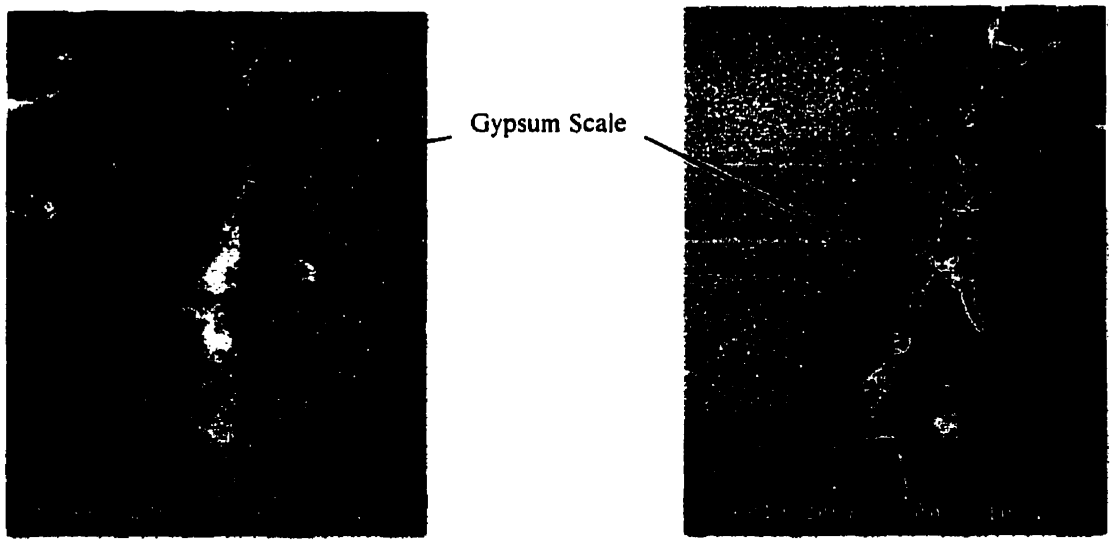

Figure 26: Effect of 100ppm Dowfax 2A1 Surfactant (a), and 10g/L Artificial Gypsum Seed (b) on gypsum scale morphology

Reactor conditions: 70°C, pH = 5.5, 6.4 (respectively), no metal sulphates in the acid feed.

4.2 Calcium Oxide Total Neutralization Reactor

Like the calcium carbonate reactor, scale growth was observed to occur in the calcium oxide total neutralization reactor after an induction period that was generally two to six hours long. The induction period was usually (but not always) inversely proportional to the scale growth rate: the higher the growth rate, the shorter the induction period. Unlike the calcium carbonate reactor however, it was hard to tell whether heterogeneous nucleation was taking place during the induction period, or whether it was particles from the bulk solution attaching to the stainless steel rods. There was not always a clearly defined surface layer with gypsum needles growing outward from it.

The scale itself was similarly ambiguous. An example is shown in Figure 27.

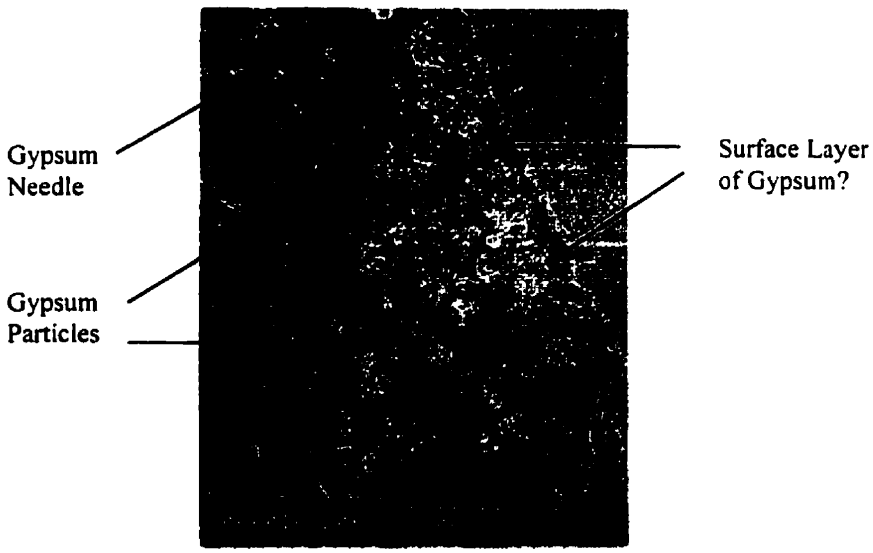

Figure 27: SEM cross-section of a scale growth rod after 8h in the reactor.

Reactor conditions: 40°C, residence time=30min, pH=11.0, no magnesium sulphate in the acid feed.

It was made up of a combination of growing gypsum needles, and what appeared to be agglomerated reactor particles. It was therefore hard to distinguish differences in morphology, in all but the most extreme examples. Also, although these particles seem to be spaced well apart in the photo, they actually formed a solid, cohesive layer of scale.

Linear growth of gypsum scale during the growth period was again observed. R^2 values calculated by linear regression on the growth portions of these curves, were always greater than 0.98.

4.2.1 Effect of pH

Figure 28 shows the specific gypsum scale growth rates at different pH values, in the calcium oxide total neutralization reactor, (represented by the solid lines). The graph also shows the corresponding saturation ratio versus pH data, (represented by the dashed lines). And it compares the system with no magnesium sulphate in the 10g/L sulphuric acid feed, to the system with 10g/L magnesium sulphate in the 10g/L sulphuric acid feed. For each of these experiments, the temperature was held constant at 40°C, and the residence time was 30min.

As can be seen, there was only a slight increase in the rate of specific gypsum scale formation over the range of pH that was studied for the system where no magnesium sulphate was present in the acid feed. The reason can be seen in the saturation ratios. They showed only a small increase from low to higher pH. This was due to the fact that gypsum solubility, (which is plotted for these systems in Figure 29), is

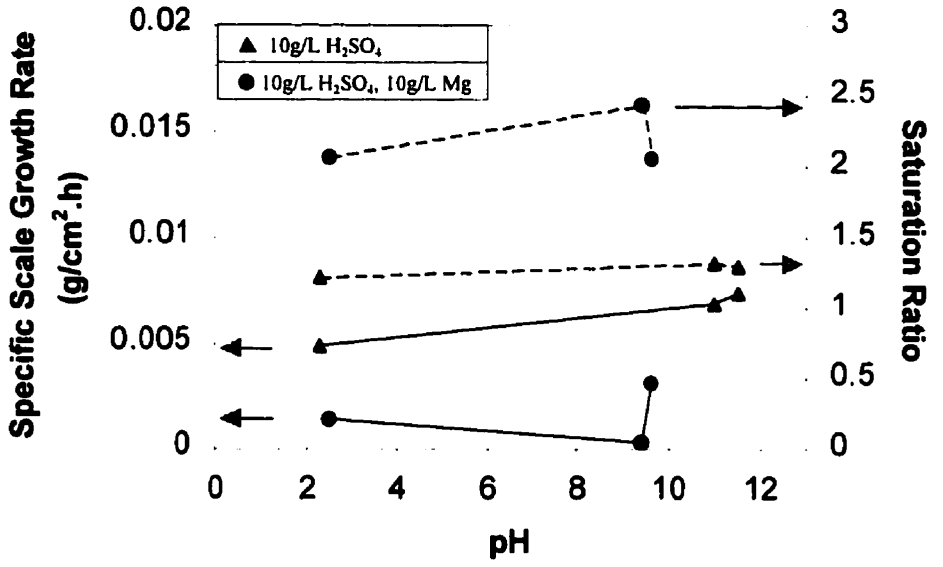

Figure 28: Specific gypsum scale growth rate and saturation ratio vs pH for the calcium oxide total neutralization reactor. The legend denotes the concentration of the inlet acid feed.

Reactor Conditions: 40°C, residence time=30min

fairly constant between pH=2.2 and pH=11. Thus, with temperature and saturation ratio essentially constant, the rate of gypsum scale formation does not vary with pH. Therefore, pH can be ignored as a factor in gypsum scale growth in the calcium oxide total neutralization reactor.

This is not the case however when magnesium is present in the acid feed, as seen in Figure 28. Ignoring for the moment the lower growth rates in this system, despite the higher saturation ratios (which will be discussed in section 4.2.4), it is clear that pH did affect scale growth in this system. At a pH of approximately 9.3, the scale growth rate was the lowest. Above and below this pH, scale growth rate increased. To make it even more puzzling, this increase corresponded with a sharp decrease in the saturation ratio.

These trends can perhaps be explained by the effect of magnesium, (which will be discussed in detail in section 4.2.4). If magnesium interferes with gypsum scale growth in the same way that nickel does, then any reactor conditions that nullify this interference would cause an increase in scale growth rate.

In these three experiments, the pH of minimum scale (pH=9.3) coincides with the onset of magnesium hydroxide precipitation. In fact, it requires a 4.5 times stoichiometric excess of calcium oxide simply to raise the pH to 9.6. Without magnesium in the acid feed, it only requires a 1.25 times excess to raise the pH to 11.3. This means that much of the magnesium in the reactor precipitates and is therefore unavailable to interfere with gypsum scale formation above a pH of 9.4. Thus, scale growth actually increases as magnesium is removed from solution.

On the other hand, the saturation ratio decreases as magnesium is consumed. The reason can be seen in Figure 29: calcium solubility increases as the common ion effect is nullified by the precipitation of sulphate (as calcium sulphate dihydrate) from magnesium sulphate. At a pH of 10.5 to 11, calcium solubility is back to normal.

Thus, one may expect the saturation ratio and scale growth rate to be equivalent to the levels in the experiments where there was no magnesium present in the acid feed, if enough calcium oxide is added to consume all of the magnesium. In Figure 28, the saturation ratio and scale growth curves do in fact seem to be converging on the saturation ratio and scale growth curves of the experiments with no magnesium sulphate in the acid feed.

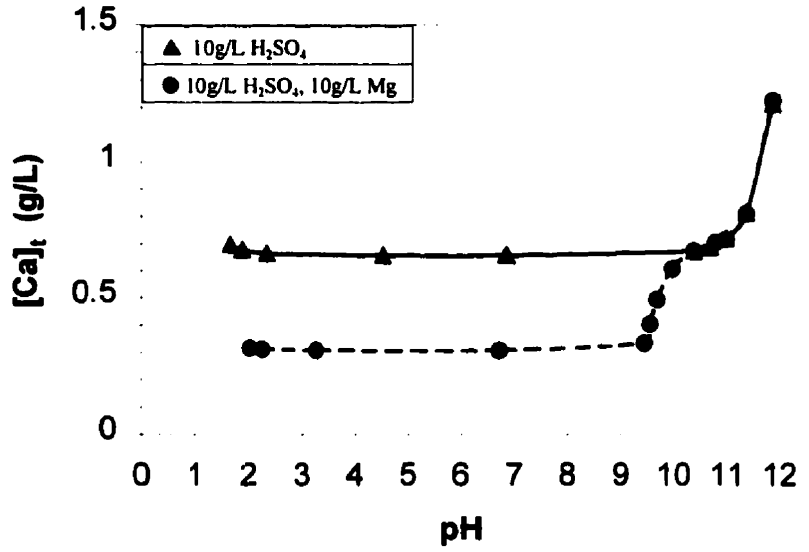

Figure 29: Calcium solubility in a saturated gypsum solution vs pH at 40°C for the two systems studied. (Calculated using MINTEQA2.)

At low pH, the scale growth rate was also higher. There is no clear explanation for this. It is possible that a buildup of positively charged H^+ ions around the gypsum scale crystals actually starts to repel or block magnesium from interfering with gypsum scale growth.

4.2.2 Effect of Temperature

Figure 30 shows the specific scale growth rate of gypsum scale at three different temperatures, in the calcium oxide total neutralization reactor. In the system with no metal sulphates present in the acid feed, there was a large (400%), continuous increase in scale growth rate between 24°C and 60°C, despite small increases in saturation ratio.

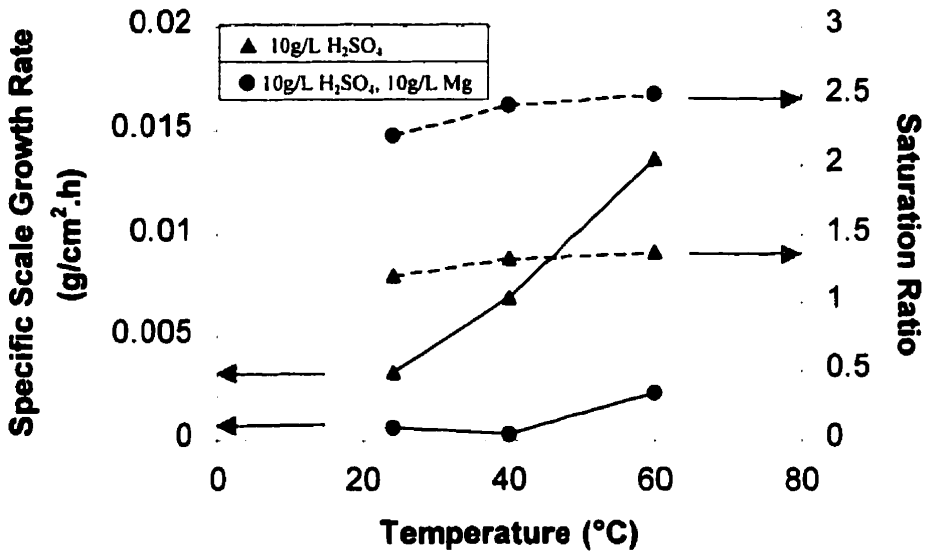

Figure 30: Specific gypsum scale growth rate and saturation ratio vs temperature for the calcium oxide total neutralization reactor.

Reactor conditions: pH≈9.3-11.0, residence time=30min

Obviously whatever mechanism is responsible for scale growth in this reactor has a dependence on saturation ratio and/or it has a dependence on temperature. This would make it similar to the calcium carbonate partial neutralization reactor. Perhaps if the temperature were increased to 90°C a similar decrease in scale growth rate would be observed. More experiments would have to be done to determine the exact dependence of scale growth rate on temperature and saturation ratio in this system.

In the system with magnesium sulphate in the acid feed, the scale growth rates were practically zero and could be considered statistically the same between 24°C and 40°C. Between 40°C and 60°C, an increase in scale growth rate was seen and it corresponded with only a small increase in saturation ratio. This is similar to the system

with no magnesium, except once again, the scale growth rates were considerably lower, (which will be explained in section 4.2.4.)

4.2.3 Effect of Residence Time

Figure 31 shows the specific gypsum scale growth rate at three different residence times.

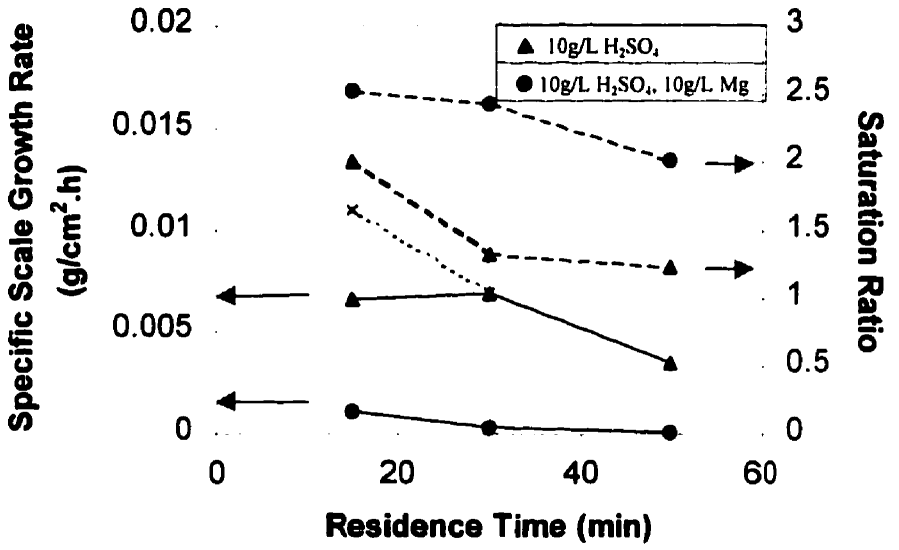

Figure 31: Specific gypsum scale growth rate and saturation ratio vs residence time for the calcium oxide total neutralization reactor.

Reactor conditions: 40°C, pH≈9.3-11.4

Generally, scale growth rate is higher at shorter residence time. In the system with no magnesium in the acid feed, there was an apparently strange result at a residence time of 15min: the scale growth rate was the same as at 30min. The reason for this was due to experimental inadequacies at short residence time.

It was observed that at 15min, scale was forming on every surface in the reactor. This included the glass walls and the Teflon stir bar. This scale was unstable and tended to flake off in large pieces. This left many large chunks of gypsum floating around inside the reactor, which were too heavy to drain out of the reactor. They were therefore acting as large seed particles that reduced the amount of scale formed on the rods. The growth rate should have been higher, and thus, a linearly extrapolated growth rate is marked with an 'x' and attached to the curve by a dashed line.

From 30min to 50min, there was a decrease in scale growth rate, which corresponded with a decrease in saturation ratio. This is the same trend that was observed in the calcium carbonate neutralization reactor, (see section 4.1.3.) However, because of the experimental inadequacy, it is not clear whether a change in the scale growth mechanism occurs between one residence time and another.

It is also hard to tell if the mechanism of scale growth changes by looking at the scale morphology. As has already been mentioned, the scale grown in this reactor seems to be a combination of growing gypsum needles and agglomerated reactor particles. The particles often obscure the needles. Figure 32 demonstrates this point by showing SEM cross-sections of scale growth magnified 300X at all three residence times.

At a residence time of 50min (Figure 32a), one long, lone gypsum needle can be seen growing outward from the stainless steel rod. The rest of the scale was made up of smaller, evenly spaced particles. The rod was completely covered in scale to the naked eye, but this photo reveals the scale to be made up of well-spaced, loosely held crystals, and therefore probably not very strong. Of the three residence times tested, 50min produces a scale morphology most beneficial from a scale abatement point of view.

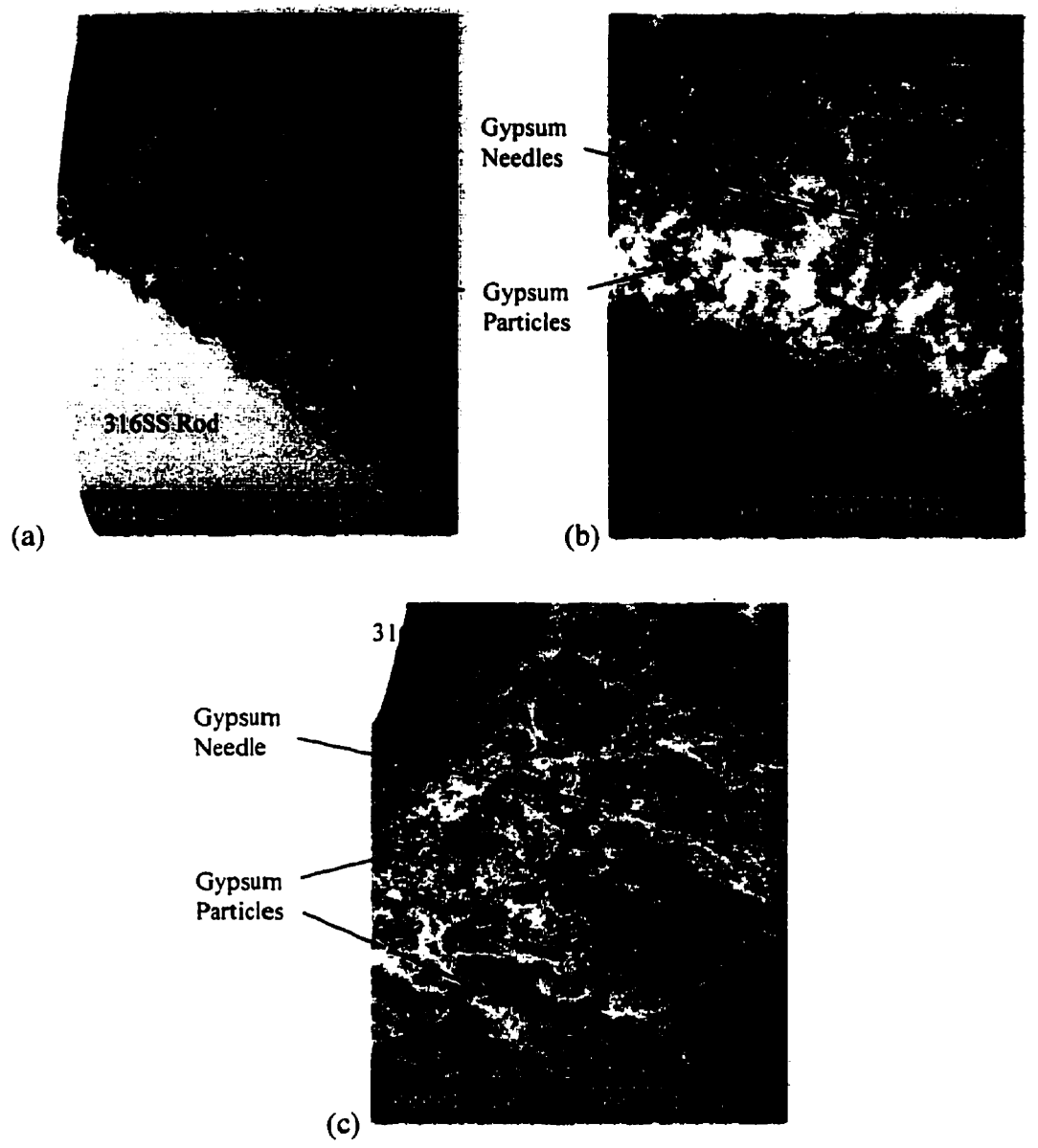

Figure 32: SEM cross-section of scale growth at residence times of: (a) 50min, (b) 30min, (c) 15min.

Reactor conditions: 40°C, pH=11.4, 11.0, 11.0 (respectively), after 8h in the reactor, with no magnesium sulphate in the acid feed.

At a residence time of 30min (Figure 32b), the scale is obscured in the photo by a dense agglomeration of particles. Several needles can be seen among them, but not

enough so that a mechanism can be deduced. All that is clear is that the scale is denser and therefore more undesirable than the scale formed at a residence time of 50min.

At a residence time of 15min (Figure 32c), the scale almost completely fills the picture. It is dense, and although porous, there are no clear spaces in between crystals. In fact, there may not even be any more individual crystals left, as the scale crystals seem to have grown together. This morphology is the least desirable of the three because it appears to be solid and crystalline. It would therefore be the hardest to remove.

In the presence of magnesium sulphate, the scale growth rates were so low that they were statistically zero, (although not actually zero). Indeed, as seen in Figure 33 at a residence time of 50min, it appears that there was no scale growth or even heterogeneous nucleation even after 8h in this reactor. This is probably due to the effect of magnesium, which will be explained in the next section. It should be noted that the bumps on the rod that can be seen in the photo are surface imperfections.

4.2.4 Effect of Magnesium Sulphate

The effect of magnesium sulphate on scale growth in the calcium oxide total neutralization reactor was similar to that of nickel in the calcium carbonate partial neutralization reactor. As has been mentioned in the previous three sections, scale growth rates were systematically lower when magnesium sulphate was present in the acid feed, than when it was absent. This was occurring despite the fact that the saturation ratios were significantly higher.

Figure 33: SEM cross-section of scale growth at a residence time of 50min.

Reactor conditions: 40°C, pH=9.6, after 8h in the reactor, with magnesium sulphate in the acid feed.

The reason for the increase in the saturation ratios is that gypsum solubility is lower due to the common ion effect. The extra sulphate in the system naturally reduces the solubility of the calcium in the system. However, this increase in saturation ratios should increase scale growth rates too. Thus, magnesium sulphate must have been inhibiting scale growth.

It is already known from literature that magnesium can inhibit gypsum crystallization by preferentially adsorbing onto growth sites [21]. Therefore it seems likely that it is absorbing onto growth sites and inhibiting scale growth, much like nickel. Also, recall from section 4.2.1 the strange pH dependence of scale growth rate in this system. This behaviour can only be explained by magnesium inhibition.

Of course, these results do not mean that adding more and more magnesium sulphate to the acid feed would continue to reduce scale growth rates. Eventually, the

common ion effect would increase the saturation ratios high enough that the effect of would be cancelled, and scale growth rates would actually start to increase.

These results are encouraging though. They show that under certain conditions, (residence time=50min, temperature=40°C, 10g/L Mg), gypsum scale growth can be inhibited to the point that it is almost zero. Perhaps the use of dolomite as the base instead of calcium carbonate and calcium oxide would have this same effect.

4.2.5 Scale Reduction

Only one anionic surfactant, (Dowfax 2A1), was tested in the total neutralization system. Gypsum seeding was only attempted once because the seed formed a solid agglomerate with the calcium oxide in the base slurry which clogged the tube in the peristaltic pump.

Figure 34 shows the results in surfactant-free experiments and experiments with 100ppm of Dowfax 2A1. The clear bars represent the system with no magnesium sulphate in the acid feed, and the solid bars represent the system with magnesium sulphate present in the acid feed.

As can be seen, the surfactant had no effect on scale growth rate, in either system at 100ppm. This is curious because anionic surfactants, (which are organic acids or organic acid salts), are thought to inhibit crystal growth by dissociating and then adsorbing onto crystal surfaces. They are therefore expected to be most effective at high pH, which favours dissociation.

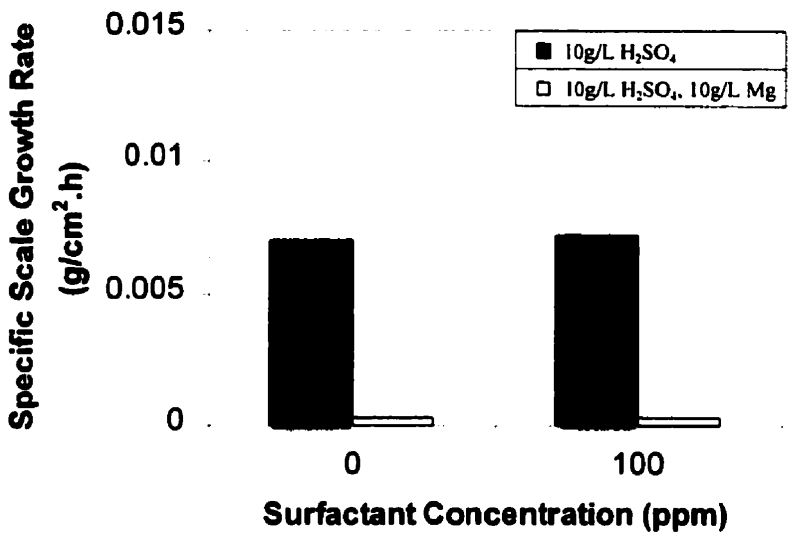

Figure 34: Effect of Dowfax 2A1 surfactant on the specific gypsum scale growth rate during calcium oxide total neutralization.

Reactor Conditions: 40°C, pH≈9.3-11.2, residence time=30min

This surfactant only seemed to be effective in the calcium carbonate system at medium pH with no metal sulphates in the acid feed. This underlines the point about the unpredictability of the effectiveness of surfactants that was discussed in section 2.4.4.

Figure 35 shows the effect of adding gypsum seed to the base slurry. Over a 50% reduction in scale growth rates was achieved when a seed concentration of 10g/L was used. It does this by providing a surface on which gypsum could precipitate, other than the scale growth rods. This is exactly the same effect as was seen in the calcium carbonate reactor.

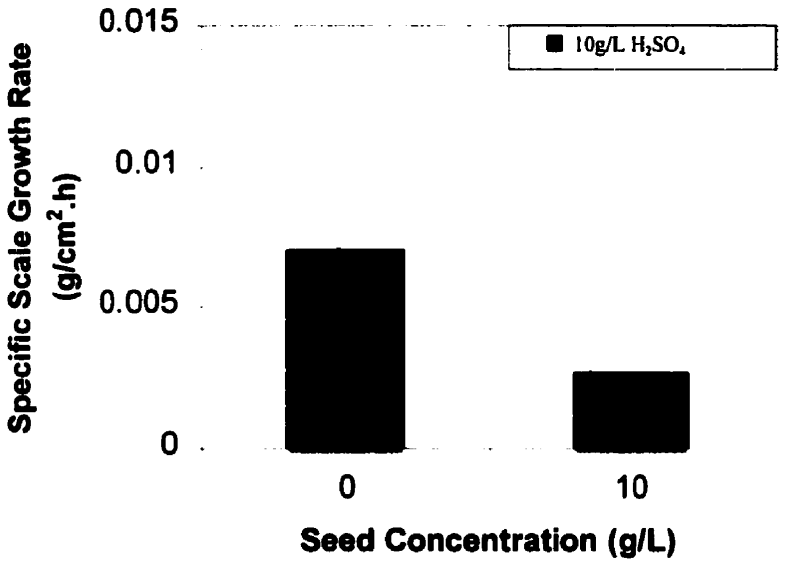

Figure 35: Effect of gypsum seed on the specific gypsum scale growth rate during calcium oxide total neutralization.

Reactor Conditions: 40°C, pH=11.0, 8.0, residence time=30min

Figure 36 shows SEM cross-sections of gypsum scale grown in the absence (a) and in the presence (b) of 10g/L artificial gypsum seed. The seed has simply provided an alternate surface for gypsum to precipitate. This reduces the amount of total scale and results in fewer agglomerated particles and no large gypsum needles.

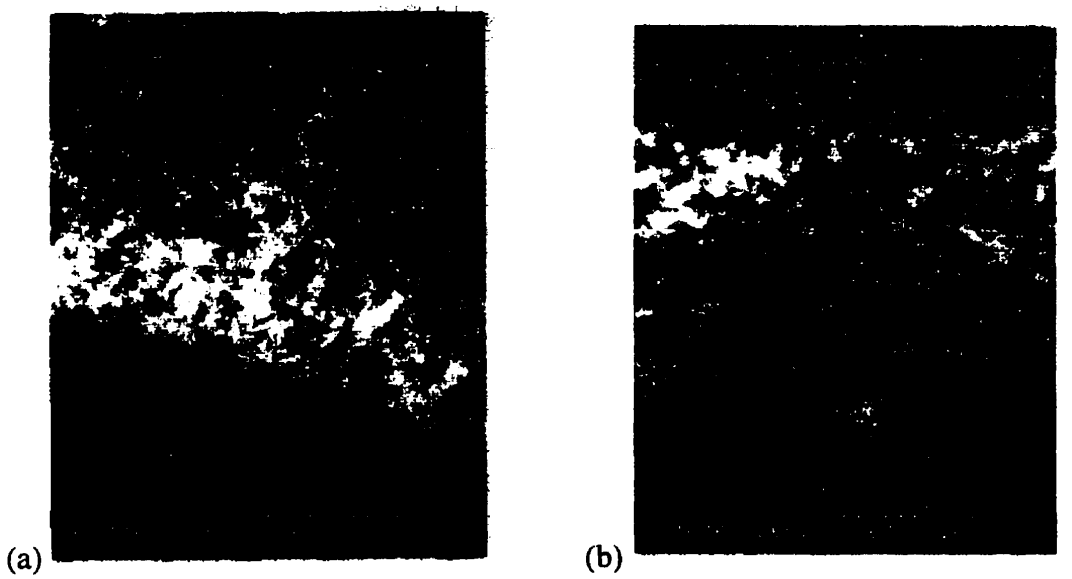

Figure 36: Effect of (a) 0g/L gypsum seed, (b) 10g/L gypsum seed on gypsum scale morphology during calcium oxide total neutralization.

Reactor Conditions: 40°C, pH=11.1, 8.0, residence time=30min, no magnesium sulphate in the acid feed

5. Conclusions

5.1 Calcium Carbonate Partial Neutralization Reactor

1.) Gypsum scale growth occurs after an induction period, during which time heterogeneous nucleation is probably taking place.

2.) Scale growth is in the form of gypsum needles growing outward from a surface layer of gypsum.

3.) Gypsum scale growth rate decreases with increasing agitation speed. This is caused by increasing mechanical shear of the gypsum scale needles at the higher speed.

4.) Gypsum scale growth rate is not significantly affected by pH. The reason is that the saturation ratio is also not significantly affected by pH, because gypsum solubility is constant above a pH of 2.2.

5.) Gypsum scale growth rate increases between a temperature of 50°C and 70°C, but decreases between 70°C and 90°C. This is caused by a similar increase and decrease in the saturation ratio. This is explained by offsetting solubility and kinetic effects.

6.) Gypsum scale growth rate decreases with increasing residence time. This is caused by decreases in the saturation ratio. However, scale growth rate has a greater dependence on changes in saturation ratio at a short residence time (15min) than at a long residence time (50min). This indicates that the scale growth mechanism is different at different residence times, (i.e. different saturation ratios).

7.) At a short residence time (15min) the scale morphology indicates a diffusion-controlled growth mechanism, while at longer residence times (i.e. 30min, 50min), the scale morphology indicates a mononuclear or screw dislocation growth mechanism.

8.) Nickel ions seem to inhibit gypsum scale growth. Scale growth rates are systematically lower in the presence of nickel, despite the fact the that saturation ratios are significantly higher. Nickel is either blocking surface growth sites, or is being preferentially adsorbed over calcium by the gypsum scale crystals.

9.) Sulphonated anionic surfactants inhibit gypsum scale growth when no metal sulphates are present in the acid feed. This inhibition is as high as 50% when the surfactant concentration is 100ppm. However, with iron, aluminum, and nickel sulphates in the acid feed there is no inhibition. In fact, in one case there is an increase in scale growth rate. It appears that the surfactants are either poisoned by metal sulphates, or that they provide no additional benefit to the nickel inhibition.

10.) Artificial gypsum seeding reduces scale growth rates by 71% at a seed concentration of 10g/L, with no metal sulphates in the acid feed. With metal sulphates in the acid feed, the scale growth rate reduction is 60%.

5.2 Calcium Oxide Total Neutralization Reactor

1.) Gypsum scale growth occurs after an induction period, during which time heterogeneous nucleation or attachment of particles from the bulk solution is probably taking place.

2.) Resulting scale growth is a combination of small agglomerated particles and growing gypsum needles.

3.) Gypsum scale growth rate is not significantly affected by pH, except when magnesium is present in the acid feed. The reason is that the saturation ratio is also not significantly affected by pH, because gypsum solubility is constant above a pH of 2.2.

4.) Gypsum scale growth rate increases between 24°C and 60°C. This is caused by small increases in the saturation ratio, and perhaps enhanced by the increase in temperature.

5.) Gypsum scale growth rate decreases with increasing residence time. This is caused by decreases in the saturation ratio. However, due to an experimental inadequacy, it is not clear whether the scale growth mechanism is different at different residence times.

6.) The scale grown at a residence time of 50min is less dense and therefore more favourable from a scale abatement point of view, than the scale grown at residence times of 30min or 15min.

7.) Magnesium ions seem to inhibit gypsum scale growth. Under some conditions, (e.g. residence time = 50min), magnesium almost completely inhibits gypsum scale growth. Like nickel, it does this by either blocking surface growth sites, or by being preferentially adsorbed over calcium by the gypsum scale crystals.

8.) Sulphonated anionic surfactants have no effect on gypsum scale growth.

9.) Artificial gypsum seeding reduces scale growth rates by over 50% at a seed concentration of 10g/L.

6. Recommendations

More experimental work could be done with the purpose of elucidating the prevailing mechanism of scale growth in all systems. This could perhaps involve the use of *in situ* crystal examination using atomic force microscopy, to study the gypsum crystal growth mechanisms on a microscopic level. Knowing the mechanism, a model could perhaps be developed to predict the conditions under which gypsum scale is most likely to form, as well as the rate at which it will grow.

Analysis of the scale formed in the presence of nickel and magnesium sulphate should also be conducted to determine if these ions are being incorporated into the crystals, or just blocking surface growth sites. EDX and XPS analysis would be best for this purpose.

The most crucial future work should be to study scale reduction through seeding or seed recycling, different surfactants, longer residence times, lower temperatures, or a combination of these. In other words, attack gypsum scale with any and all means of reduction possible. This could include the use of new scale reduction technologies such as magnetic or electric fields.

In the meantime, to reduce gypsum scale in industry, longer residence times and lower temperatures should be effective in both continuous reactors. Bases containing magnesium (such as dolomite) might also prove effective in reducing scale. Gypsum seeding using recycled seed from the outlet of the reactor is probably the best and cheapest method of scale reduction. The unpredictable nature of surfactants and the lack

of understanding of how and why they work on gypsum makes them poor choices for scale reduction at present.

7. Bibliography

[1] Hasson, D., "Precipitation Fouling", Fouling of Heat Transfer Equipment, Hemisphere Publishing Corp., Washington, D.C. (1981) 527-568

[2] Nadafi, F., "A Preliminary Literature Survey on: Mineral Scaling (Especially Gypsum) in Chemical Industries", Unpublished, Toronto (1996) 6,

[3] Perdikis, P., "Scale Formation in Batch Reactor Under Pressure Acid Leaching of a Limonitic Laterite", M.A.Sc. Thesis, Department of Chemical Engineering and Applied Chemistry, University of Toronto, (1996) 1,2,

[4] Rogers, L.A., K.Varughese, S.M.Prestwich, G.G.Wagget, M.H.Salimi, J.E.Oddo, E.Street Jr. and M.Tomson, "Use of Inhibitors for Scale Control in Brine-Producing Gas and Oil Wells", SPE Production Engineering, **5**, (1990) 77-82

[5] Amjad, Z., "Applications of Antiscalants to Control Calcium Sulfate Scaling in Reverse Osmosis Systems", Desalination, **54**, (1985) 263-276

[6] Butt, F.H., F.Rahman, and U.Baduruthamal, "Evaluationof SHMP and advanced scale inhibitors for control of CaSO4, SrSO4, and CaCO3 scales in RO desalination", Desalination, **109**, (1997) 323-332

[7] Bansal, B., H.Muller-Steinhagen, X.D.Chen, "Effect of Suspended Particles on Crystallization Fouling in Plate Heat Exchangers", Journal of Heat Transfer, **119**, (August 1997) 568-574

[8] Nulty, J.H., B.Grace and D.Cunningham, "Control of Calcium Based Scales In Australian Mineral Processing", Australian Institute of Mining and Metallurgy Publ.Sec., **2**, (1991) 185-188

[9] Hand, R.J., "Calcium sulphate hydrates: a review", British Ceramic Transactions, **96**, no.3 (1997) 116-120

[10] Ostroff, A.G., "Conversion of Gypsum to Anhydrite in Aqueous Salt Solutions", Geochimica et Cosmochimica Acta, **28**, (1964) 1363-1372

[11] Posnjak, E., "The System $CaSO_4$-H_2O", American Journal of Science, **35-A**, (1938) 247-272

[12] Personal correspondence with INCO technical services.

[13] Okita, Y., "Gypsum Scale Control in Neutralization" Unpublished Inco Memo, (1996)

[14] Dirksen, J.A. and T.A.Ring, "Fundamentals of Crystallization: Kinetic Effects on Particle Size Distributions and Morphology", Chemical Engineering Science, **46**, no.10, (1991) 2389-2427

[15] Stumm, W., Chemistry of the Solid-Water Interface, John Wiley & Sons, Inc., New York (1992) 211-241

[16] Pakter, A. "The Precipitation of Calcium Sulphate Dihydrate from Aqueous Solution", Journal of Crystal Growth, **21**, (1974)

[17] Christoffersen, M.R., J.Christoffersen, M.Weijnen, and G.Van Rosmalen "Crystal Growth of Calcium Sulphate Dihydrate at Low Supersaturation", Journal of Crystal Growth, **58**, (1982) 585-595

[18] Rubisov, D.H., and V.G.Papangelakis, "Mathematical Modelling of the Transient Behaviour of CSTRs with Reactive Particulates: Part 1 – The Population Balance Framework", Canadian Journal of Chemical Engineering, **74**, (June 1996) 353-362

[19] Tadros, M.E. and I.Mayes, "Linear Growth Rates of Calcium Sulfate Dihydrate Crystals in the Presence of Additives", Journal of Colloidal and Interface Science, **72**, no.2, (1979) 245-254

[20] Klepetsanis, P.G. and P.G.Koutsoukos, "Precipitation of Calcium Sulfate Dihydrate at Constant Calcium Activity", Journal of Crystal Growth, **98**, (1989) 480-486

[21] Hamdona, S.K., R.B.Nessim, and S.M.Hamza, "Spontaneous Precipitation of Calcium Sulphate Dihydrate in the Presence of some Metal Ions", Desalination, **94**, (1993) 69-80

[22] McCartney, E.R. and A.E.Alexander, "The Effect of Additives upon the Process of Crystallization I: Crystallization of Calcium Sulfate", Journal of Colloid Science, **13**, (1958) 383-396

[23] Öner, M., Ö.Dogan, and G. Öner, "The influence of polyelectrolytes architecture on calcium sulfate dihydrate growth retardation", Journal of Crystal Growth, **186**, (1998) 427-437

[24] Smith, B.R. and A.E.Alexander, "The Effect of Additives on the Process of Crystallization II: Further Studies on Calcium Sulphate", Journal of Colloidal and Interface Science, **34**, no.1, (1970) 81-90

[25] Weijnen, M. and G.M.van Rosmalen, "The Role of Additives and Impurities in the Crystallization of Gypsum", Industrial Crystallization 84, Elsevier Science Publishers, Amsterdam, (1984) 61-66

[26] Leao, V.A., V.S.T.Ciminelli and S.D.F.Rocha, "Organic Additives in Gypsum Precipitation", A. Sutulov Memorial Volume, Vol.III, Chemical Metallurgy, Universidad de Concepcion, Concepcion-Chile, (1994) 243-255

[27] Ross, R.J. and K.C.Low, "Polyaspartate Scale Inhibitors - Biodegradable Alternatives to Polyacrylates", Materials Performance, April (1997) 53-57

[28] Amjad, Z., "Calcium Sulfate Dihydrate Scale Formation on Heat Exchanger Surfaces in the Presence of Inhibitors", Materials Performance, November (1989) 52-55

[29] Nancollas, G.H., W.White, F.Tsai and L.Maslow, "The Kinetics and Mechanism of Formation of Calcium Sulfate Scale Minerals - The Influence of Inhibitors", Corrosion NACE, **35**, no.7, (1979) 304-308

[30] Ney, P., Zeta-Potentiale und Flotierbarkeit von Mineralen, Springer-Verlag, New York, (1973) 103-106

[31] Liu, S.-T., and G.H.Nancollas, "The Kinetics of Crystal Growth of Calcium Sulfate Dihydrate", Journal of Crystal Growth, **6**, (1970) 281-289

[32] Omelon, S. & G.P.Demopolous, "Gypsum Crystallization in Waste Water Treatment", (Conference Presentation) TMS Annual Meeting, Orlando, Fla. (1997)

[33] Gainey, R.J., C.A.Thorp and E.A.Caldwallader, "$CaSO_4$ Seeding Prevents $CaSO_4$ Scale", Industrial and Engineering Chemistry, **55**, no.3, (1963) 39-43

[34] Allison, J.D., S.B.Brown, and K.J.Novo-Gradac, MINTEQA2/PRODEFA2, A Geochemical Assessment Model for Environmental Systems: Version 3.0 User's Manual, Office of Research and Development, U.S.E.P.A. Athens, GA, (1991)

[35] Langmuir, D., & D.Melchior, Geochim. Cosmochim. Acta, **49**, (1985) 2423

[36] Barton, P., and T.Vatanatham, "Kinetics of limestone neutralization of acid waters", Environmental Science & Technology, **10**, (1976) 262-266

[37] Smith, B.R., and F.Sweet, "The Crystallization of Calcium Sulfate Dihydrate", Journal of Colloid and Interface Science, **37**, no.3, (1971) 612-618

[38] Hasson, D., J.Addai-Mensah, and J.Metcalfe, "Filterability of Gypsum Crystallized in Phosphoric Acid Solution in the Presence of Ionic Impurities", I&EC Research, **29**, (1990) 867-875

[39] Magini, M. X-Ray Diffraction of Ions in Aqueous Solution: Hydration and Complex Formation, CRC Press, Boca Raton, Florida. 1988. 69,73,78,106,121

Appendix A: Raw Data

The following section presents the raw data for the experimental study of gypsum scale formation. Temperature and pH represent the average steady state temperature and pH for that run. Stoichiometric ratio is the starting ratio of base (calcium carbonate or calcium oxide) to sulphuric acid that was being added to the reactor. Scale growth rates are given in $g/cm^2.h$. Sample calculations for stoichiometric ratio, specific scale growth rate and saturation ratio are given at the end of this section.

A.1 Calcium Carbonate Partial Neutralization Reactor

Raw data for the calcium carbonate partial neutralization reactor experiments with no metal sulphates in the acid feed are given in Table A1, and Table A2. Table A1 is the data from the scale growth study experiments, while Table A2 is the data from the scale reduction experiments.

Table A1: Raw data for the calcium carbonate partial neutralization experiments with no metal sulphates in the acid feed.

Temperature (°C)	Residence Time (min)	pH/ Stoichiometric Ratio (B/A)	Saturation Ratio	Induction Period	Specific Scale Growth Rate ($g/cm^2.h$)
70	15	6.0/1.47	1.18	2.1	0.0152
	30	6.2/1.47	1.14	4.0	0.0083
	50	6.3/1.47	1.02	5.4	0.0071
70	30	2.2/0.98	1.13	3.6	0.0080
		5.9/1.18	1.15	3.9	0.0086
		6.2/1.47	1.14	4.0	0.0083
		6.3/1.96	1.15	3.9	0.0086
50	30	6.0/1.47	1.11	3.5	0.0063
70		6.2/1.47	1.14	4.0	0.0083
90		6.3/1.47	1.06	3.7	0.0045

Table A2: Scale reduction raw data for the calcium carbonate partial neutralization experiments with no metal sulphates in the acid feed.

Temp (°C)	Res. Time (min)	pH/ Stoich. Ratio (B/A)	Surfactant [2A1] (ppm)	Surfactant [3B2] (ppm)	Surfactant [OS] (ppm)	Gypsum Seed Conc. (g/L)	Induct. Period	Specific Scale Gr. Rate ($g/cm^2.h$)
70	30	6.2/1.47	0	0	0	0	4.0	0.0083
		6.1/1.47	1	0	0	0	4.0	0.0083
		6.1/1.47	10	0	0	0	4.0	0.0061
		5.8/1.47	100	0	0	0	4.5	0.0043
		6.1/1.47	0	10	0	0	4.5	0.0059
		6.1/1.47	0	100	0	0	4.3	0.0036
		6.1/1.47	0	0	100	0	5.0	0.0059
		6.4/1.47	0	0	0	5	4.7	0.0047
		6.4/1.47	0	0	0	10	6.7	0.0024

Raw data for the calcium carbonate partial neutralization experiments with metal sulphates in the acid feed are given in Table A3, and Table A4. Table A3 is the data from the scale growth study experiments, while Table A4 is the data from the scale reduction experiments. The concentrations of nickel, aluminum, and iron were 5g/L, 2g/L and 1g/L respectively, which was their initial concentrations in the 30g/L H_2SO_4 feed solution.

Table A3: Raw data for the calcium carbonate partial neutralization experiments with nickel, aluminum and iron sulphates in the acid feed.

Temperature (°C)	Residence Time (min)	pH/ Stoichiometric Ratio (B/A)	Saturation Ratio	Induction Period	Specific Scale Growth Rate ($g/cm^2.h$)
70	15	5.5/1.47	1.49	2.8	0.0120
	30	5.8/1.47	1.41	4.7	0.0053
	50	5.8/1.47	1.10	4.2	0.0022
70	30	2.5/0.98	1.31	4.3	0.0041
		5.8/1.47	1.41	4.7	0.0053
		6.2/1.96	1.36	4.8	0.0052
50	30	5.8/1.47	1.18	4.2	0.0047
70		5.8/1.47	1.41	4.7	0.0053
90		5.9/1.47	1.20	5.4	0.0022

Table A4: Scale reduction raw data for the calcium carbonate partial neutralization experiments with nickel, aluminum and iron sulphates in the acid feed.

Temp (°C)	Res. Time (min)	pH/ Stoich. Ratio (B/A)	Surfactant [2A1] (ppm)	Surfactant [3B2] (ppm)	Surfactant [OS] (ppm)	Gypsum Seed Conc. (g/L)	Induct. Period	Specific Scale Gr. Rate ($g/cm^2.h$)
70	30	5.8/1.47	0	0	0	0	4.7	0.0053
		5.5/1.47	100	0	0	0	5.1	0.0057
		5.4/1.47	0	100	0	0	2.7	0.0062
		5.4/1.47	0	0	100	0	4.7	0.0131
		6.0/1.47	0	0	0	10	5.7	0.0021

A.2 Calcium Oxide Total Neutralization Experiments

Raw data for the calcium oxide total neutralization reactor experiments with no magnesium sulphate in the acid feed are given in Table A5, and Table A6. Table A5 is the data from the scale growth study experiments, while Table A6 is the data from the scale reduction experiments.

Table A5: Raw data for the calcium oxide total neutralization experiments with no magnesium sulphate in the acid feed.

Temp (°C)	Residence Time (min)	pH/ Stoichiometric Ratio (B/A)	Saturation Ratio	Induction Period	Specific Scale Growth Rate ($g/cm^2.h$)
40	15	11.0/1.14	2.00	1.3	0.0066
	30	11.0/1.14	1.20	2.9	0.0069
	50	11.4/1.14	1.23	0.8	0.0035
40	30	2.3/0.98	1.21	3.0	0.0049
		11.0/1.14	1.20	2.9	0.0069
		11.5/1.25	1.17	3.5	0.0074
24	30	10.9/1.14	1.20	1.3	0.0033
40		11.0/1.14	1.20	2.9	0.0069
60		10.4/1.14	1.30	3.4	0.0136

Table A6: Scale reduction raw data for the calcium oxide total neutralization experiments with no magnesium sulphate in the acid feed.

Temp (°C)	Residence Time (min)	pH/ Stoich. Ratio (B/A)	Surfactant [2A1] (ppm)	Gypsum Seed Conc. (g/L)	Induction Period	Specific Scale Growth Rate ($g/cm^2.h$)
40	30	11.0/1.14	0	0	2.9	0.0069
		11.2/1.14	100	0	4.5	0.0072
		8.0/1.14	0	10	4.8	0.0027

Raw data for the calcium oxide total neutralization experiments with magnesium sulphate in the acid feed are given in Table A7, and Table A8. Table A7 is the data from the scale growth study experiments, while Table A8 is the data from the scale reduction experiments. The concentration of magnesium was 10g/L, which was its initial concentration in the 10g/L H_2SO_4 feed solution.

Table A7: Raw data for the calcium oxide total neutralization experiments with magnesium sulphate in the acid feed.

Temp (°C)	Residence Time (min)	pH/ Stoichiometric Ratio (B/A)	$[Mg^{2+}]$ (g/L)	Saturation Ratio	Induction Period	Specific Scale Growth Rate ($g/cm^2.h$)
40	15	9.4/1.5	10	2.53	4.4	0.0011
	30	9.4/1.5	10	2.43	5.1	0.0003
	50	9.6/1.5	10	2.01	4.6	0.00006
40	30	2.5/1.14	10	2.07	5.7	0.0014
		9.4/1.5	10	2.43	5.1	0.0003
		9.6/4.56	10	2.06	4.5	0.0031
24	30	10.0/1.5	10	2.71	5.2	0.0006
40		9.4/1.5	10	2.43	5.1	0.0003
60		9.3/1.5	10	2.33	5.1	0.0023

Table A8: Scale reduction raw data for the calcium oxide total neutralization experiments with no magnesium sulphate in the acid feed.

Temp (°C)	Residence Time (min)	pH/ Stoich. Ratio (B/A)	Surfactant [2A1] (ppm)	Gypsum Seed Conc. (g/L)	Induction Period	Specific Scale Growth Rate ($g/cm^2.h$)
40	30	9.4/1.5	0	0	5.1	0.00027
		9.3/1.5	100	0	5.9	0.00027

Appendix B: Sample Calculations

B.1 Stoichiometric Amount

To calculate the stoichiometric amount, the calcium carbonate partial neutralization example will be used:

30g/L of $H_2SO_{4(aq)}$ represents 0.306mol/L, (i.e. 30/98.06 mol/L).

H_2SO_4 reacts 1:1 with $CaCO_3$,by equation (1):

$$H_2SO_{4\,(aq)} + CaCO_{3\,(s)} + H_2O_{(l)} \Rightarrow CaSO_4 \cdot 2H_2O_{(s)} + CO_{2\,(g)} \uparrow$$

Thus, assuming complete reaction, 0.306mol/L of $CaCO_3$ is needed for neutralization. This represents a mass of

0.306mol/L * 100.08g/mol = 30.6g/L

which is the stoichiometric amount of $CaCO_3$ required to partially neutralize 30g/L of H_2SO_4.

The stoichiometric ratio is calculated by dividing this number into the actual amount of calcium carbonate that was used. Thus if 30g/L was used, the stoichiometric ratio would be 30/30.6 = 0.98.

B.2 Specific Scale Growth Rate

In a typical experiment, sample rods were weighed and marked. They were then placed in the reactor. Every two hours, one sample rod was removed and weighed again and the specific mass of scale growth was plotted versus time. To get the specific scale

growth rate, linear regression was performed on the slope of the growth portion of the curve, (i.e. the portion of the curve after the induction period). As an example, the data from one experiment is shown in Table B1. It is plotted in Figure B1.

Table B1: Experimental data from a scale growth experiment in the calcium carbonate partial neutralization reactor.

Experimental Conditions	Time (h)	Mass of Rod Before Scaling (g)	Mass of Rod After Scaling (g)	Mass of Scale (g)	Surface Area of Scale on Rod (cm^2)	Specific Scale Growth (g/cm^2)
T=70°C	0	0.0000	0.0000	0.0000	0.00	0
R.t.=30min	2	23.5789	23.5795	0.0006	8.56	7E-05
PH=6.2	4	23.5517	23.5817	0.0300	8.56	0.0035
No metal Sulphates in acid feed	6	23.6173	23.7645	0.1472	8.56	0.0172
	8	23.6009	23.8412	0.2403	8.41	0.0286
	10	23.4976	23.9356	0.4380	8.71	0.0503
	12	23.6121	24.2140	0.6019	8.56	0.0703

Assuming the induction period is 4h, the data from 4h to 12h is used to calculate the linear regression using Excel. The results are as follows:

Growth Rate Equation: Specific Growth=Growth Rate*time+Constant

Specific Growth=0.0083t-0.033

$\therefore$ Growth Rate=0.0083g/cm^2.h

$\therefore$ Induction Period=3.98h (i.e.-Constant/Growth Rate)

The calculated induction period was very close to the assumed one!

The R^2 value was 0.984, and the standard error of the specific growth rate was 0.0006g/cm^2.h.

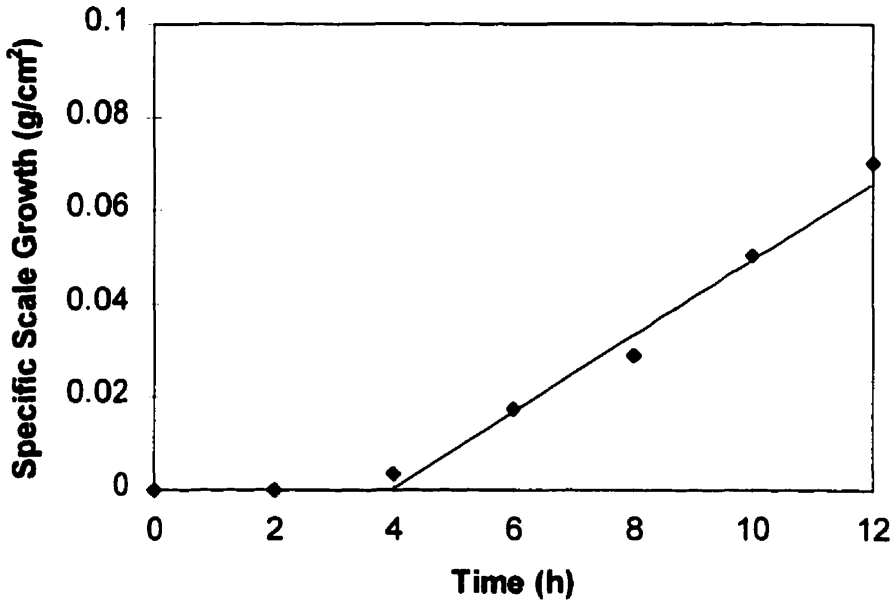

Figure B1: Specific scale growth vs time for calcium carbonate partial neutralization reactor.

Reactor conditions: Temperature=70°C, residence time=30min, pH=6.2, no metal sulphates in the acid feed.

B.3 Saturation Ratio

The saturation ratio calculations were simple. The mean (of three samples) total calcium was determined by ICP-AES to be 0.666g/L. It was calculated using MINTEQA2 to be 0.584g/L. Therefore, the saturation ratio was 0.666/0.584=1.14.

Appendix C: Sources of Error

C.1 Reproducibility

In order to assess the validity of this scale measurement technique, five experiments were performed under identical conditions in the calcium carbonate partial neutralization reactor. The conditions were temperature 70°C, residence time 30min, calcium carbonate concentration 45g/L, and sulphuric acid concentration 30g/L. The results are given in Table C1.

Table C1: Scale growth rate reproducibility data

Experiment Number	Temperature (°C)	Residence Time (min)	Average Steady State pH	Specific Scale Growth Rate ($g/cm^2.h$)
1	70	30	6.2	0.00830
2	70	30	6.3	0.00856
3	70	30	6.2	0.00863
4	70	30	6.2	0.00826
5	70	30	6.2	0.00860

The mean value in these ten experiments were pH=6.2 and a specific scale growth rate equal to $0.00847 g/cm^2.h$. The standard deviation of the specific scale growth rate was $0.00018 g/cm^2.h$. Thus, the 95% confidence interval for the experimental data was ± 4.2% of the mean. All five data points were within that range. This indicates fairly good reproducibility.

The variation is plotted in Figure C1. As can be seen, all five specific scale growth rates were within 3% of the average, and the scatter was good. Thus, the method is acceptable from a reproducibility standpoint.

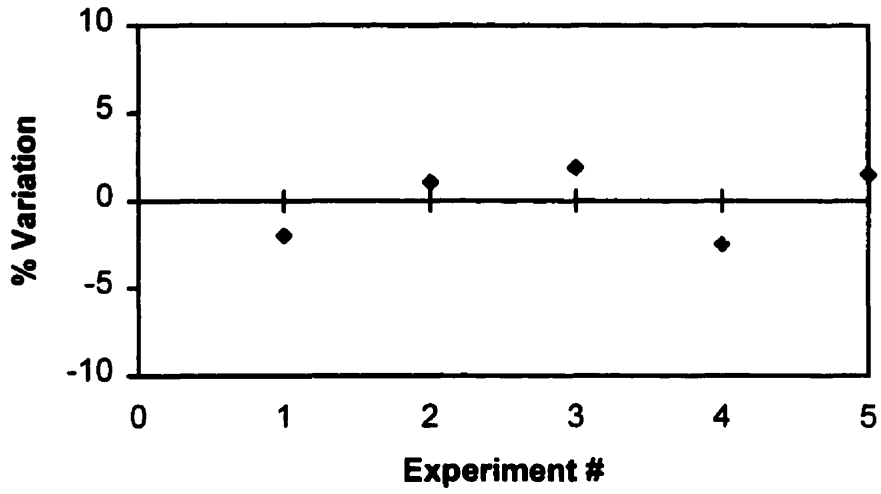

Figure C1: Specific scale growth rate variation in the calcium carbonate partial neutralization experiments

C.2 Effect of Rinsing

In order to determine the error introduced by the rinsing of the scale growth rods, 10 dry, scaled rods were weighed, rinsed, allowed to dry, and then weighed again. This test was to help quantify the amount of loose gypsum needles removed during rinsing, as well as the amount that dissolved. The results are shown in Table C2.

Table C2: Effect of Rinsing on 10 Scaled Sample Rods.

Rod #	Mass Before Rinse (g)	Mass After Rinse (g)	Difference (g)	% Difference
1	0.1066	0.1028	0.0038	3.6
2	0.1421	0.1344	0.0077	5.4
3	0.1125	0.1060	0.0065	5.8
4	0.1744	0.1699	0.0045	2.6
5	0.1305	0.1266	0.0039	3.0
6	0.1109	0.1065	0.0044	4.0
7	0.1518	0.1452	0.0066	4.3
8	0.1189	0.1166	0.0023	1.9
9	0.1646	0.1632	0.0014	0.9
10	0.1188	0.1168	0.0020	1.7

Thus, the average amount of scale that was removed during rinsing was only 3.3%. Since most of that was loose scale, which is of no consequence to this study, the amount of gypsum that dissolved was probably less than 1%. This is an acceptable error because it would be approximately the same for all scale growth rods. This also means that it would not affect the slope of the scale growth plots, (i.e. the scale growth rate). The reason is that the linear portion of the growth curves would only shift down slightly, and therefore the slope would be the same. Only the induction period would be affected by 3.3%, and that is of no concern.

C.3 Use of MINTEQA2 to Calculate Gypsum Solubility

There have been many studies that have focused on gypsum solubility in pure and mixed metal sulphate solutions. Unfortunately, most of these focused on gypsum as a component of brine or groundwater. They were therefore most concerned with the

solubility of gypsum in mixed solutions containing sodium, magnesium, chloride and sulphate. Examples of these papers include Adler, Glater, and McCutchan (1979) [C1], Arslan and Dutt (1993) [C2], Marshall and Slusher (1966) [C3], and (1968) [C4], Power, Fabuss and Satterfield (1966) [C5], Raju and Atkinson (1990) [C6], Tanji (1969) [C7], and Tanji and Doneen (1966) [C8]. The lone exception to this focus on brine was a study by Umetsu, Mutalala and Tozawa (1989) [C9], which examined calcium sulfate solubility in solutions of zinc, magnesium, copper and cobalt sulfates over a temperature range of 25 to 200°C. However, none of the systems that were studied involved mixed metal sulphate solutions.

Despite the seemingly limited applicability of the other studies, many of them contained useful methods of calculating gypsum solubility in aqueous solution [C1], [C2], [C3], [C7], [C8]. The most important conclusion from these studies was that in aqueous solution up to 2m ionic strength and less than 100°C temperature (which is the range of this study), an extended Debye-Hückel equation or the Davies equation would accurately predict gypsum solubility. This is important because the computer program MINTEQA2 [C10] uses the Davies equation to calculate gypsum solubility.

This means that the choice of MINTEQA2 as a means of calculating gypsum solubility would not necessarily introduce a large error. However, it was discovered that the choice of solubility constant ($K_{sp,\ gypsum}$) can have a profound effect on the gypsum solubility values calculated using MINTEQA2. The reason is that MINTEQA2 has its own database of thermodynamic constants (such as K_{SP}) that it uses to calculate equilibrium aqueous species concentrations. Because of its size, this database does not necessarily contain the most accurate thermodynamic constants. It therefore allows the

user to input other constants from literature. The user's choice of K_{SP} is crucial in ensuring accurate, reliable solubility predictions.

Thus, in order to determine which values of K_{sp} give the most accurate results when used in MINTEQA2, the K_{sp} values of Langmuir & Melchior [C11], Lu & Fabuss (1968) [C12], and Ostroff (1964) [C13], were used in MINTEQA2 to determine calcium solubility in a pure saturated gypsum solution over a wide temperature range. The results were compared to experimental solubility data from Marshall & Slusher (1966) [C3], Power, Fabuss, & Satterfield (1966) [C5], Seidell [C14], and Calmanovici, Gabas, & Laguerie (1993) [C15]. This comparison is shown in Figure C2. As can be seen, there is good agreement between MINTEQA2-calculated results using the K_{sp} values of Langmuir & Melchior [C11], with the experimental literature data. Therefore, their K_{sp} values were used in MINTEQA2 throughout this study to calculate gypsum solubility.

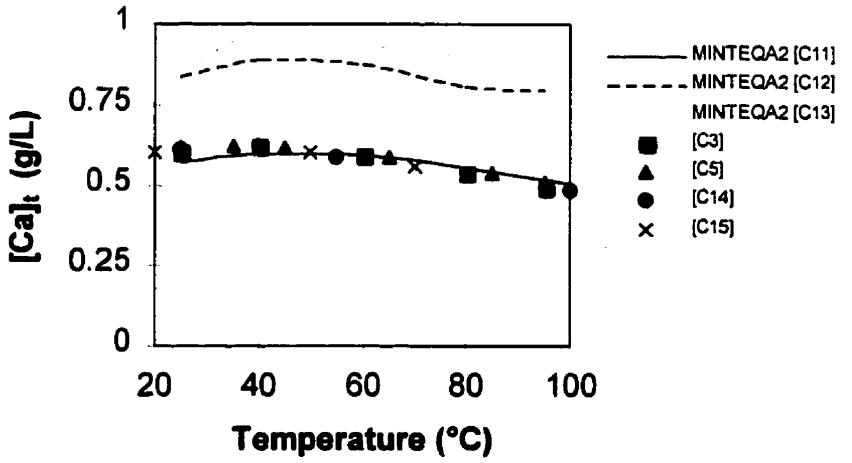

Figure C2: Gypsum solubility (given as total calcium) vs temperature for pure solution. The graph shows a comparison between MINTEQA2-calculated calcium solubility using K_{sp} values from [C11], [C12] and [C13], with experimental data from several studies.

Appendix C.3 References

[C1] Adler, M.S., J.Glater, and J.W.McCutchan, "Prediction of Gypsum Solubility and Scaling Limits in Saline Waters", Journal of Chemical and Engineering Data, **24**, no.3, (1979) 187-192

[C2} Arslan, A., and G.R.Dutt, "Solubility of Gypsum and its Prediction in Aqueous Solutions of Mixed Electrolytes", Soil Science, **155**, no.1, (1993) 37-47

[C3] Marshall, W.L., and R.Slusher, "Thermodynamics of Calcium Sulfate Dihydrate in Aqueous Sodium Chloride Solutions: 0-110°C", Journal of Physical Chemistry, **70**, no.12, (1966) 4015-4027

[C4] Marshall, W.L., and R.Slusher, "Aqueous Systems at High Temperature: Solubility to 200°C of Calcium Sulfate and its Hydrates in Sea Water and Saline Water Concentrates, and Temperature-Concentration Limits", Journal of Chemical and Engineering Data, **13**, no.1, (1968) 83-93

[C5] Power, W.H., B.M.Fabuss, and C.N.Satterfield, "Transient Solute Concentrations and Phase Changes of Calcium Sulfate in Aqueous Sodium Chloride", Journal of Chemical and Engineering Data, **11**, no.2, (1966) 149-154

[C6] Raju, K.U.G., and G.Atkinson, "The Thermodynamics of "Scale" Mineral Solubilities. 3. Calcium Sulfate in Aqueous NaCl", Journal of Chemical and Engineering Data, **35**, (1990) 361-367

[C7] Tanji, K.K., "Solubility of Gypsum in Aqueous Electrolytes as Affected by Ion Association and Ionic Strengths up to 0.15M and at 25°C", Environmental Science and Technology, **3**, no.7, (1969) 656-661

[C8] Tanji, K.K., and L.D.Doneen, "Predictions on the Solubility of Gypsum in Aqueous Salt Solutions", Water Resources Research, **2**, no.3, (1966) 543-548

[C9] Umetsu, Y., B.K.Mutalala, and K.Tozawa, "Solubility of Calcium Sulfate in Solutions of Zinc, Magnesium, Copper and Cobalt Sulfates over a Temperature Range of 25 to 200°C", Journal of Mining and Metallurgy of Japan, **6**, (1989) 13-22

[C10] Allison, J.D., S.B.Brown, and K.J.Novo-Gradac, MINTEQA2/PRODEFA2, A Geochemical Assessment Model for Environmental Systems: Version 3.0 User's Manual, Office of Research and Development, U.S.E.P.A. Athens, GA, (1991)

[C11] Langmuir, D., & D.Melchior, Geochim. Cosmochim. Acta, **49**, (1985) 2423

[C12] Lu, C.H., & B.Fabuss, I&EC P.D.D., **7**, (1968), 206

[C13] Ostroff, A.G., "Conversion of Gypsum to Anhydrite in Aqueous Salt Solutions", Geochimica et Cosmochimica Acta, **28**, (1964) 1363-1372

[C14] Seidell, A., & W.Linke, Solubilities of Inorganic and Metal Inorganic Compounds, 4th Edition, ACS, Washington, D.C. (1958)

[C15] Calmanovici, C.L., N.Gabas, and C.Laguerie, "Solubility Measurements for Calcium Sulfate Dihydrate in Acid Solutions at 20, 50, and 70°C", Journal of Chemical and Engineering Data, **38**, no.4, (1993) 534-536

Appendix D: SEM Pictures

The following picture gallery contains SEM photos taken of scale growth rod cross-sections, under selected reactor conditions. They are arranged in order to illustrate the effects of these different conditions (pH, temperature, residence time, metal sulphates, surfactants, seeding) on scale growth morphology.

D.1 Calcium Carbonate Partial Neutralization Reactor

D.1.1 Effect of pH

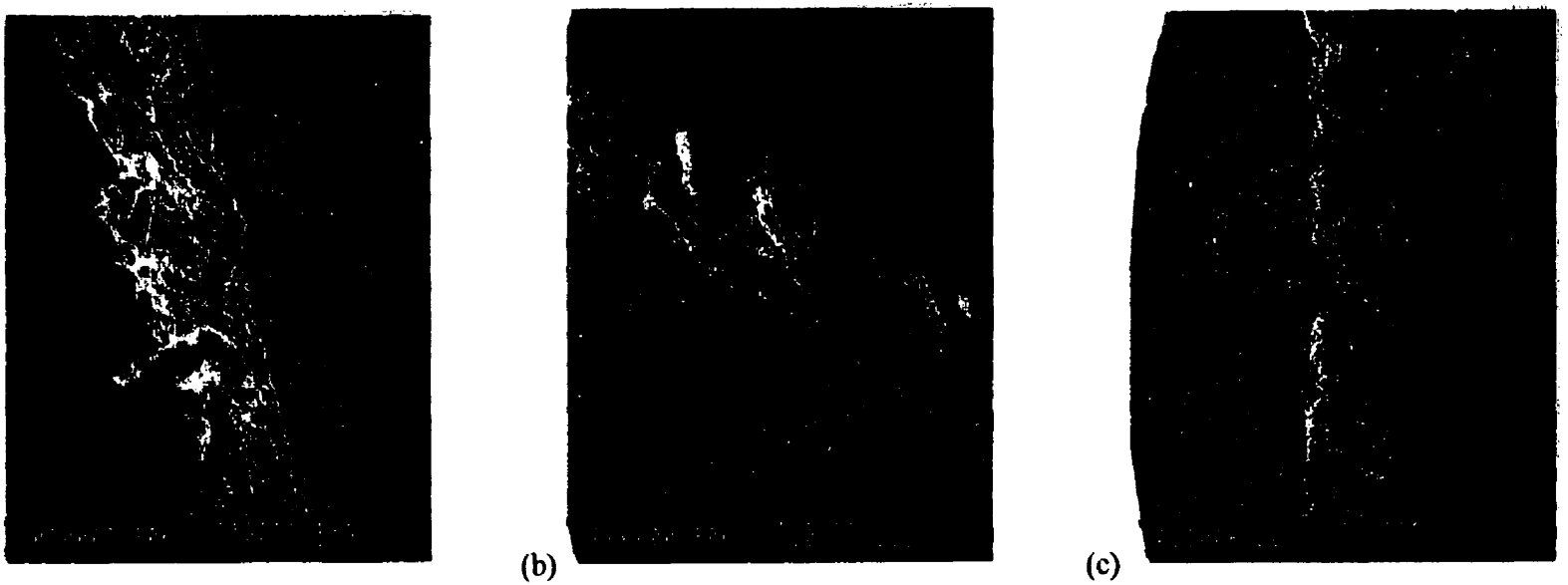

Figure D1: SEM cross-section (300X) showing gypsum scale from the calcium carbonate partial neutralization reactor on 316SS rods.

Reactor conditions: pH = (a) 2.5, (b) 5.8, (c) 6.2, temperature=70°C, residence time = 30min, with metal sulphates in the acid feed, after 8h in the reactor.

D.1.2 Effect of Temperature

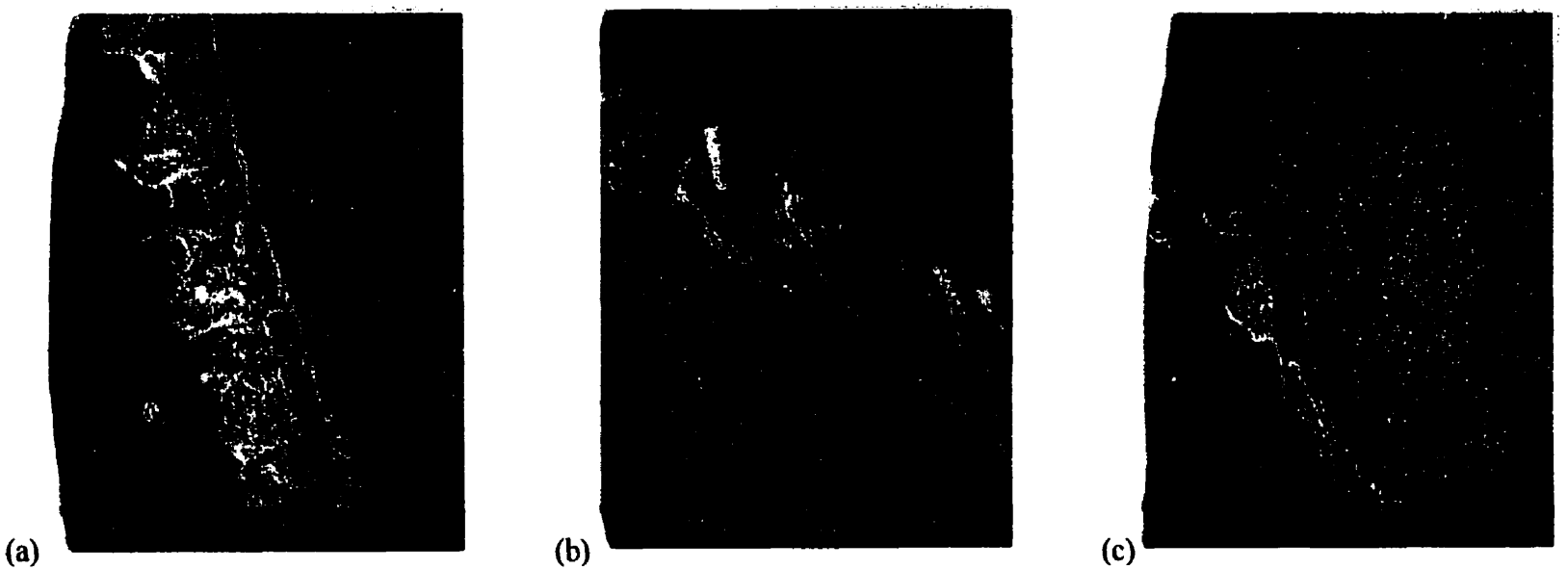

Figure D2: SEM cross-section (300X) showing gypsum scale from the calcium carbonate partial neutralization reactor on 316SS rods.

Reactor conditions: pH ≈ 5.8-5.9, temperature = (a) 50°C, (b) 70°C, (c) 90°C, residence time = 30min, with metal sulphates in the acid feed, after 8h in the reactor.

D.1.3 Effect of Residence Time

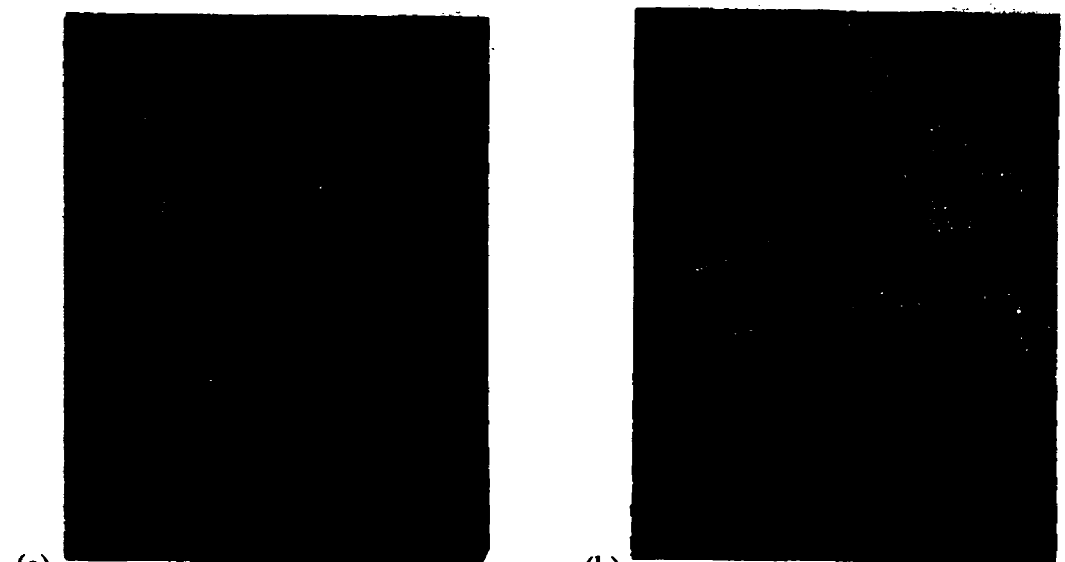

Figure D3: SEM cross-section (100X) showing gypsum scale from the calcium carbonate partial neutralization reactor on 316SS rods.

Reactor conditions: pH = (a) 5.9, (b) 6.2, temperature=70°C, residence time = (a) 15min, (b) 30min, no metal sulphates in the acid feed, after 12h in the reactor.

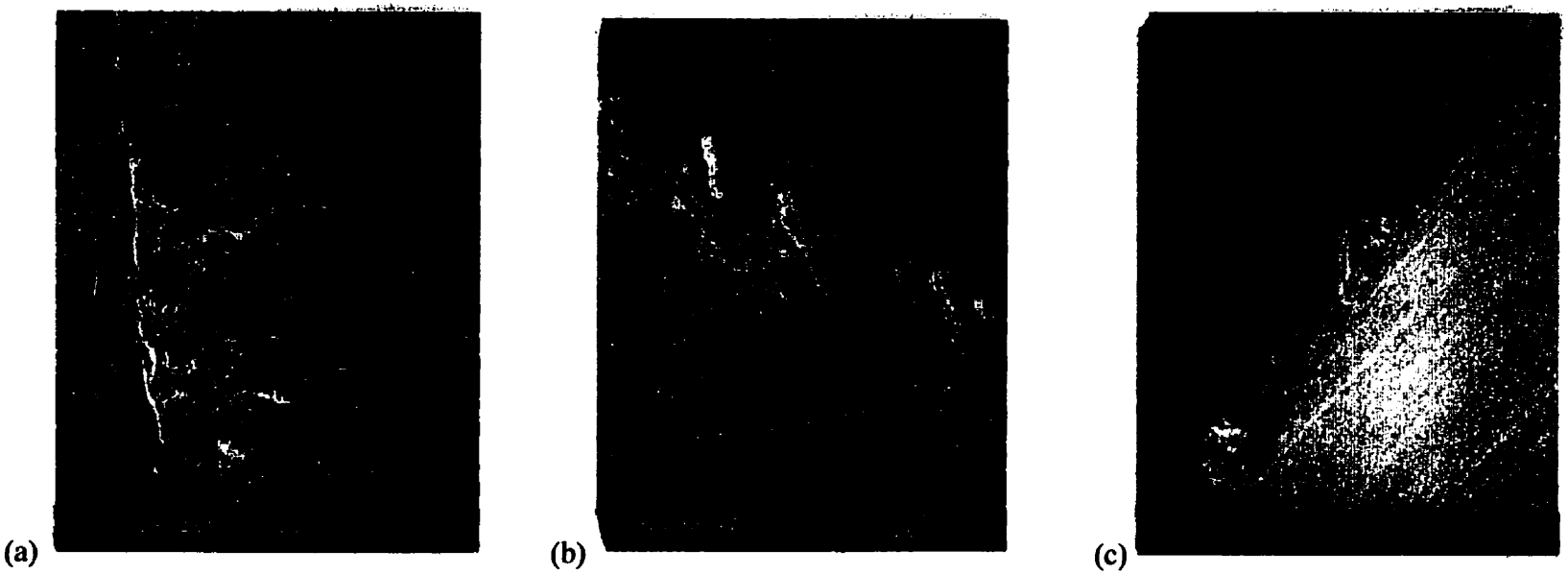

Figure D4: SEM cross-section (300X) showing gypsum scale from the calcium carbonate partial neutralization reactor on 316SS rods.

Reactor conditions: pH ≈ 5.5-5.8, temperature = 70°C, residence time = (a) 15min, (b) 30min, (c) 50min, with metal sulphates in the acid feed, after 8h in the reactor.

D.1.4 Effect of Nickel

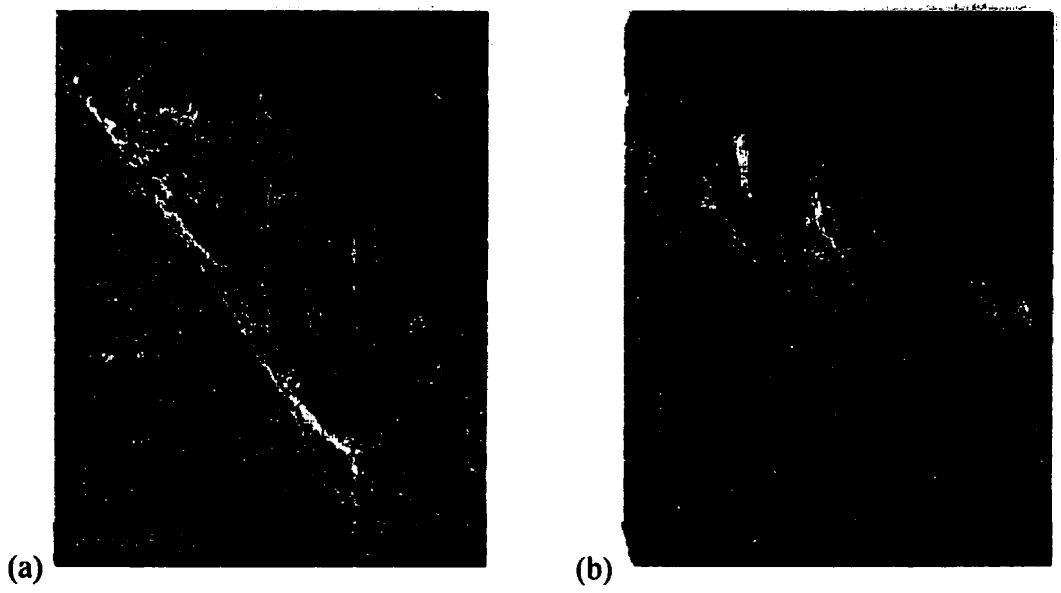

Figure D5: SEM cross-section (300X) showing gypsum scale from the calcium carbonate partial neutralization reactor on 316SS rods.

Reactor conditions: pH ≈ 5.8, temperature = 70°C, residence time = 30min, with (a) iron (III) and aluminum sulphates in the acid feed (no nickel), (b) with iron (III), aluminum and nickel sulphates in the acid feed, after 8h in the reactor.

D.1.5 Effect of Surfactants

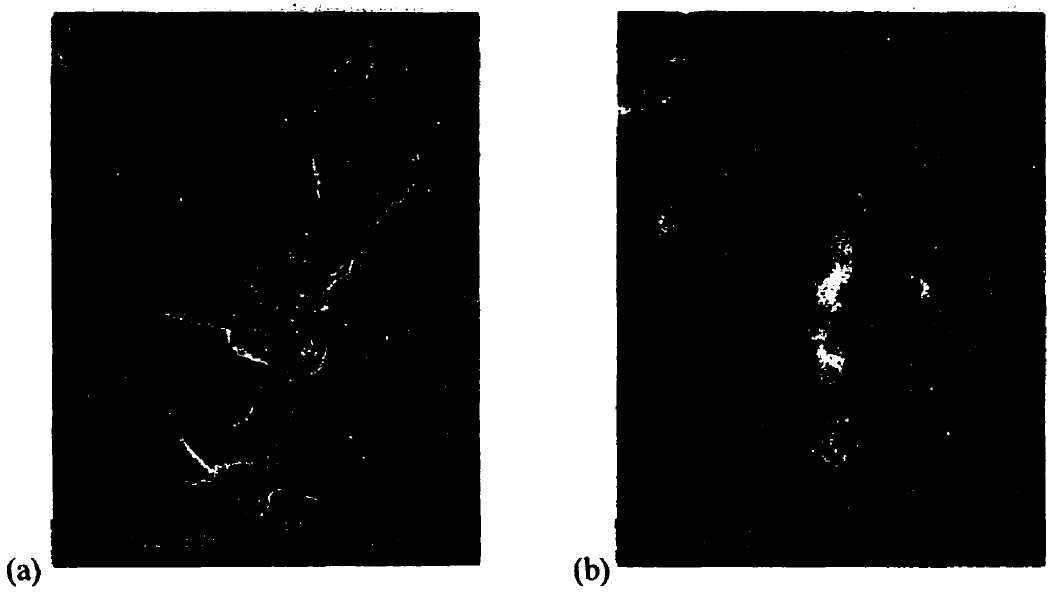

Figure D6: SEM cross-section (300X) showing gypsum scale from the calcium carbonate partial neutralization reactor on 316SS rods.

Reactor conditions: pH ≈ 6.2, 5.8, temperature = 70°C, residence time = 30min, with (a) no surfactant, (b) 100ppm Dowfax 2A1 surfactant, after 8h in the reactor.

D.1.6 Effect of Seeding

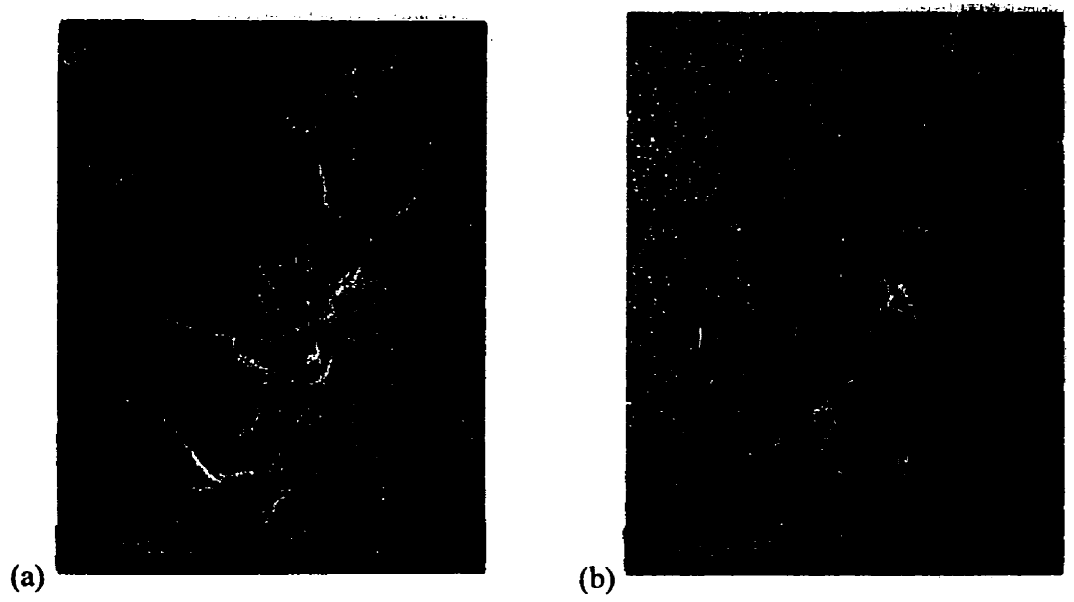

Figure D7: SEM cross-section (300X) showing gypsum scale from the calcium carbonate partial neutralization reactor on 316SS rods.

Reactor conditions: pH ≈ 6.2, 6.4, temperature = 70°C, residence time = 30min, with (a) no gypsum seeding, (b) with 10g/L gypsum seed in the calcium carbonate base feed, after 8h in the reactor.

D.2 Calcium Oxide Total Neutralization Reactor

D.2.1 Effect of pH

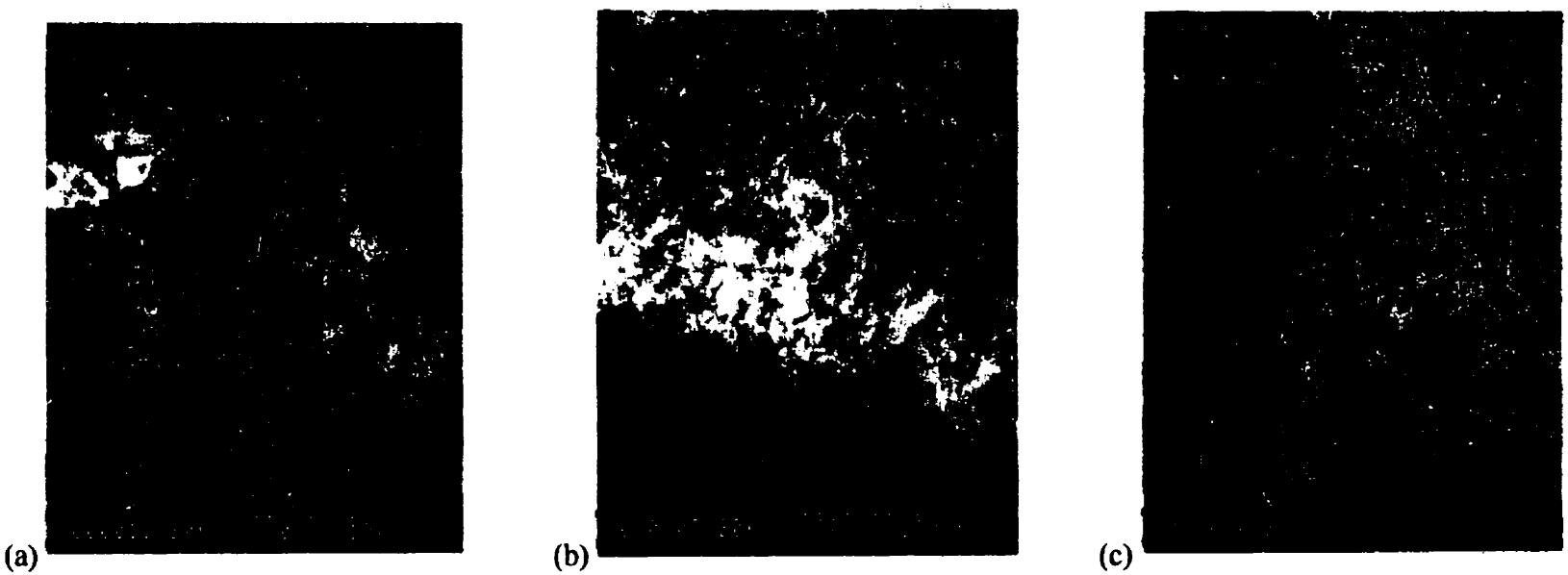

Figure D8: SEM cross-section (300X) showing gypsum scale from the calcium oxide total neutralization reactor on 316SS rods.

Reactor conditions: pH = (a) 2.3, (b) 11.0, (c) 11.5, temperature=40°C, residence time = 30min, with no magnesium sulphate in the acid feed, after 8h in the reactor.

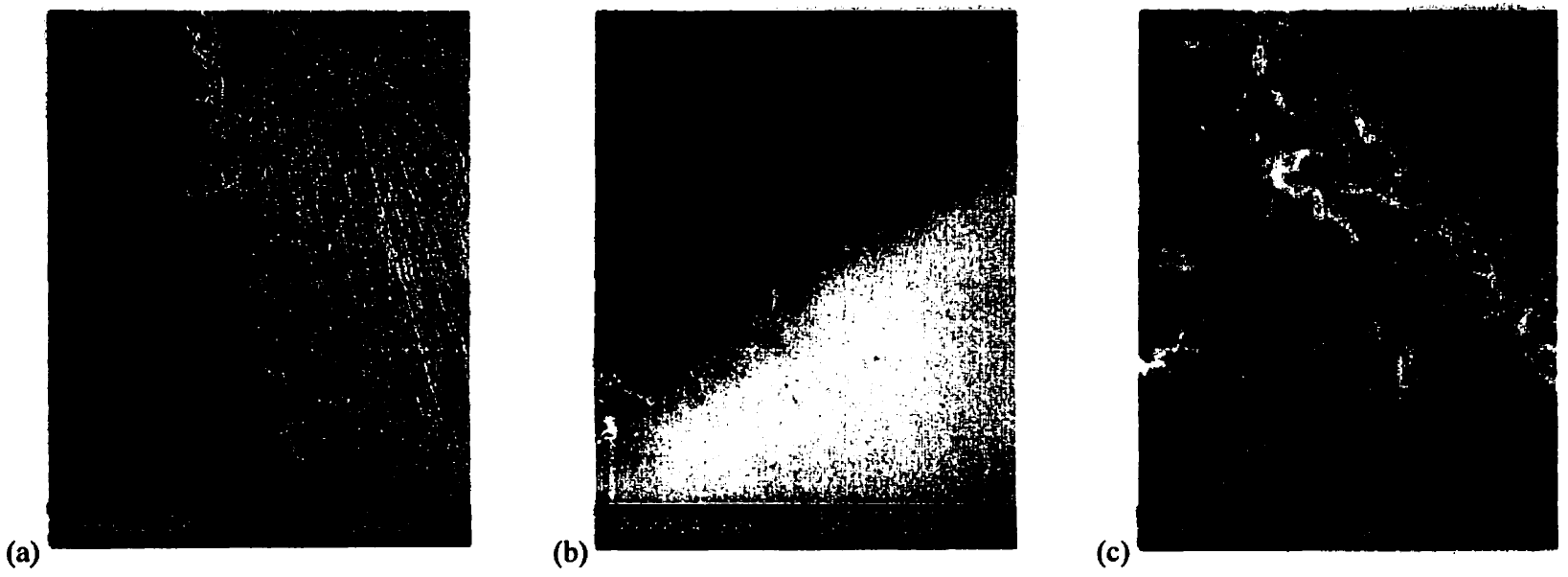

Figure D9: SEM cross-section (300X) showing gypsum scale from the calcium oxide total neutralization reactor on 316SS rods.

Reactor conditions: pH = (a) 2.5, (b) 9.4, (c) 9.6, temperature=40°C, residence time = 30min, with magnesium sulphate in the acid feed, after 8h in the reactor.

D.2.2 Effect of Temperature

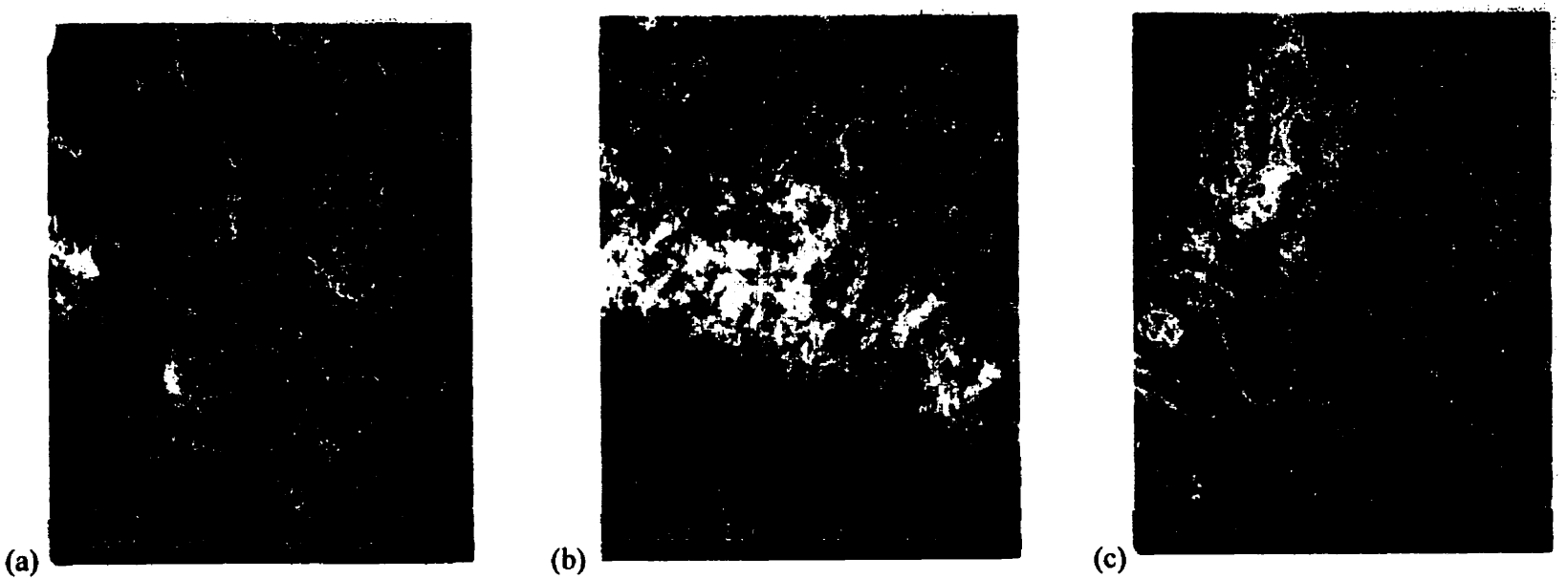

Figure D10: SEM cross-section (300X) showing gypsum scale from the calcium oxide total neutralization reactor on 316SS rods.

Reactor conditions: pH ≈ 10.4-11.0, temperature = (a) 24°C (b) 40°C, (c) 60°C, residence time = 30min, with no magnesium sulphate in the acid feed, after 8h in the reactor.

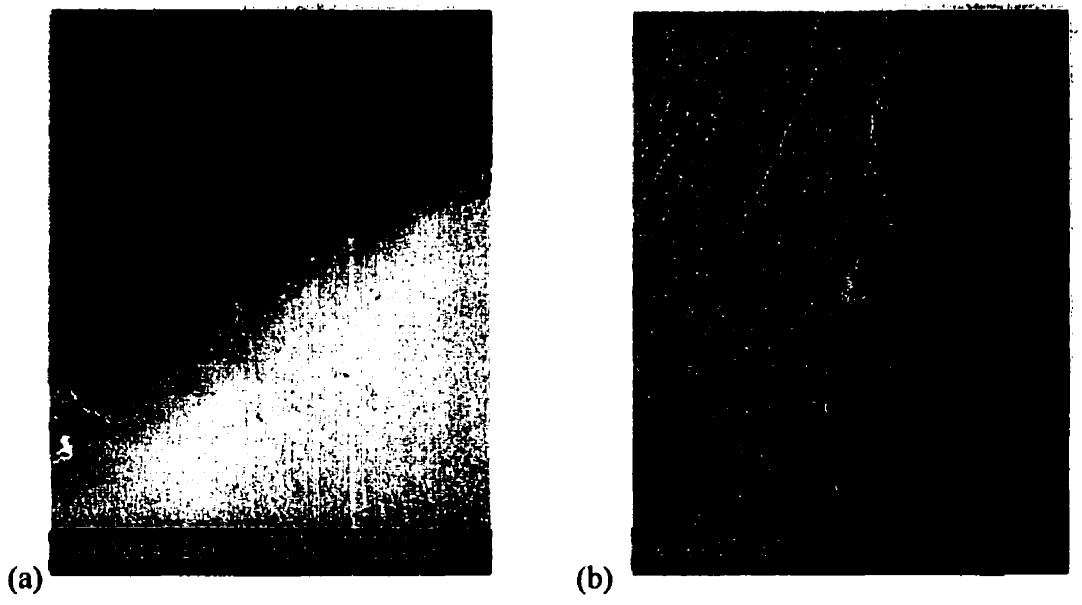

Figure D11: SEM cross-section (300X) showing gypsum scale from the calcium oxide total neutralization reactor on 316SS rods.

Reactor conditions: pH ≈ 9.3-9.4, temperature = (a) 40°C, (b) 60°C, residence time = 30min, with magnesium sulphate in the acid feed, after 8h in the reactor.

D.2.3 Effect of Residence Time

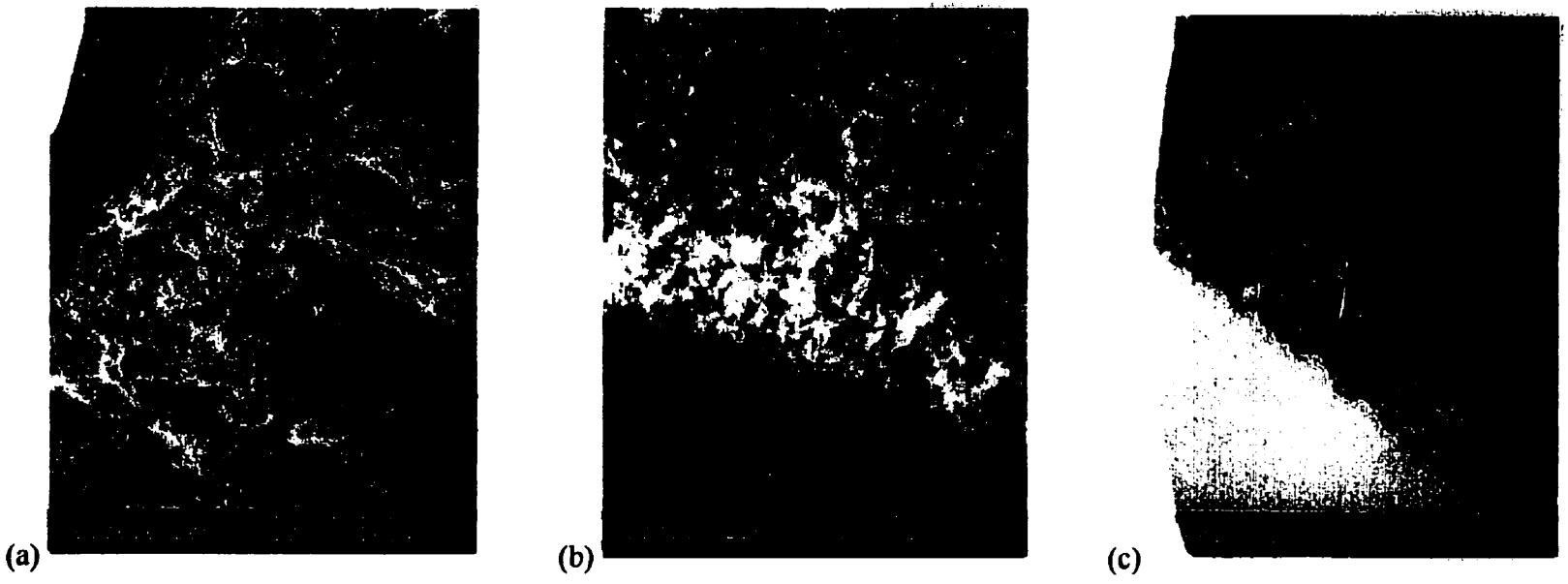

Figure D12: SEM cross-section (300X) showing gypsum scale from the calcium oxide total neutralization reactor on 316SS rods.

Reactor conditions: pH ≈ 11.0-11.4, temperature = 40°C, residence time = (a) 15min, (b) 30min, (c) 50min, with no magnesium sulphate in the acid feed, after 8h in the reactor.

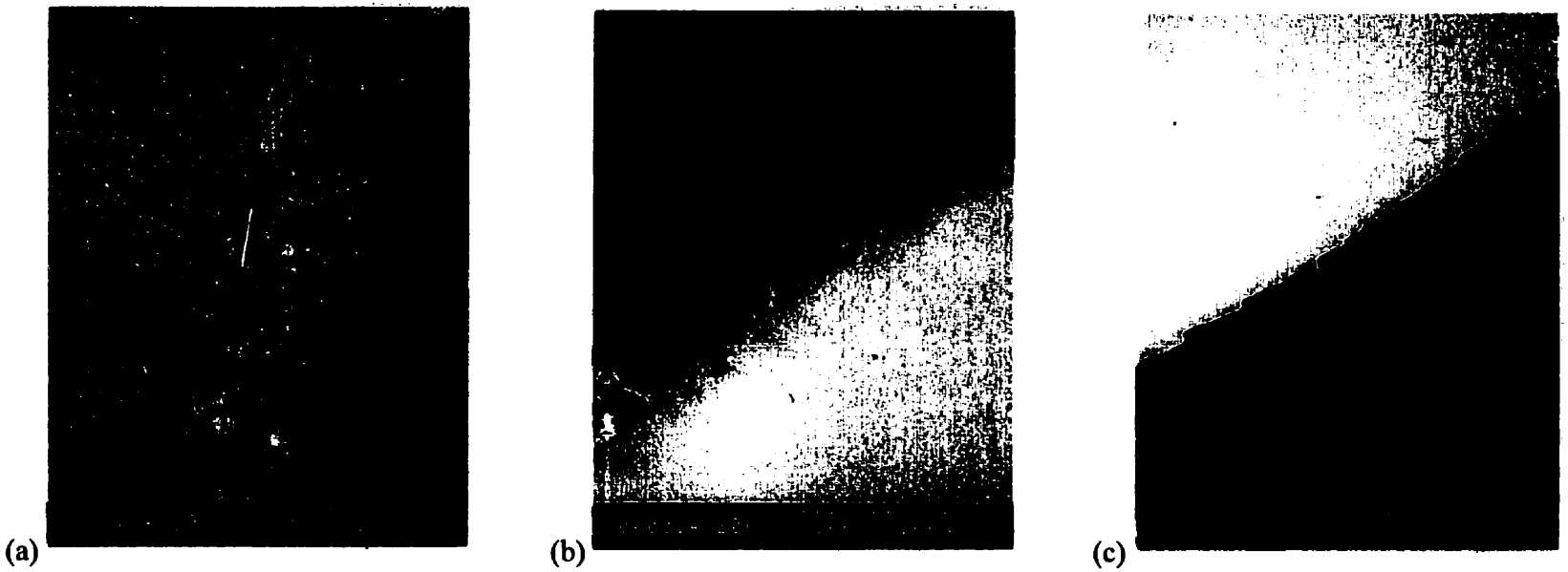

Figure D12: SEM cross-section (300X) showing gypsum scale from the calcium oxide total neutralization reactor on 316SS rods.

Reactor conditions: pH ≈ 11.0-11.4, temperature = 40°C, residence time = (a) 15min, (b) 30min, (c) 50min, with magnesium sulphate in the acid feed, after 8h in the reactor.

D.2.4 Effect of Magnesium

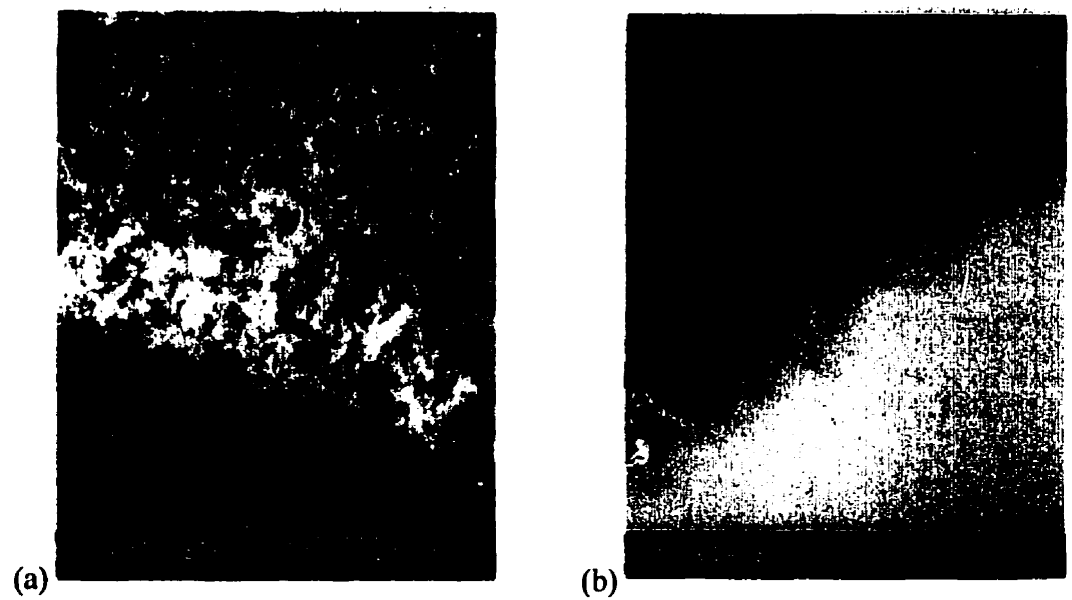

Figure D13: SEM cross-section (300X) showing gypsum scale from the calcium oxide total neutralization reactor on 316SS rods.

Reactor conditions: pH = 11.0, 9.4, temperature = 40°C, residence time = 30min, with (a) no magnesium sulphate in the acid feed, (b) with 10g/L magnesium sulphate in the acid feed, after 8h in the reactor.

D.2.5 Effect of Seeding

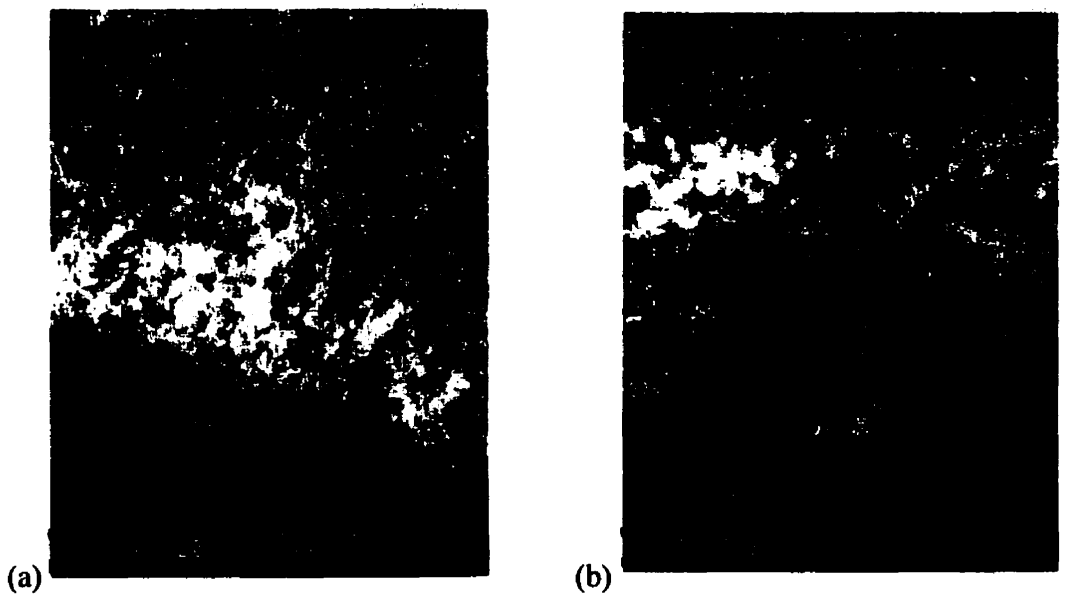

Figure D14: SEM cross-section (300X) showing gypsum scale from the calcium oxide total neutralization reactor on 316SS rods.

Reactor conditions: pH = 11.0, 8.0, temperature = 40°C, residence time = 30min, with (a) no gypsum seeding, (b) with 10g/L gypsum seed in the calcium oxide feed, after 8h in the reactor

Appendix E: Particle Size Analyses

The following section contains particle size distributions (PSD's) of the reactor slurry sampled at different reactor conditions. They are arranged in order to illustrate the effects of the different conditions (pH, temperature, residence time, metal sulphates, surfactants, seeding) on reactor slurry (bulk solution) particle sizes.

E.1 Calcium Carbonate Partial Neutralization Reactor

Figure E1 shows the particle size distribution for the calcium carbonate that was used in these experiments.

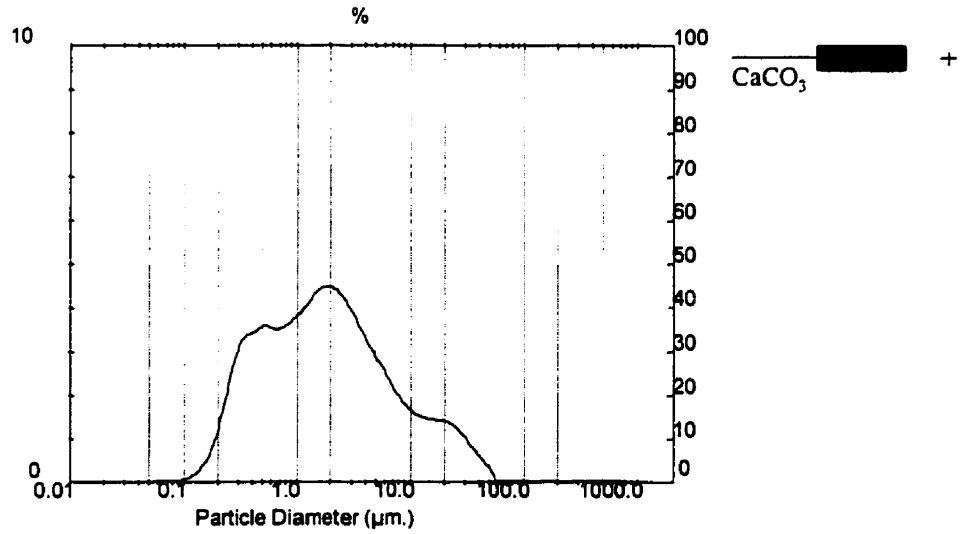

Figure E1: PSD of calcium carbonate used in partial neutralization

E.1.1 Effect of pH

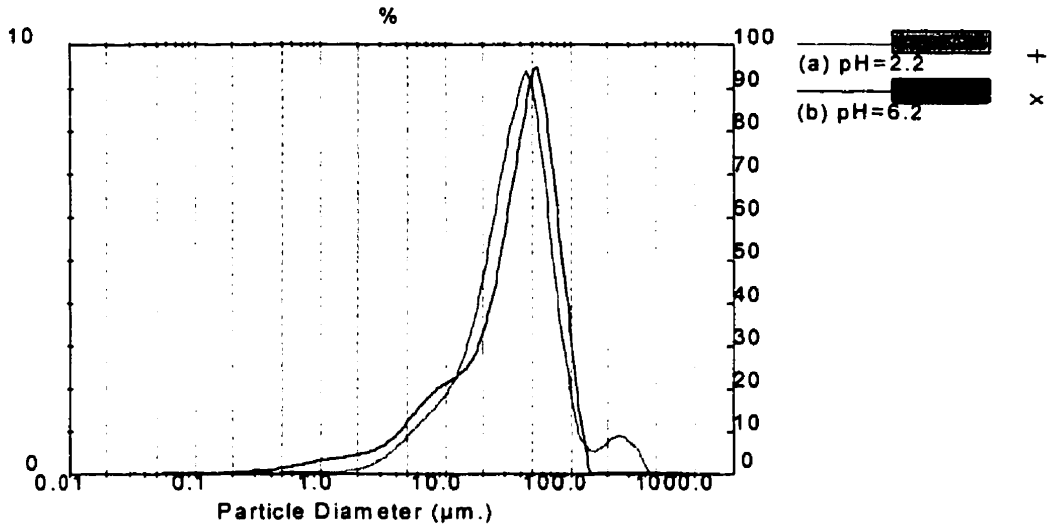

Figure E2: PSD of gypsum particles grown in the calcium carbonate partial neutralization reactor.

Reactor conditions: pH = (a) 2.2, (b) 6.2, temperature=70°C, residence time = 30min, with no metal sulphates in the acid feed.

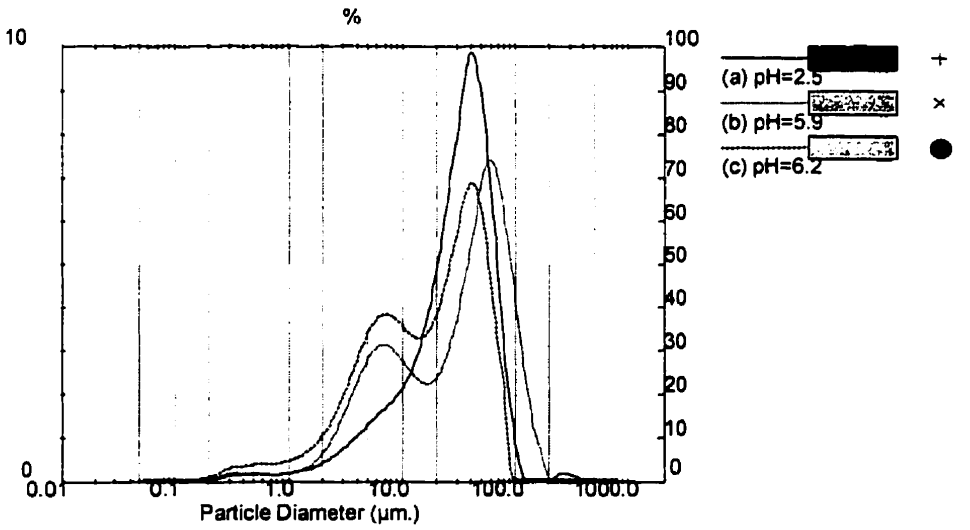

Figure E3: PSD of gypsum particles grown in the calcium carbonate partial neutralization reactor.

Reactor conditions: pH = (a) 2.5, (b) 5.9, (c) 6.2, temperature=70°C, residence time = 30min, with metal sulphates in the acid feed.

E.1.2 Effect of Temperature

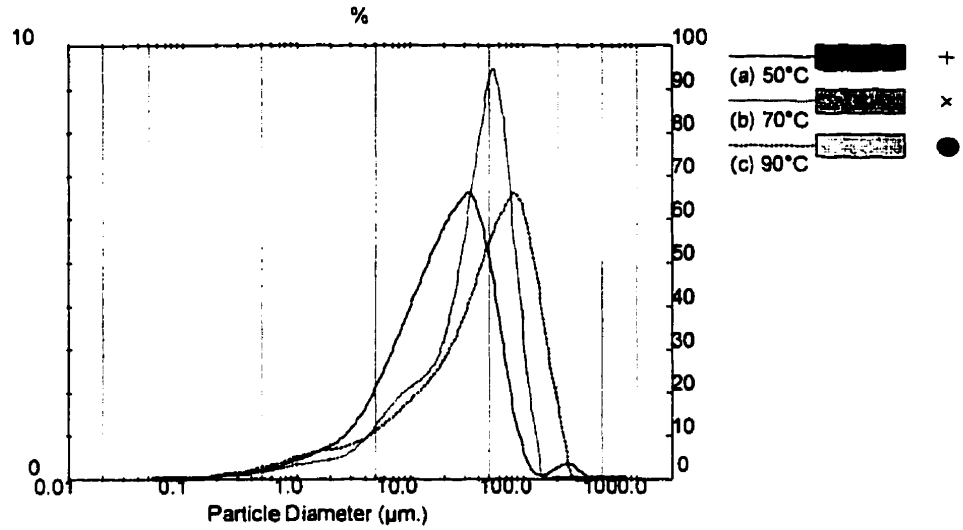

Figure E4: PSD of gypsum particles grown in the calcium carbonate partial neutralization reactor.

Reactor conditions: pH = 6.0-6.3, temperature = (a) 50°C, (b) 70°C, (c) 90°C, residence time = 30min, with no metal sulphates in the acid feed.

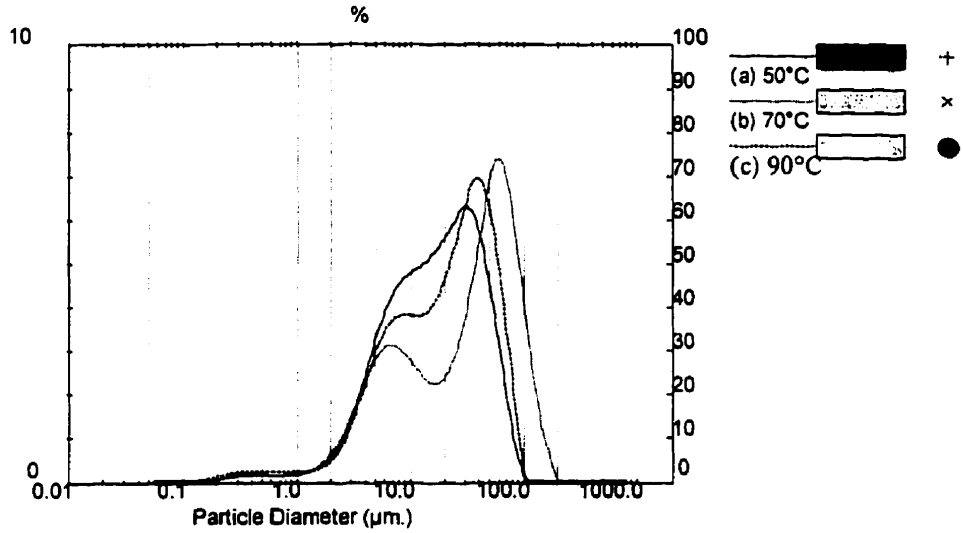

Figure E5: PSD of gypsum particles grown in the calcium carbonate partial neutralization reactor.

Reactor conditions: pH = 5.8-5.9, temperature = (a) 50°C, (b) 70°C, (c) 90°C, residence time = 30min, with metal sulphates in the acid feed.

E.1.3 Effect of Residence Time

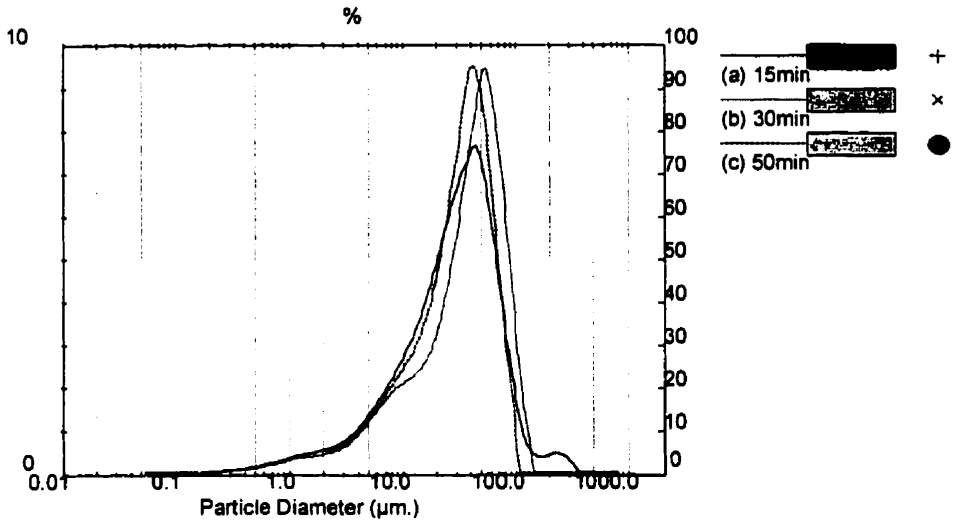

Figure E6: PSD of gypsum particles grown in the calcium carbonate partial neutralization reactor.

Reactor conditions: pH = 6.0-6.2, temperature=70°C, residence time = (a) 15min, (b) 30min, (c) 50min, with no metal sulphates in the acid feed.

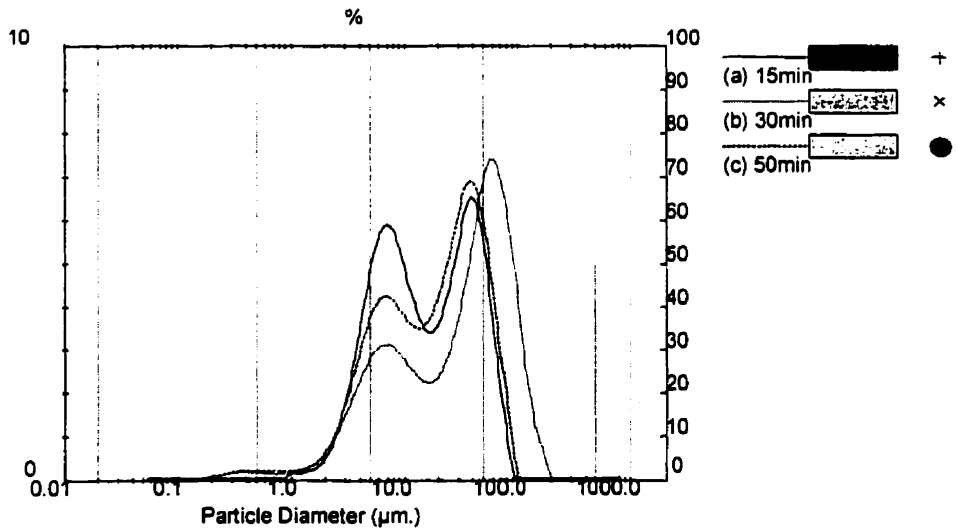

Figure E7: PSD of gypsum particles grown in the calcium carbonate partial neutralization reactor.

Reactor conditions: pH = 5.5-5.8, temperature=70°C, residence time = (a) 15min, (b) 30min, (c) 50min, with metal sulphates in the acid feed.

E.1.4 Effect of Surfactants at 100ppm

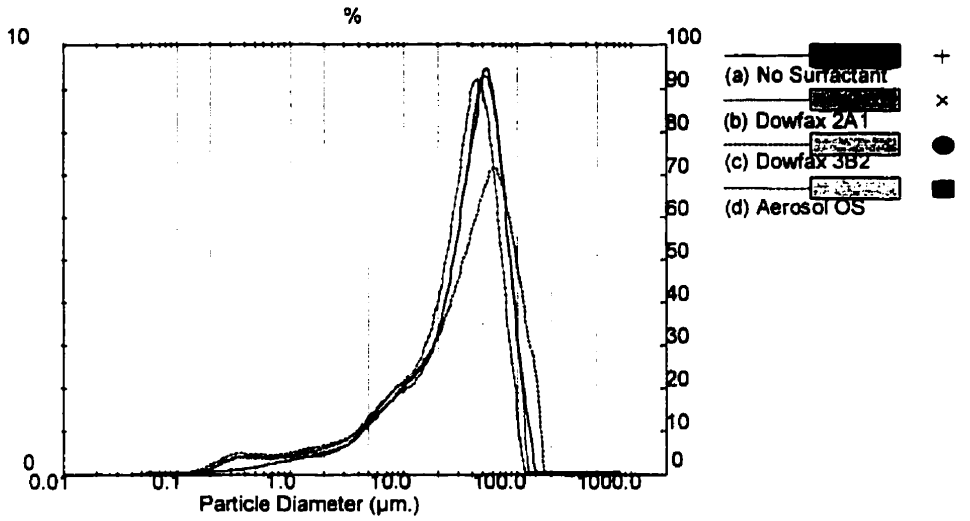

Figure E8: PSD of gypsum particles grown in the calcium carbonate partial neutralization reactor.

Reactor conditions: pH = 5.8-6.1, temperature=70°C, residence time = 30min, with (a) no surfactant, (b) Dowfax 2A1, (c) Dowfax 3B2, (d) Aerosol OS, with no metal sulphates in the acid feed.

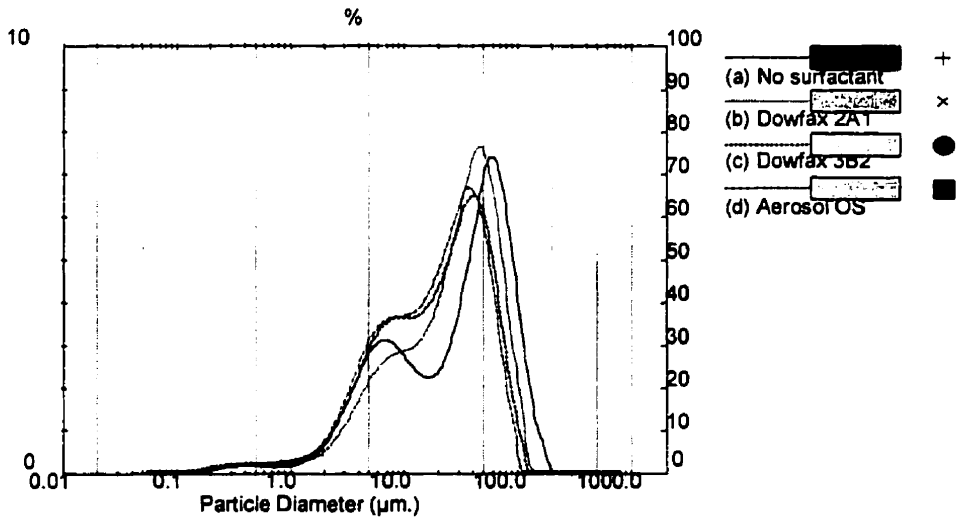

Figure E9: PSD of gypsum particles grown in the calcium carbonate partial neutralization reactor.

Reactor conditions: pH = 5.4-5.5, temperature=70°C, residence time = 30min, with (a) no surfactant, (b) Dowfax 2A1, (c) Dowfax 3B2, (d) Aerosol OS, with metal sulphates in the acid feed.

E.1.5 Effect of Seeding

Figure E10 shows the particle size distribution for the calcium carbonate that was used in these experiments, as well as the seed-containing calcium carbonate distributions.

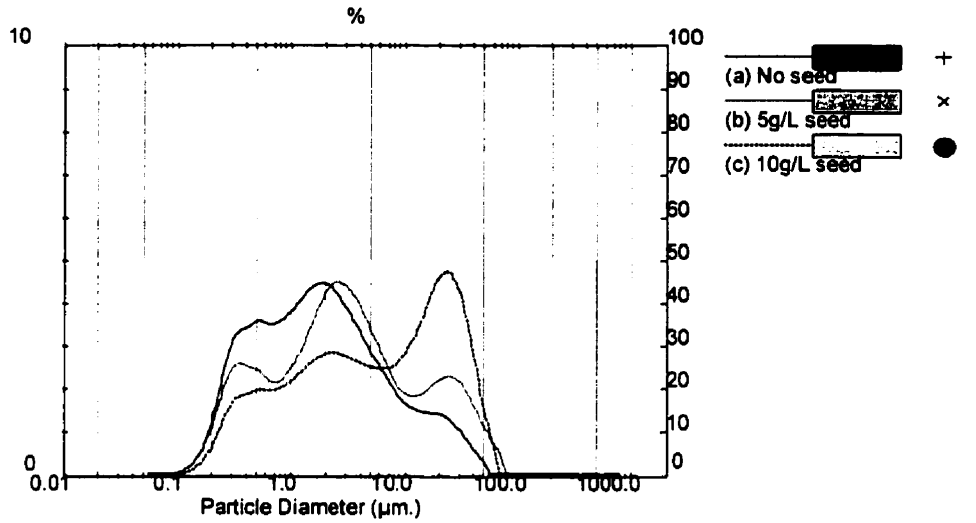

Figure E10: PSD of (a) calcium carbonate, (b) calcium carbonate + 5g/L gypsum seed, (c) calcium carbonate + 10g/L gypsum seed, used in partial neutralization "Effect of Seeding" experiments.

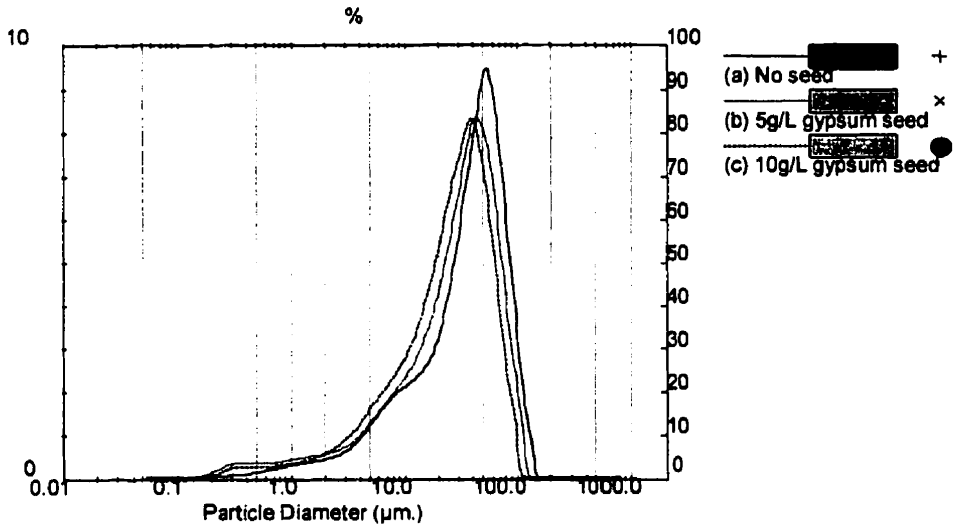

Figure E11: PSD of gypsum particles grown in the calcium carbonate partial neutralization reactor.

Reactor conditions: pH = 6.2-6.4, temperature=70°C, residence time = 30min, with (a) no seed, (b) 5g/L gypsum seed in $CaCO_3$, (c) 10g/L gypsum seed in $CaCO_3$, with no metal sulphates in the acid feed.

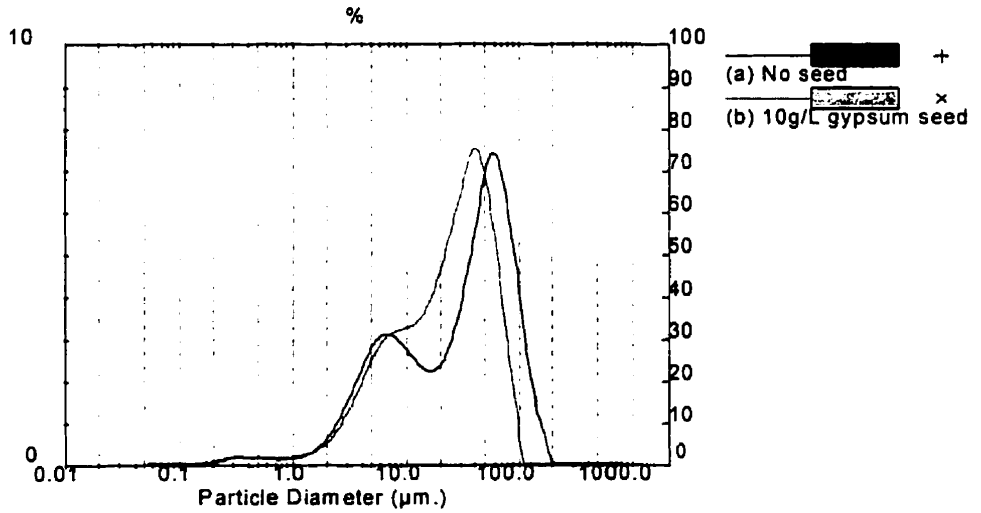

Figure E12: PSD of gypsum particles grown in the calcium carbonate partial neutralization reactor.

Reactor conditions: pH = 5.8, 6.0, temperature=70°C, residence time = 30min, with (a) no seed, (b) 10g/L gypsum seed in $CaCO_3$, with metal sulphates in the acid feed.

E.2 Calcium Oxide Total Neutralization Reactor

Figure E13 shows the particle size distribution for the calcium oxide that was used in these experiments.

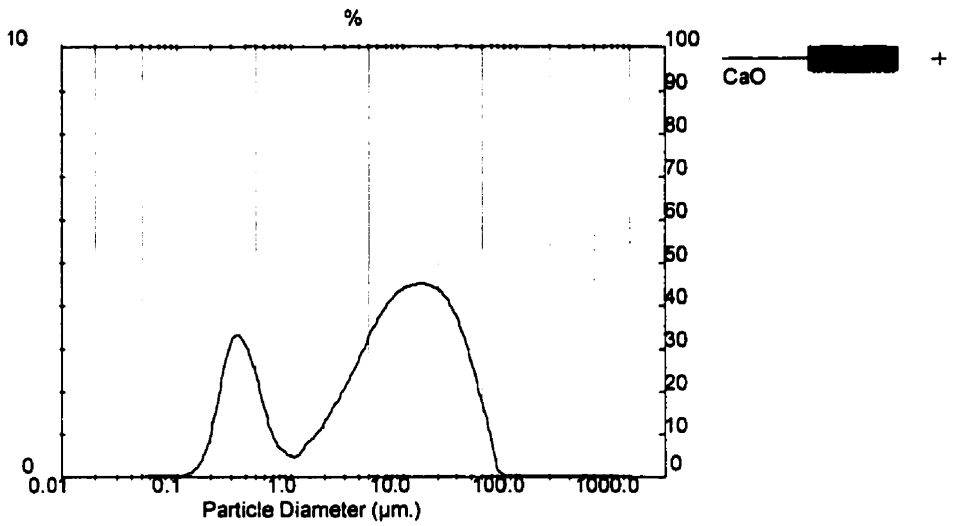

Figure E13: PSD of calcium oxide used in total neutralization

E.2.1 Effect of pH

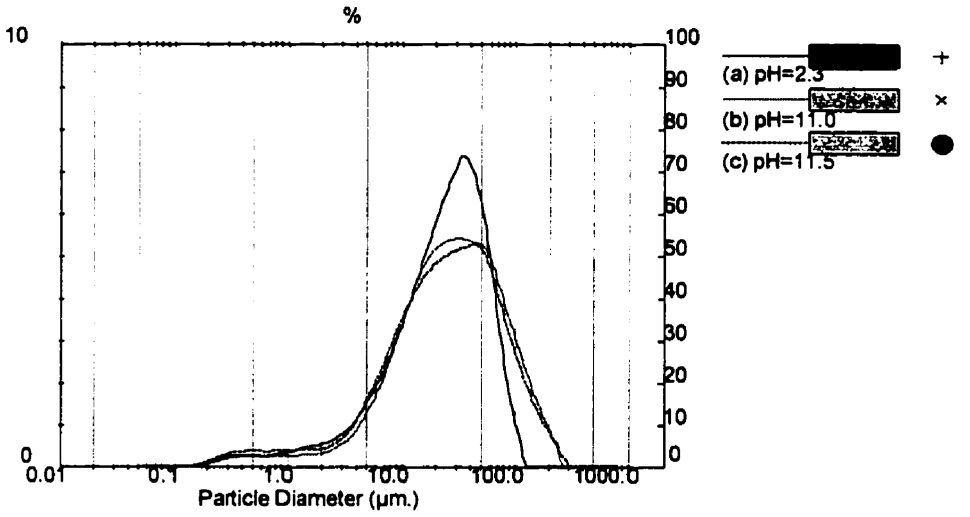

Figure E14: PSD of gypsum particles grown in the calcium oxide total neutralization reactor.

Reactor conditions: pH = (a) 2.3, (b) 11.0, (c) 11.5, temperature=40°C, residence time = 30min, with no magnesium sulphate in the acid feed.

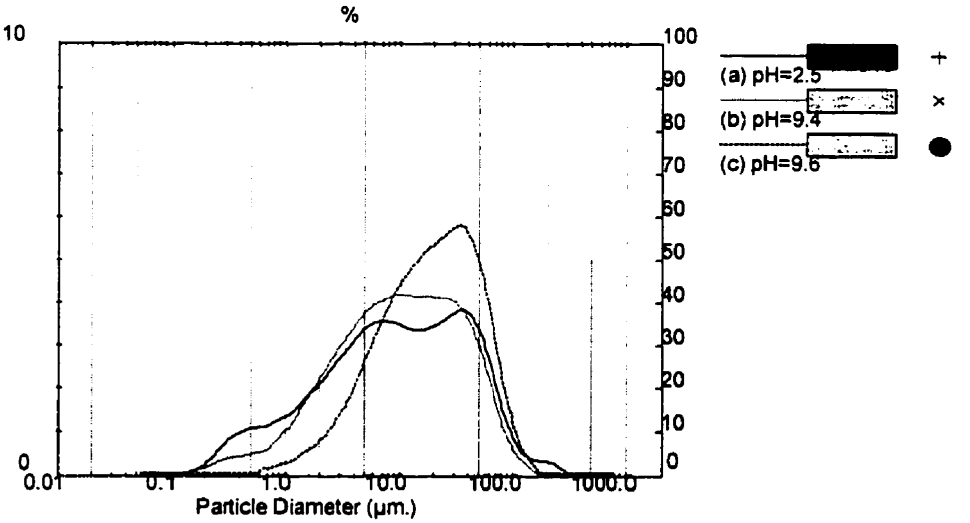

Figure E15: PSD of gypsum particles grown in the calcium oxide total neutralization reactor.

Reactor conditions: pH = (a) 2.5, (b) 9.4, (c) 9.6, temperature=40°C, residence time = 30min, with magnesium sulphate in the acid feed.

E.2.2 Effect of Temperature

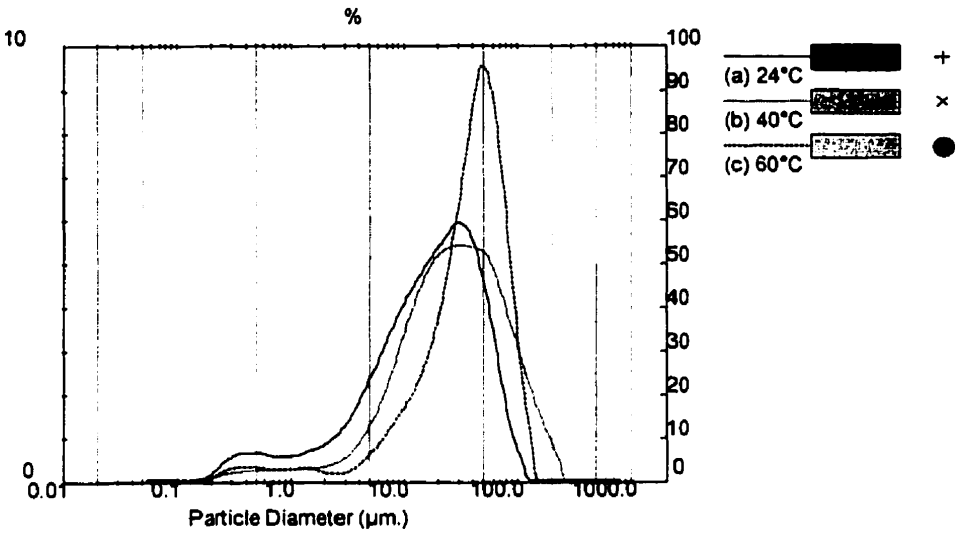

Figure E16: PSD of gypsum particles grown in the calcium oxide total neutralization reactor.

Reactor conditions: pH = 10.4-11.0, temperature = (a) 24°C, (b) 40°C, (c) 60°C, residence time = 30min, with no magnesium sulphate in the acid feed.

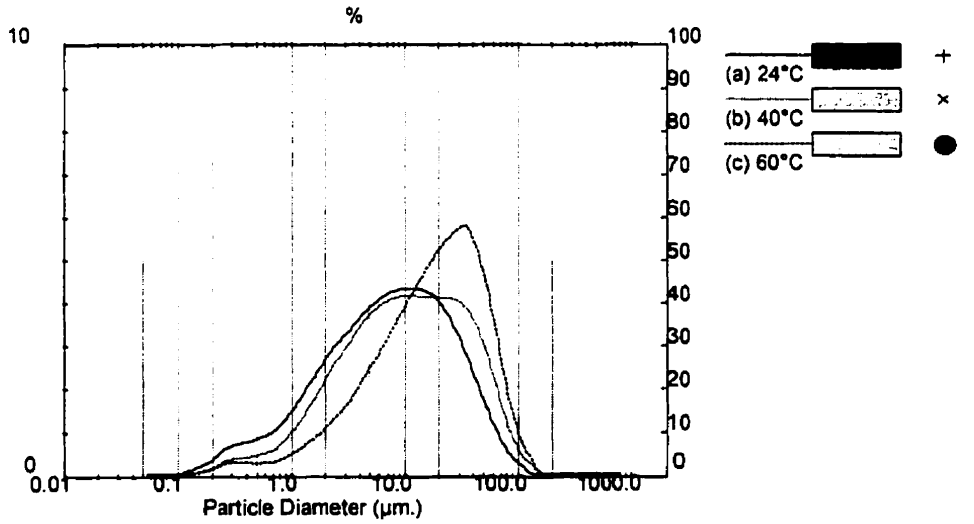

Figure E17: PSD of gypsum particles grown in the calcium oxide total neutralization reactor.

Reactor conditions: pH = 9.3-10.0, temperature = (a) 24°C, (b) 40°C, (c) 60°C, residence time = 30min, with magnesium sulphate in the acid feed.

E.2.3 Effect of Residence Time

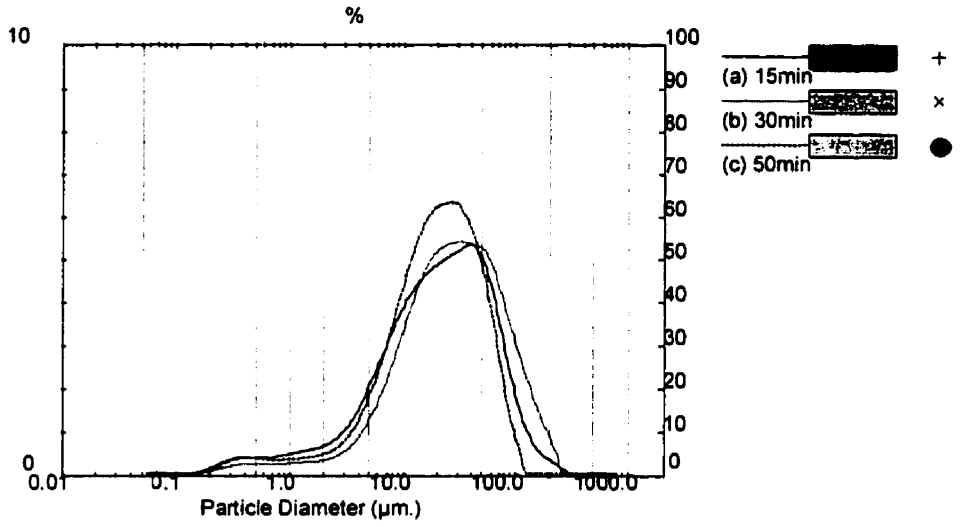

Figure E18: PSD of gypsum particles grown in the calcium oxide total neutralization reactor.

Reactor conditions: pH = 11.0-11.4, temperature=40°C, residence time = (a) 15min, (b) 30min, (c) 50min, with no magnesium sulphate in the acid feed.

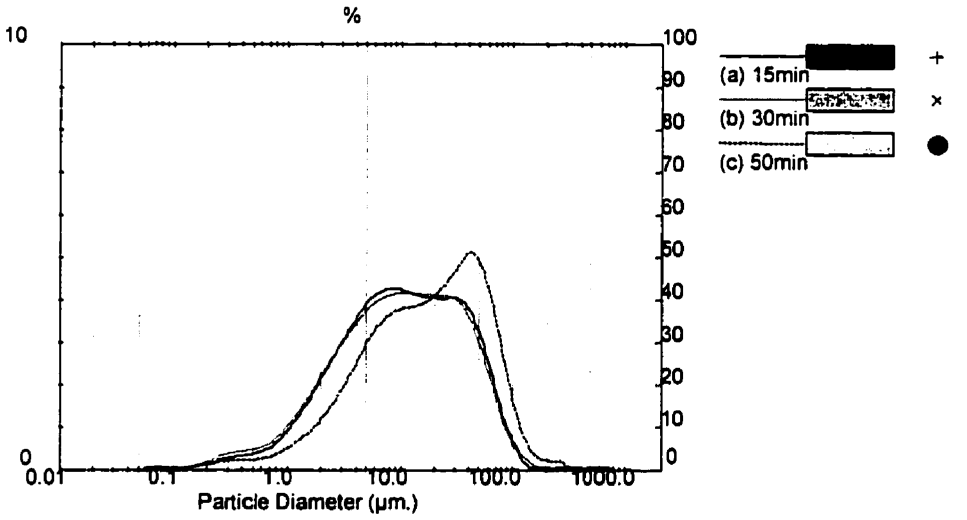

Figure E19: PSD of gypsum particles grown in the calcium oxide total neutralization reactor.

Reactor conditions: pH = 9.4-9.6, temperature=40°C, residence time = (a) 15min, (b) 30min, (c) 50min, with magnesium sulphate in the acid feed.

E.2.4 Effect of Surfactants

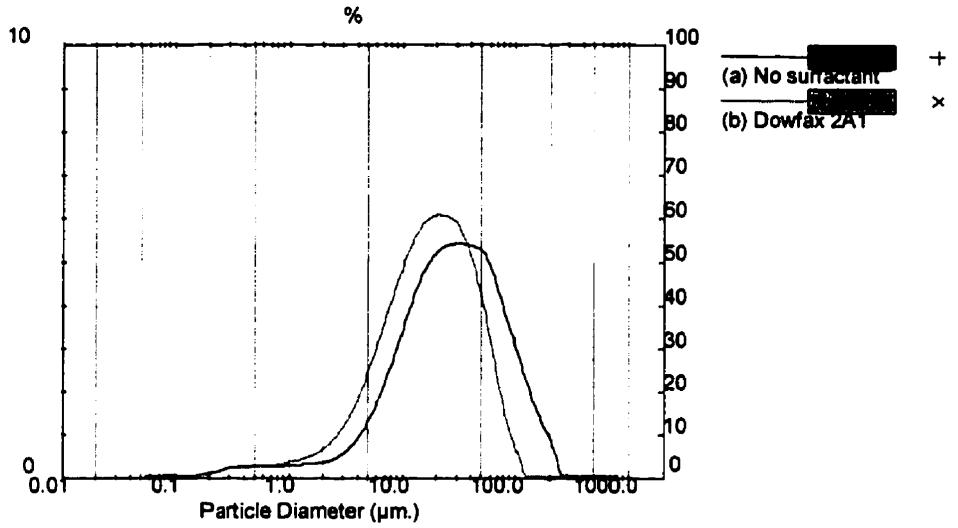

Figure E20: PSD of gypsum particles grown in the calcium oxide total neutralization reactor.

Reactor conditions: pH = 11.0-11.2, temperature=40°C, residence time = 30min, with (a) no surfactant, (b) 100ppm Dowfax 2A1, with no magnesium sulphate in the acid feed.

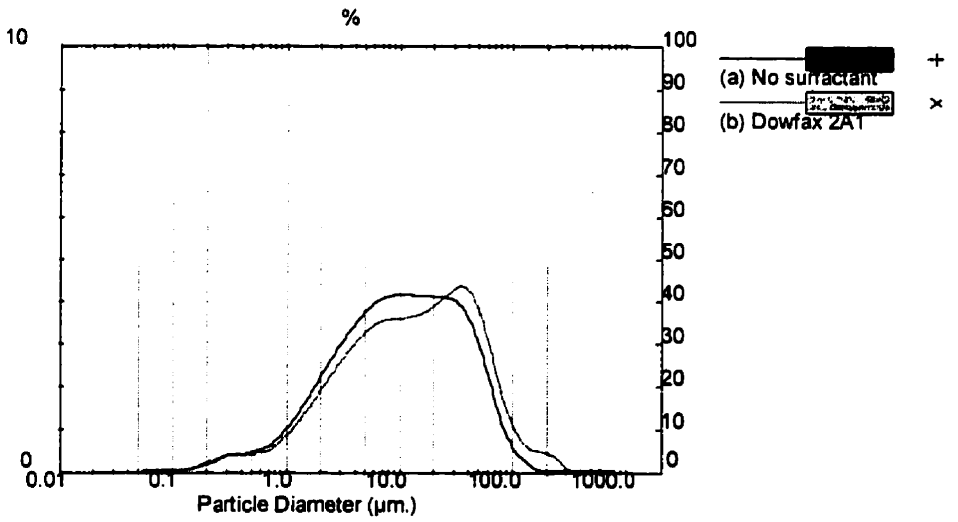

Figure E21: PSD of gypsum particles grown in the calcium oxide total neutralization reactor.

Reactor conditions: pH = 9.3-9.4, temperature=40°C, residence time = 30min, with (a) no surfactant, (b) Dowfax 2A1, with magnesium sulphate in the acid feed.

E.2.5 Effect of Seeding

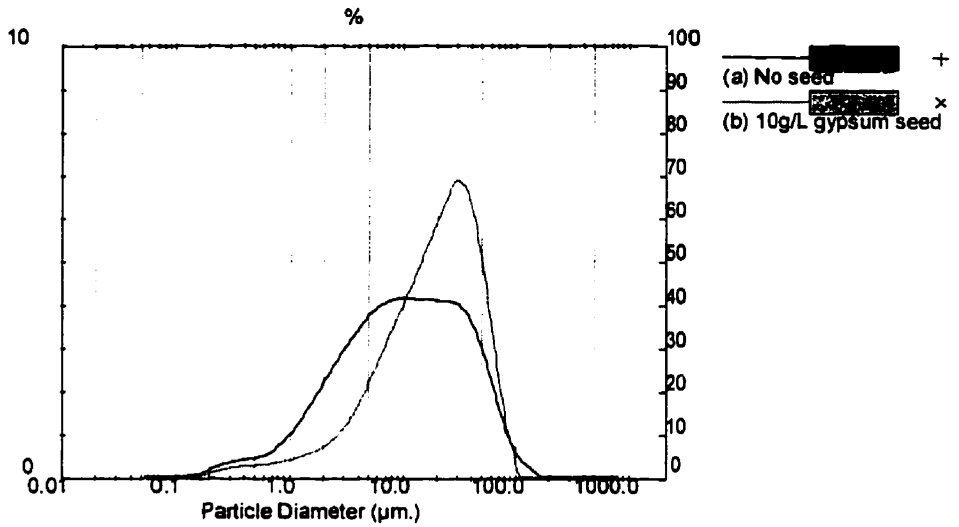

Figure E22: PSD of gypsum particles grown in the calcium oxide total neutralization reactor.

Reactor conditions: pH = 11.0, 8.0, temperature=40°C, residence time = 30min, with (a) no seed, (b) 10g/L gypsum seed in CaO, with magnesium sulphate in the acid feed.